TESIS DOCTORAL
NOA MÍGUEZ RODRÍGUEZ

SINTESÍS DE OLIGOSACÁRIDOS Y GLICOCONJUGADOS BIOACTIVOS EMPLEANDO ENZIMAS GLICOSÍDICAS

UNIVERSIDAD AUTÓNOMA DE MADRID
Departamento de Biología Molecular
Madrid, 2019

Departamento de Biología Molecular
Facultad de Ciencias
Universidad Autónoma de Madrid

SINTESÍS DE OLIGOSACÁRIDOS Y GLICOCONJUGADOS BIOACTIVOS EMPLEANDO ENZIMAS GLICOSÍDICAS

NOA MÍGUEZ RODRÍGUEZ
Graduada en Biología

MEMORIA
Para optar al grado de Doctora por la Universidad Autónoma de Madrid

DIRECTORES
Dr. Francisco José Plou Gasca
Dr. Antonio Ballesteros Olmo

Instituto de Catálisis y Petroleoquímica
Consejo Superior de Investigaciones Científicas

TUTOR
Dr. Manuel Soto Álvarez

Madrid, 2019

FRANCISCO JOSÉ PLOU GASCA, DR. EN CIENCIAS QUÍMICAS, INVESTIGADOR CIENTÍFICO DEL CSIC

ANTONIO BALLESTEROS OLMO, DR. EN CIENCIAS QUÍMICAS, PROFESOR DE INVESTIGACIÓN "AD HONOREM" DEL CSIC

CERTIFICAN: Que el presente trabajo "Síntesis de oligosacáridos y glicoconjugados bioactivos empleando enzimas glicosídicas", que constituye la Memoria que presenta la Graduada en Biología por la Universidad de Vigo, Noa Míguez Rodríguez, para optar al grado de Doctora, ha sido realizado bajo su dirección en el Departamento de Biocatálisis del Instituto de Catálisis y Petroleoquímica del CSIC, Campus de Excelencia Internacional UAM + CSIC, Madrid.

Y para que conste, firma el presente certificado en Madrid en mayo de 2019,

Dr. Francisco J. Plou

Dr. Antonio Ballesteros

A mi familia

A Viejo

"The truth is that the world is full of dragons, and none of us are as powerful or cool as we'd like to be. And that sucks. But when you're confronted with that fact, you can either crawl into a hole and quit, or you can get out there, take off your shoes, and Bilbo it up."

— Patrick Rothfuss

AGRADECIMIENTOS

Gracias a todos los que han participado y ayudado en esta Tesis, tanto a nivel científico, como a nivel personal:

Primero, gracias a todas las instituciones que han posibilitado, con su financiación, la realización de esta Tesis Doctoral. Gracias a los proyectos Nacionales BIO2013-48779-C4-1-R y BIO2016-76601-C3-1-R. Gracias también a la Acción COST (Systems Biocatalysis), por su ayuda para costear los gastos de la estancia y congresos.

Al departamento de Biología Molecular de la UAM por facilitarme toda la burocracia asociada a esta tesis.

Gracias a mi Director de Tesis, Dr. Francisco J. Plou Gasca. Kiko, muchas gracias por acogerme en tu laboratorio desde el máster, por confiar en mí y por tu apoyo y guía durante todos estos años.

Gracias a mi Director, Dr. Antonio Ballesteros, por sus consejos, sus anécdotas en cualquier lugar del mundo, su entusiasmo y los picnics en el bosque.

Gracias al Dr. Miguel Alcalde por mantener los ánimos altos y las palabras de apoyo.

Gracias también a mi tutor, el Dr. Manuel Soto, por su disposición y ayuda en todos los trámites que ha conllevado este trabajo.

Gracias a todos los grandes investigadores que han colaborado en esta Tesis: A la Dra. María Fernández Lobato y a todo su grupo del CBMSO por las enzimas, y los ánimos. A la Dra. Julia Sanz y a los miembros de su grupo del IQFR por los estudios cristalográficos. Al Servicio Interdepartamental de Investigación de la UAM, por los análisis de espectrometría de masas y análisis elemental. Al Prof. Jesús Jiménez Barbero y a la Dra. Ana Poveda (CIC-BioGUNE) por la realización e interpretación de los espectros de RMN. Gracias a la Prof. María Ribeiro, de la Universidad de Lisboa por acogerme en su laboratorio y enseñarme novedosas técnicas de inmovilización de enzimas. A Ramiro de Novozymes por aportarme enzimas y grandes ideas. A Ramón de Análisis Vínicos por todas las columnas y los consejos sobre cromatografía.

Gracias también a todas las personas que forman el ICP. Gracias a todo el personal de recursos humanos, secretaría, la Unidad de Apoyo, almacén, informática, limpieza, prevención…por facilitarnos el día a día y ayudarnos en todo lo posible.

Gracias a todos mis compañeros de laboratorio por la compañía, el aprendizaje y la diversión; Paloma, Lucía, Bárbara, Joselu, Fadia y David. Gracias a Lopa por aguantarme cada día, responder mis millones de preguntas y hacerme *llorar* cuando era necesario. Gracias también por el Mad Cool, la Sci-fy y Gato.

Gracias Bárbara por tu alegría y energía contagiosas. Gracias Fadia por las partidas de Mario Kart y los Jarritos. Gracias David por ser el mejor *pequeño lacayo* que existe. Gracias a Lucía por su amabilidad y sus consejos. Gracias a Joselu por tus amenas conversaciones.

Gracias a "los de arriba", por todos los buenos momentos de los últimos años. Muchas gracias Javi por los juegos de mesa, las tardes de fútbol y sobre todo el Javibus (es broma). Gracias a Patch (y minipatch) por amenazarme con las manazas para que cumpliera el calendario y las conversaciones en *balleno*. Gracias a Berni y a Pati por los atracones de pulpo y tortilla de verano, y los viajes en Pato. Gracias a Xavi por el mejor momento de la historia de Faunia. Gracias también a Iván por las partidas de ping-pong que algún día jugaremos.

Gracias también al Dr. Manuel Ferrer y a los *Manolos*: Moni, Cris, Rafa, Pepe, Sandra, Laura, David y Sergio, gracias por los cafés y las tartas. Gracias Moni por lavarme el cerebro para que adoptara a Puchi. Gracias *Gremlin* por los viernes de Spyro, los documentales de peces y los Mochito, Peanut, Derpi, Lagartijo, Nubecita, Ade y Bichou. Gracias también por los findes de piscina y el voleibol asesino (gracias Aitor por la parte que te corresponde). Gracias a *Lady Flor* y a Laura por los tests de personalidad y las risas compartidas.

Gracias a Manolito y a Lara por hacer que Madrid se parezca un poquito más a Galicia.

Gracias a mis compañeras de piso Marta y Elena por los ratos compartidos y los ánimos estos últimos meses. También gracias a Puchi por ser la alegría de la casa, por el caballito, el dinosaurio y demás locuras.

También quiero agradecer a mis amigos de Pontevedra, Sabela, Elena, Pedro, Emma, Gabo, César y Elisa, por estar conmigo todos estos años y por lo bien que lo hemos pasado.

Gracias a Alba y Cibrán por ser mis amigos desde siempre.

Gracias a mi madre, mi padre y mis hermanos David e Isaac por su cariño y apoyo incondicional todos estos años. También gracias a Viejo que, aunque ya no está siempre será el rey de la casa. Gracias a los Memekos, Milikito, Tupi y Hachiko por todas las risas.

GENERAL INDEX

Content index i
Figures index iv
Tables index viii
Abbreviations & acronyms xi
Summary xiii
Presentación..... xv

CONTENT INDEX

1. INTRODUCTION **1**
1.1 Bioactive oligosaccharides **3**
1.2 Bioactive glycoconjugates. Glycosylation **6**
1.3 Glycosidic enzymes **7**
1.4 Neo-fructooligosaccharides production **8**
1.5 Fructosylation of polyphenols. Glycosylation of hydroxytyrosol **11**
1.6 Production of acidic XOS **13**
1.7 Chitooligosaccharides production **15**
1.8 Enzyme immobilization **18**
2. OBJECTIVES **23**
3. MATERIALS AND METHODS **27**
3.1 Materials **29**
3.1.1 Enzymes 29
3.1.2 Reagents 29
3.1.3 Immobilization carriers 30
3.1.4 Buffer solutions 30
3.2 Enzyme characterization **31**
3.2.1 β-Frutofuranosidase activity 31
3.2.2 Endoxylanase activity 31
3.2.3 Protein concentration 31
3.3 Analytical methods **31**
3.3.1 TLC 31
3.3.2 HPLC 32
3.3.3 HPAEC-PAD 33
3.3.4 Semipreparative HPLC 35
3.3.5 Mass spectrometry (MS) 36
3.3.6 Nuclear magnetic resonance 37
3.3.7 Elemental analysis 37
3.4 Transfructosylation assays with pXd-INV **38**

3.4.1 Acceptor/Inhibitor screening 38
3.4.2 Enzymatic synthesis of fructosylated phenols 38
3.4.3 Fructosylation of HT and reaction optimization 38
3.4.4 Purification of Fru-HQ and Fru-HT 39
3.4.5 Crystallization and X-Ray structure determination 39
3.5 β-Fructofuranosidase immobilization 39
3.5.1 Entrapment in PVA lenses 39
3.5.2 Binding to carriers 40
3.5.3 Apparent activity 41
3.5.4 Operational stability of immobilized biocatalysts 41
3.5.5 Thermostability of PVA hydrogels 43
3.5.6 Large-scale immobilization in Sepabeads EC-HA 43
3.6 Neo-FOS production in reactors with immobilized pXd-INV 43
3.6.1 Batch reactor 43
3.6.2 Packed-bed reactor 43
3.7 Production of acidic XOS 44
3.7.1 Enzymatic hydrolysis of beechwood xylan 44
3.7.2 Acidic XOS purification 44
3.7.3 Large-scale production and purification of acidic XOS 44
3.7.4 Scavenging of ABTS radical 45
3.8 Large-scale production of COS 46
4. RESULTS AND DISCUSSION 47
4.1 Production of neo-FOS by immobilized pXd-INV 49
4.1.1 Immobilization of pXd-INV in PVA hydrogels 49
4.1.2 Immobilization of pXd-INV by ionic binding 50
4.1.3 Operational stability of the immobilized biocatalysts 51
4.1.4 Thermal stability of PVA-based biocatalyst 52
4.1.5 Production of FOS by PVA-entrapped pXd-INV 53
4.1.6 Batch reactor for neo-FOS production with PVA-based biocatalyst 56
4.1.7 Packed-bed reactor for neo-FOS production with Sepabeads biocatalyst 57
4.2 Fructosylation of phenolic compounds with pXd-INV 59

4.3 Production of fructosylated hydroxytyrosol conjugates by pXd-INV 65

4.3.1 Fructosylation of HT by pXd-INV 65

4.3.2 Structural and molecular analysis of HT fructosylation by pXd-INV.. 69

4.3.3 Site-Directed mutagenesis of pXd-INV 70

4.4 Enzymatic production of acidic XOS 72

4.4.1 Production of neutral and acidic XOS 73

4.4.2 Anion-exchange purification of acidic XOS 74

4.4.3 Antioxidant activity of acidic XOS 77

4.5 Large-scale production of COS 79

4.5.1 Large-scale procedure for COS synthesis 79

4.5.2 Characterization of COS mixtures 84

5. GENERAL DISCUSSION 91

5.1 Neo-FOS production by immobilized pXd-INV 93

5.2 Fructosylation of phenolic compounds by pXd-INV 96

5.3 Production of acidic XOS 99

5.4 Large-scale production of COS 101

6. CONCLUSIONS 103

7. REFERENCES 109

APPENDIX I 131

APPENDIX II 137

FIGURES INDEX

Figure 1.1 Schematic representation of enzymatic glycosylation with GHs, GTs and TGs. **6**

Figure 1.2 Fructooligosaccharides structure. a) Inulin-type FOS. b) Levan-type FOS. c) Neo-FOS. d) Mixed-FOS..... **9**

Figure 1.3 General scheme of xylan structure. Violet: 4-O-methyl-α–D-glucuronopyranosyl. Yellow: acetyl. Red: α-D-glucose. Blue-orange: α-L-coumaroyl arabinose Blue-green: α-L-feruloyl arabinose..... **14**

Figure 1.4 Structure of the three main types of chitooligosaccharides (COS): fully acetylated (faCOS), partially acetylated (paCOS) and fully deacetylated (fdCOS). **17**

Figure 1.5 Scheme of enzyme immobilization methodologies **20**

Figure 3.1. Immobilization of pXd-INV by entrapment in PVA. **40**

Figure 3.2. Micro-scale assay for the determination of apparent activity and operational stability of immobilized biocatalysts **42**

Figure 3.3. Anion-exchange purification of acidic XOS **45**

Figure 4.1. Operational stability of each biocatalyst: a) PVA (Initial activity 35.5 U); b) EC-EA and EC-HA (Initial activity 41.8 U); c) EC-EA and EC-HA (Initial activity 4.18 U). Reaction conditions: 100 g/L of sucrose in sodium acetate buffer (pH 5.0) at 50 ºC for 20 min. Values are referred to the activity of the biocatalyst in the first cycle **52**

Figure 4.2. Thermostability of pXd-INV entrapped in PVA lenses after incubating at 4-60 ºC for 24 h in 100 mM sodium acetate buffer (pH 5.0)..... **53**

Figure 4.3. a) HPAEC-PAD chromatogram of the reaction of 600 g/L of sucrose at 30 ºC with pXd-INV immobilized in PVA lenses. (1) Glucose; (2) Fructose; (3) Sucrose; (4) 1-Kestose; (5) Blastose; (6) Neokestose; (7) Neonystose. b) Structure of the FOS synthesized by the PVA-entrapped enzyme. The sucrose skeleton is represented in green..... **54**

Figure 4.4. Kinetics of FOS formation with PVA-entrapped pXd-INV. Reaction conditions: 600 g/L of sucrose in 100 mM sodium acetate buffer (pH 5.0) at 30 ºC **55**

Figure 4.5. Batch stirred tank reactor system for FOS production with PVA-entrapped pXd-INV (PVA-pXd-INV). Reaction conditions: 600 g/L of sucrose in 100 mM sodium acetate buffer (pH 5.0) at 30 ºC..... **56**

Figure 4.6. Operational stability of the immobilized biocatalyst (PVA-pXd-INV) in a batch reactor. Reaction conditions per cycle: 600 g/L of sucrose in 100 mM sodium acetate buffer (pH 5.0) at 30 ºC for 26 h **57**

Figure 4.7. Packed bed reactor system for FOS production with pXd-INV immobilized in Sepabeads EC-HA (HA-pXd-INV). Reaction conditions: 600 g/L of sucrose in 100 mM sodium acetate buffer (pH 5.0) at 50 ºC **58**

Figure 4.8. Operational stability of the immobilized biocatalyst (HA-pXd-INV) in a packed bed reactor. Reaction conditions: 600 g/L of sucrose in 100 mM sodium acetate buffer (pH 5.0) was fed at 0.03 mL/min and the column was kept at 50 ºC **59**

Figure 4.9. HPLC analysis of the assays with (A) hydroquinone (HQ); (B) catechol; (C) EGCG and (D) p-nitrophenol. Reaction conditions 100 g/L of sucrose and 20 g/L of phenolic compound in 100 mM sodium acetate buffer (pH 5.0) at 60 ºC. Red: PDA detector; Black: ELSD detector **61**

Figure 4.10. TLC analysis of reactions in presence of a) Hydroquinone (HQ) and b) Hydroxytyrosol (HT) observed at UV light. Reaction conditions: 100 g/L of sucrose and 20 g/L of phenolic compound in 100 mM sodium acetate buffer (pH 5.0) at 60 ºC. **62**

Figure 4.11. FOS production in absence and presence of various phenolic compounds. Reaction conditions: 100 g/L of sucrose and 20 g/L of phenolic compound in 100 mM sodium acetate buffer (pH 5.0) at 60 ºC. **63**

Figure 4.12. Predicted structure of the obtained HQ derivative (4-hydroxyphenyl-*β*-D-fructofuranoside) **65**

Figure 4.13. Surface depiction of pXd-INV-D80A with fructose and two phenolic compounds in the active site. a) Crystals soaked with fructose and EGCG (both in green) and b) Crystals soaked with fructose (orange) and HQ (light green). **65**

Figure 4.14. HPLC analysis of the HT fructosylation assay catalyzed by pXd-INV. Reaction conditions: 300 g/L of sucrose and 25 g/L of HT in 100 mM sodium acetate buffer (pH 5.0) at 60 ºC. a) Chromatogram employing a NH2 column and PDA detector. (HT) Hydroxytyrosol; (Fru-HT1 and Fru-HT2) Hydroxytyrosol fructosides. b) HPAEC-PAD chromatogram with a PA1 column. Peaks: (1) Glucose; (2) Fructose; (3) Sucrose; (4) 1-Kestose; (5) Neokestose. **66**

Figure 4.15. Production of fructosylated hydroxytyrosol derivatives (Fru-HT1 and Fru-HT2) with pXd-INV. a) Effect of HT concentration with sucrose concentration fixed at 100 g/L. b) Effect of sucrose concentration with HT concentration set at 25 g/L. The different sucrose and HT assayed concentrations are displayed on each panel.. ..... **67**

Figure 4.16. Production of fructosylated hydroxytyrosol conjugates (Fru-HT1 and Fru-HT2) and FOS by pXd-INV represented as a function of sucrose consumption under optimum reaction conditions (300 g/L of sucrose as donor and 25 g/L of HT as acceptor in 100 mM sodium acetate buffer, pH 5.0, at 60 ºC).. ..... **68**

Figure 4.17. Structure of Fru-HT1 (3,4-dihydroxyphenyl ethyl *β*-D-fructofuranoside) determined by NMR. **68**

Figure 4.18. Surface depiction of pXd-INV-D80A with both substrates and product bound in the active site. a) Crystals soaked with fructose (light green) and HT

(dark green). HT was located in three positions labelled as HT1, HT2 and HT3. b) Crystals soaked with the fructosylated product (fructose in light red and HT in dark red) purified by HPLC. Fru-HT1 is the main product characterized by NMR, and it will be formed when HT is located at HT1 binding site. Fru-HT2 is produced when HT fructosylation occurs at the HT2 position. The 2Fo-Fc electron density maps are contoured at 1 σ **70**

Figure 4.19. Reaction scheme of HT fructosylation by pXd-INV. Fru-HT1 is the main product characterized by NMR and Fru-HT2 is a secondary product identified by crystallography. **70**

Figure 4.20. Production of fructosylated hydroxytyrosol conjugates (Fru-HT1 and Fru-HT2) and FOS under optimum reaction conditions (300 g/L of sucrose as donor and 25 g/L of HT as acceptor in 100 mM sodium acetate buffer, pH 5.0, at 60 ºC), represented as a function of sucrose consumption, employing the mutants. a) pXd-INV-Q341S and b) pXd-INV-N342Q **71**

Figure 4.21. HPAEC-PAD chromatogram of the hydrolysis of 2% xylan at 3 and 48 h with Depol 670L. (Ara) Arabinose; (Glc) Glucose; (Xyl) Xylose; (Xyl_2) Xylobiose; (Xyl_3) Xylotriose; (Xyl_4) Xylotetraose; (Xyl_5) Xylopentaose; (Xyl_6) Xylohexaose **73**

Figure 4.22. HPAEC-PAD analysis of the a) Neutral fraction and b) Acidic fraction. Identified peaks: (1) Xylose; (2) Xylobiose. (*) Main peak of the acidic fraction **74**

Figure 4.23. Characterization of the acidic fraction by mass spectrometry (MALDI-TOF). Peaks: X2_MeGlcA (methyl-glucuronic xylobiose); X3_MeGlcA (methyl-glucuronic xylotriose); X4_MeGlcA (methyl-glucuronic xylotetraose); X5_MeGlcA (methyl-glucuronic xylopentaose); X6_MeGlcA (methyl-glucuronic xylohexaose) **76**

Figure 4.24. Structure of 2'-O-α-(4-O-methyl-α-D-glucuronosyl)-xylobiose elucidated by NMR **77**

Figure 4.25. Antioxidant activity of neutral XOS, beechwood xylan and acidic XOS (X2_MeGlcA) **78**

Figure 4.26. Large-scale procedure for COS production **81**

Figure 4.27. Schematic representation of the reactions carried out and the products obtained for each of them **83**

Figure 4.28. HPAEC-PAD chromatogram of the COS produced with CHIT600 and Neutrase 0.8L. Reaction conditions: 1% (w/v) chitosan, 10% (v/v) Neutrase 0.8L in sodium acetate buffer (pH 5.0) at 50 ºC for 48 h. Peaks: (1) GlcN; (2) $(GlcN)_2$; (3) $(GlcN)_3$); (4) $(GlcN)_4$; (5) $(GlcN)_5$ **84**

Figure 4.29. HPAEC-PAD chromatogram of the COS produced with QS1 and CHIT42. Reaction conditions: 1% (w/v) chitosan, 10% (v/v) CHIT42 in sodium acetate buffer (pH 5.0) at 35 ºC for 48 h **86**

Figure 4.30. HPAEC-PAD chromatogram of the COS produced with CHIT1 and Neutrase 0.8L. Reaction conditions: 1% (w/v) chitosan, 10% (v/v) Neutrase 0.8L in ammonium acetate buffer (pH 5.0) at 60 ºC for 48 h **88**

Figure 4.31. HPAEC-PAD chromatogram of the COS produced with CHIT2 and Neutrase 0.8L. Reaction conditions: 1% (w/v) chitosan, 10% (v/v) Neutrase 0.8L in ammoniun acetate buffer (pH 5.0) at 60 °C for 48 h..... **89**

Figure 5.1 Schemed reaction of xylan hydrolysis by Depol 670L..... **101**

TABLES INDEX

Table 1.1 Bioactivities of oligosaccharides and oligosaccharides derivatives..... **4**

Table 1.2 Production of neo-FOS employing microbial enzymes or microorganisms **10**

Table 1.3 Fructosylation of phenolic compounds by microbial enzymes **12**

Table 3.1 Chitosans used in this Thesis **30**

Table 3.2 Buffer solutions employed in this Thesis **30**

Table 3.3 HPLC methods for transfructosylation of polyphenols and production of Fru-HT with pXd-INV. A: CH_3CN and B: H_2O..... **32**

Table 3.4 HPAEC-PAD methods for FOS analysis. A: 100 mM NaOH. B: H_2O. D: 100 mM NaOH, 600 mM CH_3COONa..... **34**

Table 3.5 HPAEC-PAD methods for XOS and COS analysis. A: 200 mM NaOH. B: H_2O. C: 200 mM CH_3COONa. D: 100 mM NaOH, 320 mM CH_3COONa..... **35**

Table 3.6 Semipreparative HPLC. A: CH_3CN and B: H_2O **36**

Table 3.7 pXd-INV immobilization conditions for the different carriers..... **41**

Table 4.1 Immobilization parameters of pXd-INV in PVA lenses with two enzyme loadings..... **50**

Table 4.2 Immobilization parameters of pXd-INV in Sepabeads EC-EA and EC-HA with two different enzyme loadings..... **51**

Table 4.3 Effect of the assayed phenolic compounds on the hydrolytic and transfructosylation activity of pXd-INV **64**

Table 4.4 Maximum production of the fructosylated HT conjugates (FOS concentration at this time) by pXd-INV and its mutants..... **72**

Table 4.5 Half-maximal scavenging activity of beechwood xylan, neutral XOS and X2_MeGlcA, compared with Trolox..... **79**

Table 4.6 Main identified signals in the MALDI-TOF mass spectrum of the reaction between chitosan CHIT600 and Neutrase 0.8L **85**

Table 4.7 Main identified signals in the MALDI-TOF mass spectrum of the reaction between chitosan QS1 and CHIT42..... **87**

Table 4.8 Main identified signals in the MALDI-TOF mass spectrum of the reaction with chitosan CHIT1 and Neutrase 0.8L **88**

Table 4.9 Main identified signals in the MALDI-TOF mass spectrum of the reaction with chitosan CHIT2 and Neutrase 0.8L **90**

Table 5.1 Production of neo-FOS with immobilized pXd-INV biocatalysts obtained in this Thesis **95**

Table 5.2 Fructosylation of phenolic compounds with pXd-INV **97**

Table 5.3 Description of the production process for each COS mixture (substrate, reaction conditions, product and MW) **102**

ABBREVIATIONS AND ACRONYMS

Aas	Redox enzymes that act in conjunction with CAZymes
ABTS	2,2'-azinobis-(3-ethylbenzothiazoline-6-sulfonic acid)
AGOS	Algar oligosaccharides
AOS	Alginate oligosaccharides
BSA	Bovine Serum Albumin
CAZy	Carbohydrate Active enZymes database
CAZymes	Carbohydrate Active enZymes
CEs	Carbohydrate Esterases
CHIT1	Chitosan from ANFACO-CECOPESCA (4 kDa, 94.7% DD)
CHIT2	Chitosan from ANFACO-CECOPESCA (56 kDa, 79.4% DD)
CHIT42	Chitinase of 42 kDa from *Trichoderma harzianum*
CHIT600	Chitosan from Acros Organics (600-800 kDa, >90% DD)
CIC bioGUNE	Centro de Investigación Cooperativa en Biociencias
CLEAs	Cross-Linked Enzyme Aggregates
CLECs	Cross-Linked Enzyme Crystals
COS	Chitooligosaccharides
CSIC	Consejo Superior de Investigaciones Científicas
d	Dilution rate (h^{-1})
DD	Degree of deacetylation
DDS	4,4-dimethyl-4-silapentane-1-sulfonic acid
DHB	2,5-dihydroxybenzoic acid
DNS	3,5-dinitrosalicilyc acid
DP	Degree of polymerization
EFSA	European Food Safety Authority
EGCG	Epigallocatechin gallate
ELSD	Evaporative Light Scattering Detector
faCOS	Fully acetylated COS
fdCOS	Fully deacetylated COS
FOS	Fructooligosaccharides
Fru-HQ	Hydroquinone fructoside
Fru-HT	Hydroxytyrosol fructoside
GH	Glycosyl hydrolase family
GHs	Glycosyl hydrolases
GlcN	D-glucosamine
GlcNAc	N-acetyl-D-glucosamine
$(GlcN)_n$	Chitooligosaccharide with degree of polymerization *n*
$(GlcNAc)_n$	Chitin-oligosaccharide with degree of polymerization *n*
GOS	Galactooligosaccharides
GTs	Glycosyltransferases
HA-pXd-INV	pXd-INV immobilized in Sepabeads EC-HA
HEPES	4-(2-hydroxyethyl)-1-piperazine ethanesulfonic acid

HPAEC-PAD	High Performance Anion-Exchange Cromatography with Pulsed Amperometric Detection
HPLC	High PerformanceLiquid Cromatography
HQ	Hydroquinone
HT	Hydroxytyrosol
IMOS	Isomaltooligosaccharides
IUB-IUPAC	International Union of Biochemistry - International Union of Pure and Applied Chemistry
MALDI-TOF	Matrix Assisted Laser Desorption Ionization-Time Of Flight
MOS	Mannan oligosaccharides
MS	Mass Spectrometry
MW	Molecular Weight
MWCO	Molecular Weight Cut-Off
NMR	Nuclear Magnetic Resonance
PA	Pattern of acetylation
paCOS	Partially acetylated COS
PDA	Photodiode array detector
PLs	Polysaccharide lyases
POS	Pectic oligosaccharides
PVA	Polyvinyl alcohol
PVA-pXd-INV	pXd-INV entrapped in PVA
pXd-INV	*β*-fructofuranosidase from *Xanthophyllomyces dendrorhous* (recombinant)
QS1	Chitosan from InFiQus (98 kDa, 81% DD)
QTOF	Quadrupole Time Of Flight
SC_{50}	Half-maximum scavenging concentration
SIdI	Servicio Interdepartamental de Investigación
SOS	Soybean oligosaccharides
TEAC	Trolox Equivalent Antioxidant Capacity
TGs	Transglycosidases
TLC	Thin Layer Chromatography
U	Units of enzymatic activity
UAM	Universidad Autónoma de Madrid
USA	United States of America
UV	Ultraviolet light
v/v	Volume/volume
w/v	Weight/volume
X2	Xylobiose
X2_MeGlcA	Methyl-glucuronic xylobiose
X3_MeGlcA	Methyl-glucuronic xylotriose
X4_MeGlcA	Methyl-glucuronic xylotetraose
X5_MeGlcA	Methyl-glucuronic xylopentaose
X6	Xylohexaose
X6_MeGlcA	Methyl-glucuronic xylohexaose
XOS	Xylooligosaccharides

SUMMARY

Bioactive carbohydrates and glycoconjugates possess many biological activities that can exert a beneficial effect in human health. This Thesis is focused on the enzymatic production and characterization of bioactive glycoconjugates: fructosylated derivatives of hydroquinone and hydroxytyrosol; and three families of bioactive oligosaccharides: neo-fructooligosaccharides (neo-FOS), acidic xylooligosaccharides (acidic XOS) and chitooligosaccharides (COS).

Neo-FOS production was investigated employing immobilized biocatalysts prepared by ionic binding or entrapment of the *β*-fructofuranosidase from *Xanthophyllomyces dendrorhous* (pXd-INV). The enzyme pXd-INV was entrapped in polyvinyl alcohol lenses and neo-FOS production was studied in a batch stirred tank reactor, obtaining a maximum productivity of 42 g_{FOS} L^{-1} day^{-1}. Neo-FOS synthesis was also assessed in a packed-bed bioreactor employing pXd-INV immobilized on an amino activated carrier (Sepabeads EC-HA) with an initial productivity of 218 g_{FOS} L^{-1} day^{-1}.

The ability of pXd-INV to fructosylate phenolic compounds was also evaluated. Two positive acceptors were found: hydroxytyrosol (HT) and hydroquinone (HQ). The production of HT fructosides was optimized, yielding up to 11.7 g/L. The mechanism and selectivity of the reaction, and the molecular features that determine that a phenolic compound acts as an acceptor or an inhibitor, were studied by crystallography.

The synthesis of acidic XOS was carried out with the commercial enzyme Depol 670L. Xylan hydrolysis gave rise to a mixture of neutral and acidic XOS. Acidic XOS were separated by anion-exchange chromatography and the main product was chemically characterized and identified as 2'-O-α-(4-O-methyl-α-D-glucuronosyl)-xylobiose (X2_MeGlcA). The antioxidant activity of the obtained product, neutral XOS and xylan was comparatively measured. Both X2_MeGlcA and xylan displayed scavenging activity on the ABTS radical cation.

Furthermore, an integrated methodology was developed for the enzymatic production and characterization of several COS mixtures. A proteolytic preparation (Neutrase 0.8L) and a chitinase from *Trichoderma harzanium* (CHIT42) were employed for the hydrolysis of chitosans with different deacetylation degrees and molecular weights. Thus, we synthesized several COS mixtures based on: (1) fully deacetylated COS (fdCOS); (2) partially acetylated COS (paCOS); (3) mixtures of fdCOS and paCOS.

PRESENTACIÓN

Los carbohidratos y glicoconjugados bioactivos poseen actividades biológicas que pueden ejercer un efecto beneficioso en la salud humana. La presente Tesis Doctoral se centra en la producción enzimática y caracterización de glicoconjugados bioactivos: derivados fructosilados de la hidroquinona y el hidroxitirosol; y tres familias de oligosacáridos bioactivos: neo-fructooligosacáridos (neo-FOS), xilooligosacáridos ácidos (XOS ácidos) y quitooligosacáridos (COS).

La producción de neo-FOS se investigó empleando biocatalizadores inmovilizados preparados por adsorción iónica o atrapamiento de la *β*-fructofuranosidasa de *Xanthophyllomyces dendrorhous* (pXd-INV). La enzima pXd-INV se inmovilizó en lentes de alcohol polivinílico y la producción de neo-FOS se estudió en un reactor de tanque agitado discontinuo, obteniendo 42 g_{FOS} L^{-1} día $^{-1}$. La síntesis de neo-FOS también se evaluó en un biorreactor de lecho fijo empleando pXd-INV inmovilizada en un soporte amino activado (Sepabeads EC-HA) con una productividad inicial de 218 g_{FOS} L^{-1} día $^{-1}$.

Se evaluó la capacidad de pXd-INV para fructosilar compuestos fenólicos. Se encontraron dos aceptores positivos: hidroxitirosol (HT) e hidroquinona (HQ). Se optimizó la producción de fructósidos del HT, obteniendo hasta 11.7 g/L. El mecanismo y la selectividad de la reacción, y las características moleculares que determinan si un compuesto fenólico actúa como aceptor o inhibidor, se estudiaron mediante cristalografía.

La síntesis de XOS ácidos se llevó a cabo con la enzima comercial Depol 670L. La hidrólisis del xilano produjo una mezcla de XOS neutros y ácidos. Los XOS ácidos se separaron mediante cromatografía de intercambio aniónico y el producto principal fue caracterizado químicamente e identificado como 2'-O-α-(4-O-metil-α-D-glucuronosil)-xilobiosa (X2_MeGlcA). Se analizó la actividad antioxidante del producto obtenido, comparando con XOS neutros y xilano. Tanto X2_MeGlcA como el xilano mostraron un efecto antioxidante sobre el radical ABTS.

Además, se desarrolló una metodología integrada para la producción enzimática y caracterización de varias mezclas de COS. Se empleó una preparación proteolítica (Neutrase 0.8L) y una quitinasa de *Trichoderma harzanium* (CHIT 42) para la hidrólisis de quitosanos con diferentes grados de desacetilación y peso molecular. Así, se sintetizaron varias mezclas de COS basadas en: (1) COS totalmente desacetilados (fdCOS); (2) COS parcialmente acetilados (paCOS); (3) mezclas de fdCOS y paCOS.

INTRODUCTION

1.1 Bioactive oligosaccharides

Carbohydrates are complex compounds that play an essential role in life, being the main source and storage of energy for most organisms. In addition, they are structural polymers (cellulose or chitin), form glycoconjugates (like glycolipids or glycoproteins), and play key roles in several biological functions such as cell recognition and adhesion, signal transduction, carcinogenesis and immunity (Varki, 2017). Carbohydrates can be classified by their degree of polymerization (DP) into monosaccharides, oligosaccharides or polysaccharides as determined by IUB-IUPAC terminology (IUB-IUPAC, 1982).

Oligosaccharides are defined as molecules containing a small number (2-10) of monosaccharide residues, connected by glycosidic linkages (IUB-IUPAC, 1982). They are widespread in nature, having animal, plant or microbial origin, and they are very diverse and complex molecules due to their linear and branched structures, different monomeric compositions, glycosidic linkages and degrees of polymerization.

Besides having crucial roles in biological processes (Varki, 1993), some oligosaccharides exert extra-nutritional beneficial effects in human health, receiving the name of bioactive oligosaccharides (Aluko, 2012, Hayes and Tiwari, 2015). Bioactive compounds were previously defined as essential and non-essential molecules that occur in nature, are part of the food chain, and have a positive effect in human health (Biesalski et al., 2009). Bioactive oligosaccharides have certain structural features, including non-digestible glycosidic bonds and/or non-sugar modifications (acetylation, sulfation) that enable their use beyond merely nutritional purposes.

Table1.1 summarizes some of the bioactivities of several oligosaccharides with different origins and structures and shows the considerable variety in structure and activity of oligosaccharides. Modified oligosaccharides (sulfated or acetylated sugars) seem to have a wider spectrum of activities such as antioxidant, antimicrobial or antiviral.

Table 1.1 Bioactivities of oligosaccharides and oligosaccharides derivatives.

Type of carbohydrate	Name	Bioactivities	References
Aminoglycan	**Chitooligosaccharides (COS)**	Antibacterial	(Wu et al., 2013a)
		Anticoagulant	(Kim and Rajapakse, 2005)
		Antihypertensive	(Park et al., 2003b)
		Anti-inflammatory	(Azuma et al., 2015)
		Antioxidant	(Li et al., 2012)
		Antitumor	(Huang et al., 2006)
		Antiviral	(Artan et al., 2010)
		Immuno-stimulatory	(Azuma et al., 2015)
		Neuroprotective	(Huang et al., 2015)
		Prebiotic	(Mateos-Aparicio et al., 2016)
Fructan	**Fructooligosaccharides (FOS)**	Prebiotic	(Sabater-Molina et al., 2009)
Galactan	**Galactooligosaccharide (GOS)**	Prebiotic	(Rodriguez-Colinas et al., 2013)
Hemicellulose	**Xylooligosaccharides (XOS)**	Prebiotic	(Vazquez et al., 2001)
	Arabino-XOS	Prebiotic	(Eeckhaut et al., 2008)
	Acidic-XOS	Antibacterial	(Christakopoulos et al., 2003)
		Anti-inflammatory	(Yoshino et al., 2006a)
		Antioxidant	(Valls et al., 2018)
	Mannan oligosaccharides (MOS)*	Immuno-modulatory	(Hoving et al., 2018)
		Prebiotic	(Nurhayati et al., 2018)
Starch	**Cyclodextrins**	Prebiotic	(Mussatto and Mancilha, 2007)
	Isomaltulose	Prebiotic	(Mussatto and Mancilha, 2007)
	Gentiooligosaccharides	Prebiotic	(Mussatto and Mancilha, 2007)
	Isomaltooligosaccharides (IMOS)	Prebiotic	(Kaneko et al., 1994)

Sulfated sugar	**Agar oligosaccharides (AGOS)**	Antioxidant	(Xu et al., 2018)
		Prebiotic	(Li et al., 2014)
		Anti-cancer	(Higashimura et al., 2016)
		Anti-inflammatory	(Zou et al., 2019)
	Carragenan oligosaccharides	Antioxidant	(Sun et al., 2015)
		Antiviral	(Wang et al., 2011)
		Immuno-modulatory	(Yao et al., 2014)
		Prebiotic	(Li et al., 2017)
	Fucooligosaccharides	Anticoagulant	(Kim et al., 2010)
		Antitumor	(Kasai et al., 2015)
Raffinose	**Raffinose**	Prebiotic	(Mussatto and Mancilha, 2007)
	Soybean oligosaccharides (SOS)	Prebiotic	(Espinosa-Martos and Ruperez,2006)
β-glucan	**Laminarin oligosaccharides**	Immuno-stimulatory	(Kim et al., 2006)
	Curdlan oligosaccharides	Immuno-stimulatory	(Tang et al., 2019)
		Prebiotic	(Shi et al., 2018)
Uronic acid	**Alginate oligosaccharides (AOS)**	Antibacterial	(An et al., 2009)
		Antioxidant	(Falkeborg et al., 2014)
		Antitumor	(Chen et al., 2017)
		Immuno-stimulatory	(Wang et al., 2014)
		Neuroprotective	(Tusi et al., 2011)
		Prebiotic	(Wang et al., 2006)
Galacturonan	**Pectic oligosaccharides (POS)**	Prebiotic	(Gómez et al., 2014)

*Mannan can have plant or microbial (yeast) origin.

1.2 Bioactive glycoconjugates. Glycosylation

Glycoconjugates are very complex and diverse compounds consisting of carbohydrates covalently linked to non-sugar molecules, mainly proteins, peptides and lipids (Sharon, 1986). They are ubiquitous in nature and have a fundamental role in almost every biological process including development, differentiation, fertilization, inflammation and metastasis (Hart, 2003).

Glycosylation of small bioactive molecules, such as aliphatic and aromatic alcohols, alkaloids, antibiotics, polyphenols, hormones or terpenoids, modifies their physico-chemical and biological properties, enabling the production of new glycoconjugates that may have enhanced solubility, stability, bioavailability or bioactivity (Thuan and Sohng, 2013). Thus, the transfer of a glycosyl moiety can be employed for several applications (Desmet et al., 2012).

Considering this, efficient glycosylation methodologies are very interesting at both laboratory and industrial scale. Glycosylation can be achieved by chemical and enzymatic procedures, being enzymatic synthesis the most desirable due to its high eco-efficiency. Enzymatic glycosylation can be carried out by different types of carbohydrate active enzymes (CAZymes) (**Figure 1.1**).

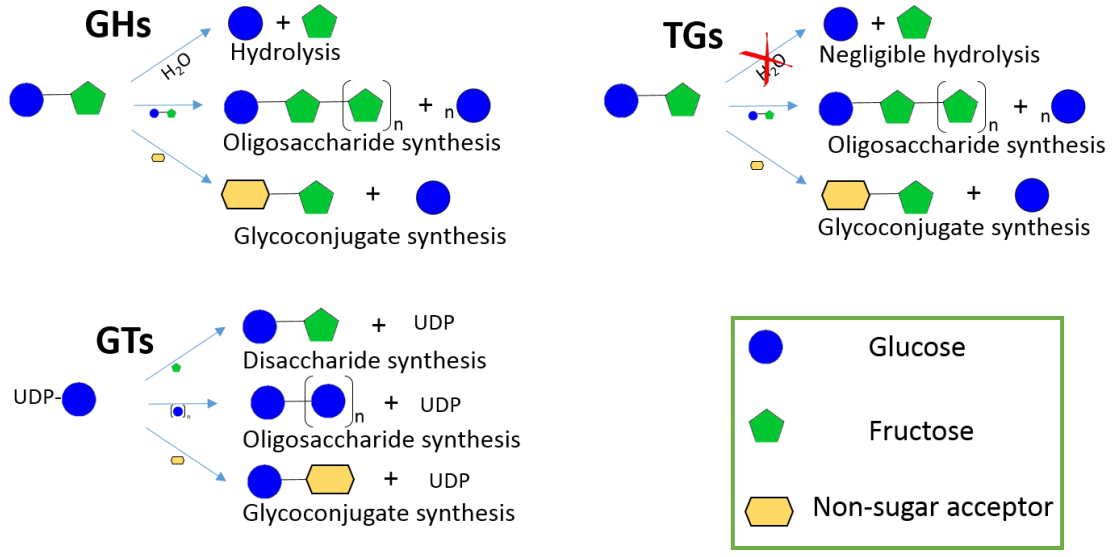

Figure 1.1 Schematic representation of enzymatic glycosylation with GHs, GTs and TGs.

1.3 Glycosidic enzymes

Among all of the biomolecules, the synthesis of oligosaccharides, glycosides or glycoconjugates is the most challenging due to the complexity and diversity of carbohydrates (Schmaltz et al., 2011). These compounds can be assembled by conventional chemical methods or enzymatic processes. However, chemical synthesis suffers from several drawbacks, including necessary protection-deprotection and purification steps, resulting in an inefficient and time-consuming process (Wen et al., 2018). Also, the use of toxic catalysts or solvents, extreme reaction conditions and the production of large amounts of waste makes chemical synthesis an environmentally irresponsible process (Desmet et al., 2012). On the other hand, enzymatic methods are stereo- and regioselective, occur in mild conditions (temperature, pH) and do not produce toxic byproducts, enabling a more efficient and eco-friendly procedure (de Roode et al., 2003).

For these reasons, the use of enzymes for oligosaccharide, glycoside or glycoconjugate synthesis has aroused great interest. The biocatalysts involved in sugar synthesis, disruption or modification receive the name of carbohydrate active enzymes (CAZymes) and are classified in the Carbohydrate Active Enzymes database (CAZy, www.cazy.org), according to their amino acid sequence similarities. At the moment, CAZy contains five classes of enzymes: glycoside hydrolases (GHs), glycosyltransferases (GTs), polysaccharide lyases (PLs), carbohydrate esterases (CEs) and enzymes that have auxiliary activities (AAs) (Drula et al., 2013).

The synthesis of oligosaccharides, glycosides and glycoconjugates can be accomplished using glycosyltransferases (EC 2.4.1.-) and glycosyl hydrolases or glycosidases (EC 3.2.1.-) (Hg Crout and Vic, 1998)(**Figure 1.1**).

GTs carry out the majority of transglycosylation reactions in nature but their use in glycochemistry is often hampered by the need of expensive nucleotide sugar donors and a challenging heterologous production (Lairson et al., 2008)

Glycosidases or glycosyl hydrolases are a widespread and diverse group of enzymes which catalyze the cleavage of glycosidic bonds (Davies and Henrissat, 1995). Also, they are one of the most efficient enzymes with enhancement rates around 10^{17}-fold (Rye and Withers, 2000) and one of the most abundant with 156

families currently registered in CAZy. GHs classification can also be based on the anomeric configuration of the reaction product or the position where they act in the substrate. Based on the first criteria, glycosidases are divided in retaining glycosidases that release products with the same anomeric configuration as the substrate and inverting glycosidases, which generate products with the opposite configuration in the anomeric carbon. According to the latter criteria, two kinds are distinguished: endo-glycosidases that cleave between internal residues in a glycosidic chain and exo-glycosidases that cut single residues at the non-reducing end of the chain (Bojarová and Kren, 2009).

In comparison with glycosyltransferases, glycosidases present various advantages, including a wide range of substrates, the use of simple sugar donors and their usual robustness. However, their utilization is also hindered since their transglycosylating activity is subordinated to their hydrolytic activity and regioselectivity is not always achieved (Bissaro et al., 2015). A rare kind of GHs called tranglycosydases (TGs) are able to catalyze the formation of glycosidic bonds with negligible hydrolysis (Bissaro et al., 2015), which makes them ideal biocatalysts for transglycosylation reactions (**Figure 1.1**). Examples of transglycosidases are levansucrases, inulosucrases or cyclodextrin glucanotransferases.

This Thesis is focused on the enzymatic synthesis of neofructooligosaccharides (neo-FOS), hydroxytyrosol fructosides, acidic xylooligosaccharides (acidic-XOS) and chitooligosaccharides (COS). In all cases the enzymes employed belong to the family of glycosidases. Their enzymatic production and bioactivity are discussed in detail.

1.4 Neo-fructooligosaccharides production

Fructooligosaccharides (FOS) are fructose oligomers linked to a sucrose skeleton by different glycosidic bonds. Depending on the nature of these linkages, FOS can be sorted in: inulin-FOS (^{1}F-FOS) with fructose monomers linked by $\beta(2\rightarrow1)$ bonds, levan-FOS (^{6}F-FOS) with $\beta(2\rightarrow6)$ linkages between fructoses, neo-FOS (^{6}G-FOS) with a $\beta(2\rightarrow6)$ bond between the glucose moiety of sucrose and fructose, and mixed FOS with both kinds of linkages (**Figure 1.2)**. FOS are present in many plants (onion, chicory, tomatoes, asparagus, etc.) as energy reserves (Roberfroid, 1993) and have prebiotic properties, promoting the development of beneficial species such as *Bifidobacterium* and *Lactobacillus* in the gastrointestinal tract (Gibson et

al., 2007). Besides their prebiotic activity, FOS can exert other beneficial activities such as improving mineral absorption (Ca^{2+}, Mg^{2+}), reducing cholesterol levels and helping to prevent colon cancer (Singh et al., 2017, Hidaka et al., 1986). In addition, FOS are water soluble, non-caloric and have a sweet taste, which makes them an interesting ingredient for functional foods. FOS have been extensively studied and are being commercialized under several brands, including Neosugar®, NutraFlora®, Meioligo®, and Actilight® (Bali et al., 2015).

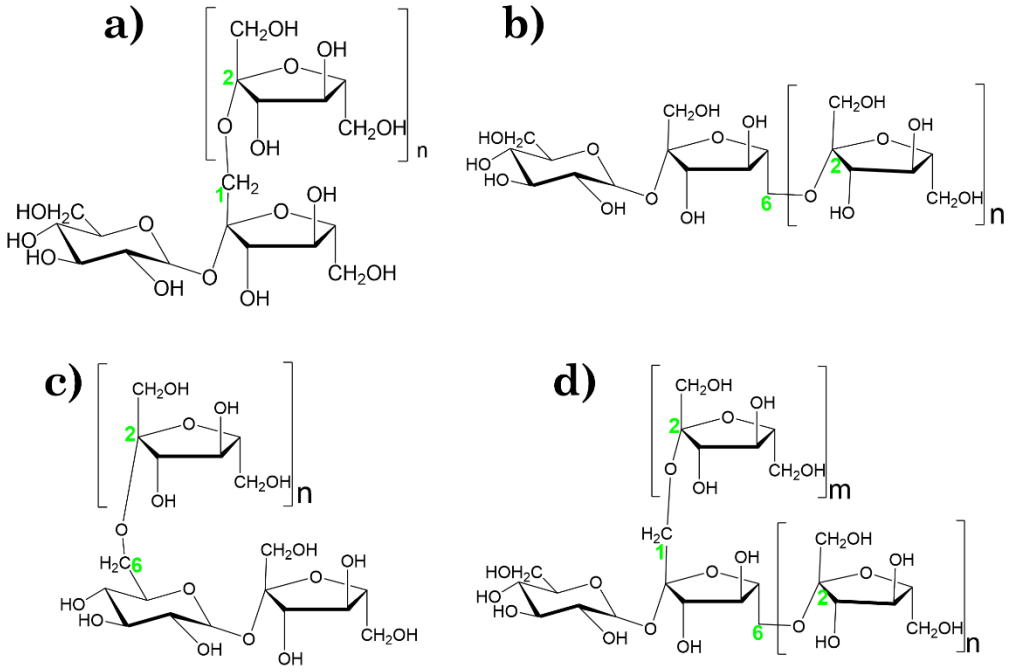

Figure 1.2 Fructooligosaccharides structure. a) Inulin-type FOS. b) Levan-type FOS. c) Neo-FOS. d) Mixed-FOS.

Inulin-type FOS are linear FOS with $\beta(2\rightarrow1)$ bonds between fructoses, being 1-kestose the smallest member of the inulin series. They can be produced by hydrolysis of inulin –easily extracted from plants (e.g. chicory)– using inulinases (EC 3.2.1.7) or by sucrose transfructosylation employing fungal (generally from *Aspergillus* strains) sucrose fructosyltransferases (EC 2.4.1.99) and β-fructofuranosidases (EC 3.2.1.26). They are the most explored and commercialized kind of FOS.

Levan-type FOS are formed by $\beta(2\rightarrow6)$ linkages and the shorter constituent is 6-kestose. As inulin-type FOS, they can be synthesized by hydrolysis of levan or by transfructosylation of sucrose utilizing levansucrases (EC 2.4.1.10) (Santos-Moriano et al., 2015). However, levan hydrolysis by levanases (EC 3.2.1.65) is inefficient due

to the inexistence of a cost-effective source of levan. Additionally, levansucrases mainly yield 6-kestose and FOS of the same series, but they can also produce other FOS like 1-kestose and neokestose, or show levanase activity (Zambelli et al., 2014, Jang et al., 2006). For these reasons, production of pure levan-type FOS is complicated and their industrial application has not been achieved.

Neo-FOS are fructooligosaccharides with $\beta(2\rightarrow6)$ bonds, but unlike in levan-type FOS, the first fructose is linked to the glucose moiety of sucrose. Several studies suggest that neo-FOS could display better physico-chemical and prebiotic properties than commercialized inulin-type FOS (Kilian et al., 2002, Lim et al., 2007). Their improved stability to temperature and pH, and their enhanced prebiotic properties make them promising ingredients for the functional food industry. However, neo-FOS are only produced by a few microbial β-fructofuranosidases and levansucrases, and in the last case, they are secondary products (Bekers et al., 2002). The production of neo-FOS using purified enzymes or whole cells is summarized in **Table 1.2**. Despite achieving the heterologous overproduction of some enzymes, the largest yield of neo-FOS reported was obtained with free whole cells (Ning et al., 2010) and their industrial application has not been accomplished.

Table 1.2 Production of neo-FOS employing microbial enzymes or microorganisms.

Microorganism	Biocatalyst	Yield (g/L)	Reference
Penicillium citrinum	Whole cell (immobilized)	49.4	(Park et al., 2005)
	Whole cell + fructosyltransferase (immobilized)	108.4	(Lim et al., 2007)
Penicillium oxalicum	β-fructofuranosidase	94.2	(Xu et al., 2015)
Xanthophyllomyces dendrorhous	Whole free cells	238	(Ning et al., 2010)
X. dendrorhous	Whole free cells	124	(Sheu et al., 2013)
X. dendrorhous	β-fructofuranosidase (Xd-INV)	168	(Linde et al., 2012)
X. dendrorhous	β-fructofuranosidase intracellular	73.9	(Chen et al., 2011)

Mixed FOS have $\beta(2\rightarrow1)$ and $\beta(2\rightarrow6)$ linkages and are mainly found in plants. They can be branched inulins or branched levans and their smaller representative is bifurcose. Agave is rich in branched fructans and its hydrolysis produces a complex mixture of FOS that is commercialized by Nekutli®.

1.5 Fructosylation of polyphenols. Glycosylation of hydroxytyrosol

Phenolic compounds are one of the most numerous, diverse and widely distributed (plant kingdom) group of molecules found in nature. They are characterized by the presence of phenolic structural features and have many biological activities, including antioxidant, anti-bacterial, cardio-protective or neuroprotective (Handique and Baruah 2002, Singh et al., 2008). Polyphenols can be classified according to their chemical structures into: phenolic acids, flavonoids, polyphenolic amides and other polyphenols. Also, phenolic compounds often occur in nature as glycosides and glycoconjugates (Tsao, 2010). As previously mentioned, glycosylation can improve the biological activities of polyphenols (Nadim et al., 2014) and, therefore, provide access to a larger number of compounds with medicinal and industrial value.

In particular, fructosylation has been previously investigated as a way to enhance the properties of several phenolic compounds (Herrera-González et al., 2017). **Table 1.3** compiles the polyphenol fructosides that have been synthesized using microbial enzymes. Interestingly, while there are many reports on glycosylated derivatives of polyphenols, only a few of them deal with fructosylation.

As shown, β-fructofuranosidases and levansucrases are the most employed enzymes for the fructosylation of phenolic compounds. Nevertheless, an inulosucrase and the residual activity (β-fructofuranosidase) of a commercial β-galactosidase have been used successfully for transfructosylation.

Table 1.3 Fructosylation of phenolic compounds by microbial enzymes.

Enzyme	Enzyme source	Polyphenol	References
Levansucrase	*Leuconostoc mesenteroides*	Hydroquinone	(Kang et al., 2009)
Inulosucrase	*Leuconostoc citreum*	Hydroquinone	(Mena-Arizmendi et al., 2011)
Levansucrase	*Bacillus subtilis*	Catechol	(Mena-Arizmendi et al., 2011)
		Hydroquinone	
		Methyl-hydroquinone	
		Resorcinol	
β-fructofuranosidase	*Arthrobacter nicotianae XM6*	Purearin	(Wu et al., 2013a)
β-fructofuranosidase	*Arthrobacter arilaitensis NJEM01*	Mangiferin	(Wu et al., 2013c)
		Purearin	
		Vitexin	
Lactozym 3000L	*Kluyveromyces lactis*	Tyrosol	(Potocka et al., 2015)
		Hydroxytyrosol	
Levansucrase	*Gluconacetobacter diazotrophicus*	Caffeic acid	(Nuñez-López et al., 2019)
		Catechin	
		Coniferyl alcohol	
		Ferulic acid	
		Mangiferin	
		Purearin	
		Resveratrol	
		Rosmarinic acid	
		Vanillin	

Olive oil is a functional food, which besides a high concentration of monounsaturated fatty acids, also contains several polyphenols (de la Torre, 2008). Phenolic compounds in olive oil can be classified in simple phenols (tyrosol, hydroxytyrosol, etc.), polyphenols (flavonoids), secoiridoids (oleuropein) and lignans (Boskou, 2006). Hydroxytyrosol (2-(3,4-dihydroxyphenyl)-ethanol) is one of the main components of olive oil, olive leafs and olives. Hydroxytyrosol (HT) can also be found in red and white wines, but always in lower quantities than in olives or olive oil (Robles-Almazan et al., 2018). Among olive oil polyphenols, HT (2-(3,4-dihydroxyphenyl)-ethanol) has the highest *in vitro* antioxidant activity (Visioli et al., 1998). In addition, hydroxytyrosol possesses strong anti-inflammatory, neuroprotective, anti-tumoral and cardio-protective properties, making HT the only phenolic compound in the market with a European Food Safety Authority health claim (EFSA Panel on Dietetic Products and Allergies, 2011). However, HT displays poor bioavailability, in spite of being well absorbed in the gastrointestinal tract (Miro-Casas et al., 2003). This low bioavailability is caused by a rapid first pass metabolism in both the gut and the liver, which transforms HT into sulfated and glucuronidated metabolites, whose bioactivity is still unclear (Giordano et al., 2015).

Glycosylation has proven to be an effective method for enhancing bioavailability and other properties in phenolic compounds, such as water solubility or stability (Torres et al., 2011, De Winter et al., 2015, González-Alfonso et al., 2018).

Hydroxytyrosol glycosylation has been barely studied, and only by enzymatic procedures. Trincone et al. were the first to report the α-glucosylation of HT employing an α-glucosidase from *Aplysia fasciata* (Trincone et al., 2012). The *β*-xylosylation was accomplished using a fungal *β*-xylosidase (Nieto-Domínguez et al., 2017) and the *β*-fructosylation was achieved by Potocka et al. utilizing the residual *β*-fructofuranosidase activity of a commercial lactase (Potocka et al., 2019).

1.6 Production of acidic XOS

Hemicellulose is the second most abundant crop waste, only after cellulose, and therefore one of the most significant resources of the biosphere. The hemicellulosic fraction contains an extensive variety of polysaccharides. Among them, xylans are the most abundant due to their presence in almost every green plant and some algi (Ebringerová et al., 2005). Xylans are bioactive polysaccharides that have aroused

great interest for the production of both bioethanol and high value-added compounds, mainly xylooligosaccharides (XOS) (Deutschmann and Dekker, 2012). Xylans are heteropolysaccharides made of a β-1,4-xylopyranose backbone that can be highly branched with other monosaccharides (mainly arabinose), acetyl side-groups, glucuronic acid, methyl-glucuronic acid and ferulic acid (**Figure 1.3**). The degree and composition of these substitutions is strongly determined by the xylan source. Thus, arabinoxylans, mainly found in softwoods and grasses, show arabinose and ferulic acid decorations, while glucuronoxylans, abundant in hardwood species, display a high degree of methylglucuronic substitutions (Ebringerová and Heinze, 2000; Teleman et al., 2002).

As a result of this complexity, the enzymatic hydrolysis of xylan requires the coordinated action of several hydrolases (mainly endoxylanases and β-xylosidases) to accomplish total breakdown. Endo-β-1,4-xylanases (EC 3.2.1.8) are glycosyl hydrolases (GH) that belong to families GH10, GH11 and GH30; they randomly hydrolyze the xylan backbone into XOS (Biely et al., 1997; Kolenová et al., 2006; Linares-Pastén et al., 2018). Then, β-xylosidases can catalyze the breakdown of XOS to achieve complete hydrolysis (Polizeli et al., 2005).

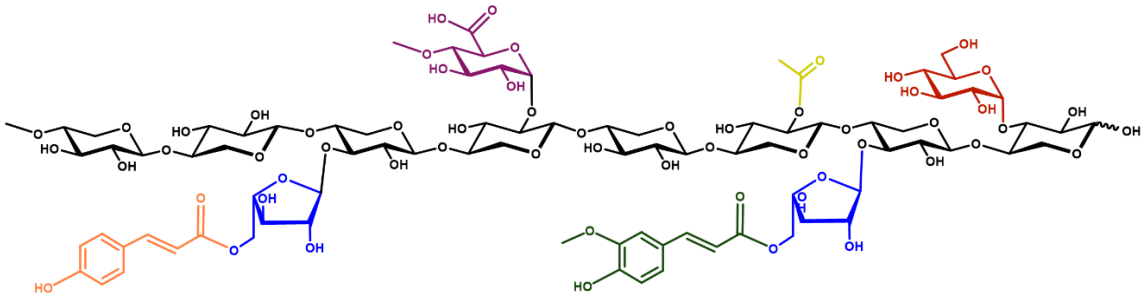

Figure 1.3 General scheme of xylan structure. Violet: 4-O-methyl-α–D-glucuronopyranosyl. Yellow: acetyl. Red: α-D-glucose. Blue-orange: α-L-coumaroyl arabinose Blue-green: α-L-feruloyl arabinose.

XOS are bioactive oligosaccharides composed of 2-10 xylose residues linked by $\beta(1\rightarrow4)$ bonds and different substitutions depending on the endoxylanase employed and the xylan source (Aachary and Prapulla, 2010; Carvalho et al., 2013; Samanta et al., 2015). There is an increasing interest in XOS due to their potential as emerging prebiotics and other health promoting properties, such as antioxidant, antitumorigenic, antiallergic, anti-inflammatory and antimicrobial (Broekaert et al.,

2011; Buruiana et al., 2017; Chung et al., 2007; Gullón et al., 2011; Imaizumi et al., 1991; Scott et al., 2014; Valls et al., 2018). In addition, XOS showed no negative effects on health or undesirable organoleptic properties, which makes them a highly promising food ingredient for functional foods (Courtin et al., 2009).

Acidic xylooligosaccharides or aldouronics (acidic XOS) are hetero-oligomers of xylose with uronic acid (glucuronic or methyl-glucuronic acids) residues randomly linked by α(1→2) bonds. They can be produced by glucuronoxylan hydrolysis using endoxylanases (Ishihara et al., 1997; Ohbuchi et al., 2009; Yamasaki et al., 2012). Several studies have reported the health inducing activities of acidic-XOS, including antibacterial effect (Christakopoulos et al., 2003), antioxidant activity (Valls et al., 2018), inhibitory effect on stress-induced gastric inflammation (Yoshino et al., 2006a), preventive effects on the development of atopic dermatitis-like symptoms and on contact hypersensitivity (Ohbuchi et al., 2010; Yoshino et al., 2006b). Moreover, some investigations have compared the activities of neutral and acidic XOS, concluding that acidic XOS possess stronger bioactivities. Interestingly, these properties are strongly related to the degree of polymerization and uronic acid ramification (Ohbuchi et al., 2010; Valls et al., 2018). These enhanced properties make them interesting ingredients for functional foods. However, the synthesis of pure acidic XOS is challenging since most endoxylanases produce a mixture of neutral and acidic XOS, making chromatographic separation a necessity. In addition, characterization and quantification of acidic XOS is complicated due to the lack of standards. Other techniques like mass spectrometry and NMR allow product identification, but quantification is still not feasible.

1.7 Chitooligosaccharides production

Chitin is a natural aminopolysaccharide composed of N-acetyl-glucosamine residues linked by $\beta(1\rightarrow4)$ bonds. It is the second most abundant polysaccharide in nature, after cellulose, and is mainly found in fungal cell walls and the exoskeletons of arthropods, like crab, shrimp, lobster, cockroach, or fly (Heggset et al., 2010). Approximately 10^{11} tons/year of chitin are produced by living organisms but, despite its widespread distribution, commercial chitin is mainly obtained from shellfish waste. Nevertheless, every year more than 10,000 tons of chitin could be extracted from crab and shrimp shells, providing a convenient and economical raw material

for the production of bioactive and high value-added compounds (Hamed et al., 2016).

Chitosan is a cationic polysaccharide consisting of D-glucosamine (GlcN) and N-acetyl-glucosamine (GlcNAc) moieties with $\beta(1\rightarrow4)$ linkages. It is obtained by complete or partial deacetylation of chitin and, unlike chitin, is rarely found in nature (Liaqat and Eltem, 2018). Chitin and chitosan are differentiated by the degree of acetylation; some studies speak of chitosan when the acetylation degree is less than 30% and chitin when it is higher than 70% (Liaqat and Eltem, 2018), while others employ the term chitosan if the acetylation degree is lower than 50% and chitin on the rest of the cases (Younes and Rinaudo, 2015). Besides being biocompatible, biodegradable and non-toxic, both polysaccharides exhibit very interesting physicochemical and biological properties (Li et al., 2016), including antioxidant, antimicrobial, anticancer and anticoagulant (Hamed et al., 2016). These beneficial properties make chitin and chitosan very interesting for numerous applications in the food, pharmaceutic, cosmetic, agriculture and textile industries (Fernandez and Ingber, 2014, Zou et al., 2016). However, they are both insoluble in aqueous solutions at neutral pH and have high viscosity, which limit their use in many applications, mainly in the food and medicine sectors (Li et al., 2016).

Chitooligosaccharides (COS), the product of chitin or chitosan hydrolysis, are homo- or hetero-oligomers of glucosamine and/or N-acetyl-glucosamine linked by $\beta(1\rightarrow4)$ bonds. They also show a wide range of biological activities (**Table 1.1**) but, unlike chitin and chitosan, they are water soluble and notably less viscous due to shorter chain lengths and free amino groups (Bahrke, 2007). COS can be obtained by physical, chemical or enzymatic degradation of chitin or chitosan (Lodhi et al., 2014). According to their degree of acetylation or deacetylation, COS can be classified in three groups: fully acetylated COS (faCOS), partially acetylated COS (paCOS) and fully deacetylated COS (fdCOS) (**Figure 1.4**). Enzymatic methodologies for COS production possess several advantages over other methods, including the use of milder conditions, more control over the final product and better reproducibility (Muanprasat and Chatsudthipong, 2017). COS enzymatic synthesis can be carried out by specific enzymes such as chitinases (EC 3.2.1.14) and chitosanases (3.2.1.132) or non-specific enzymes like proteases, pectinases, cellulases, and lipases (Pantaleone et al., 1992, Santos-Moriano et al., 2018a).

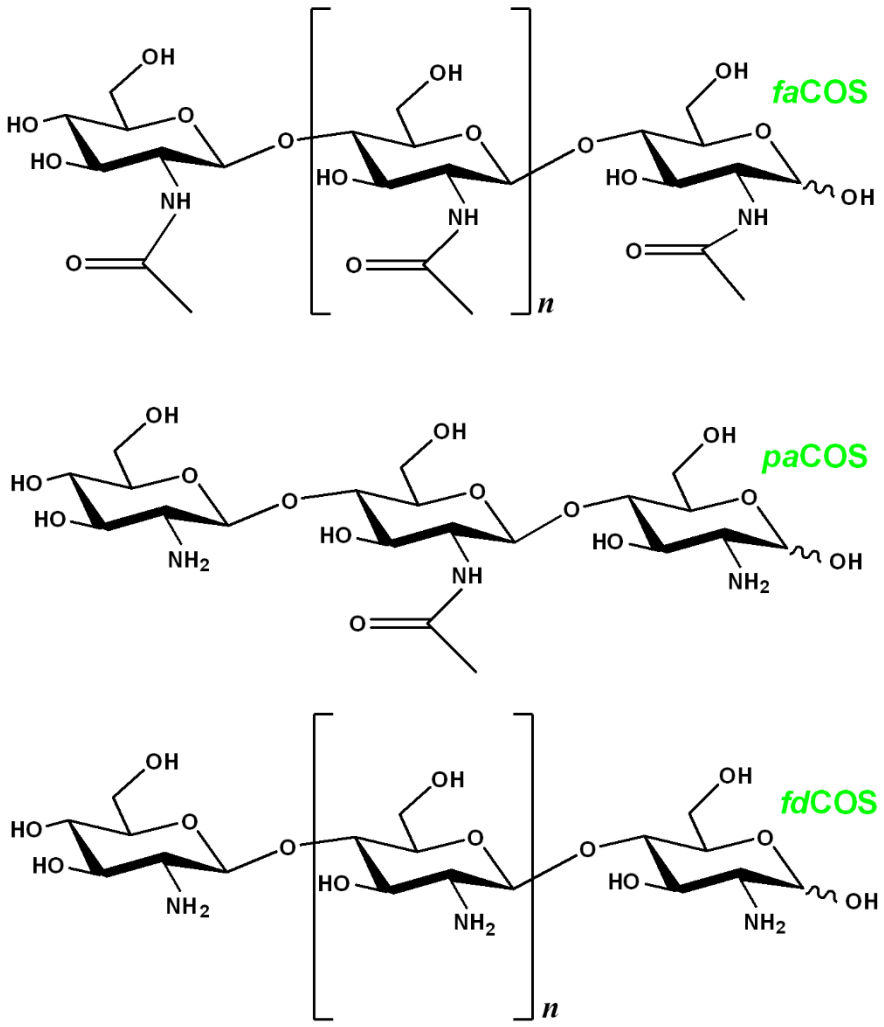

Figure 1.4 Structure of the three main types of chitooligosaccharides (COS): fully acetylated (faCOS), partially acetylated (paCOS) and fully deacetylated (fdCOS).

Chitosanases specifically endo-hydrolyze chitosan cleaving GlcN-GlcN bonds. However, some subclasses are also able to hydrolyze GlcN-GlcNAc or GlcNAc-GlcN linkages. Chitinases specifically cleave linkages between GlcNAc moieties at internal or terminal positions, but can also hydrolyze GlcN and GlcNAc bonds. This explains why chitinases can be active on chitosan and chitosanases on chitin, since chitosan is rarely 100% deacetylated and natural chitin is about 90% acetylated (Kim and Rajapakse, 2005). According to CAZy, chitosanases belong to families GH5, GH8, GH46, GH72 and GH80 (Hoell et al., 2010), whilst chitinases have been categorized into families GH18 and GH19 (Hamid et al., 2013).

The chitosanolytic activity of some unspecific enzymes such as cellulases, pectinases or lysozyme could be explained by the structural similarity between their

natural substrates and chitosan (Xia et al., 2008). However, in the case of several commercial enzymes like proteases, lipases or amylases, this activity is probably due to the presence of another contaminant enzyme (Aam et al., 2010). Nevertheless, commercial enzymes exhibit several advantages including availability, lower cost and approval for food and pharmaceutical applications (Kittur et al., 2003).

COS produced by enzymatic hydrolysis are usually complex mixtures of oligomers with different degree of polymerization, degree of deacetylation and pattern of acetylation, which depend on the source of chitosan/chitin, the specifity of the enzyme and the conditions employed (Muanprasat and Chatsudthipong, 2017, Santos-Moriano et al., 2018b). In addition, their biological activities are strongly affected by these parameters, which makes COS separation and characterization essential for the evaluation of these bioactivities, and consequently, their industrial application (Liaqat and Eltem, 2018).

The characterization of COS mixtures is still a great challenge in COS synthesis, mainly due to the lack of standards, especially for partially acetylated COS (paCOS). Various methods have been used for COS separation including size exclusion chromatography (Song et al., 2014), metal affinity chromatography (Le Devedec et al., 2008), absorption chromatography with charcoal columns (Semenuk et al., 2001), anion-exchange chromatography with pulsed amperometric detection (Cao et al., 2016 Kidibule et al., 2018) and hydrophilic interaction chromatography (Li et al., 2012). In addition, Mass spectrometry (MS) and NMR techniques have shown great potential for COS characterization (Santos-Moriano et al., 2016, Mahata et al., 2014).

1.8 Enzyme immobilization

Biocatalysis is based on the use of enzymes, which are biodegradable, biocompatible and renewable catalysts that work under mild conditions with high activity and selectivity, yielding several chemicals and commodities. Thus, biocatalysis is significantly more environmentally friendly and cost-effective than traditional chemical synthesis. However, industrial application of enzymatic procedures is frequently hampered by insufficient operational stability and arduous enzyme recovery and re-use (Sheldon, 2007).

Enzyme immobilization is a powerful tool that can overcome these drawbacks, and favor the design of industrial-scale biocatalytic procedures for the production of many compounds, including bioactive oligosaccharides or glycoconjugates. Immobilized enzymes are defined as enzymes physically confined or localized in a certain region of space with retention of their activity, and which can be used repeatedly and continuously (Katchalski-Katzir and Kraemer, 2000). An effective immobilization strategy allows an easy recovery and reutilization of the biocatalyst, facilitates product separation and enhances resistance towards inactivation by different agents (pH, temperature, organic solvents or inhibitors). The selection and optimization of an immobilization protocol (support and immobilization conditions) is always challenging since they are developed mostly on empirical basis and no rules for each type of enzyme have been established (Torres-Salas et al., 2011). A micro-scale procedure was developed by our group aiming to facilitate the screening of multiple immobilization conditions and minimize enzyme, carrier and reagent consumption (Fernández-Arrojo et al., 2015).

Despite the huge amount of publications in this field, enzyme immobilization methodologies can be classified into three categories: binding to a carrier, entrapment and crosslinking (Sheldon and van Pelt, 2013). They are represented in **Figure 1.5**.

The binding to carriers involves the attachment of the enzyme to a solid support. According to the nature of the interaction between enzyme and material, covalent and non-covalent binding can be differentiated. Non-covalent binding can be physical by unspecific forces (hydrophobic and Van de Waals interactions) or ionic. Usually both types are too weak for industrial conditions, although in some cases a satisfactory operational stability has been achieved (Rodrigues et al., 2019). On the other hand, covalent binding forms a tight union between enzyme and support that generally prevents enzyme leakage. A great variety of materials is available for enzyme binding, including polysaccharides (agarose), organic polymers (polymethacrylate, polyacrylamide) an inorganic materials (silica, diatomaceous earth). All of them can be chemically activated with reactive groups (glyoxal, epoxy, ethylenediamino, hexamethylenediamino, etc.).

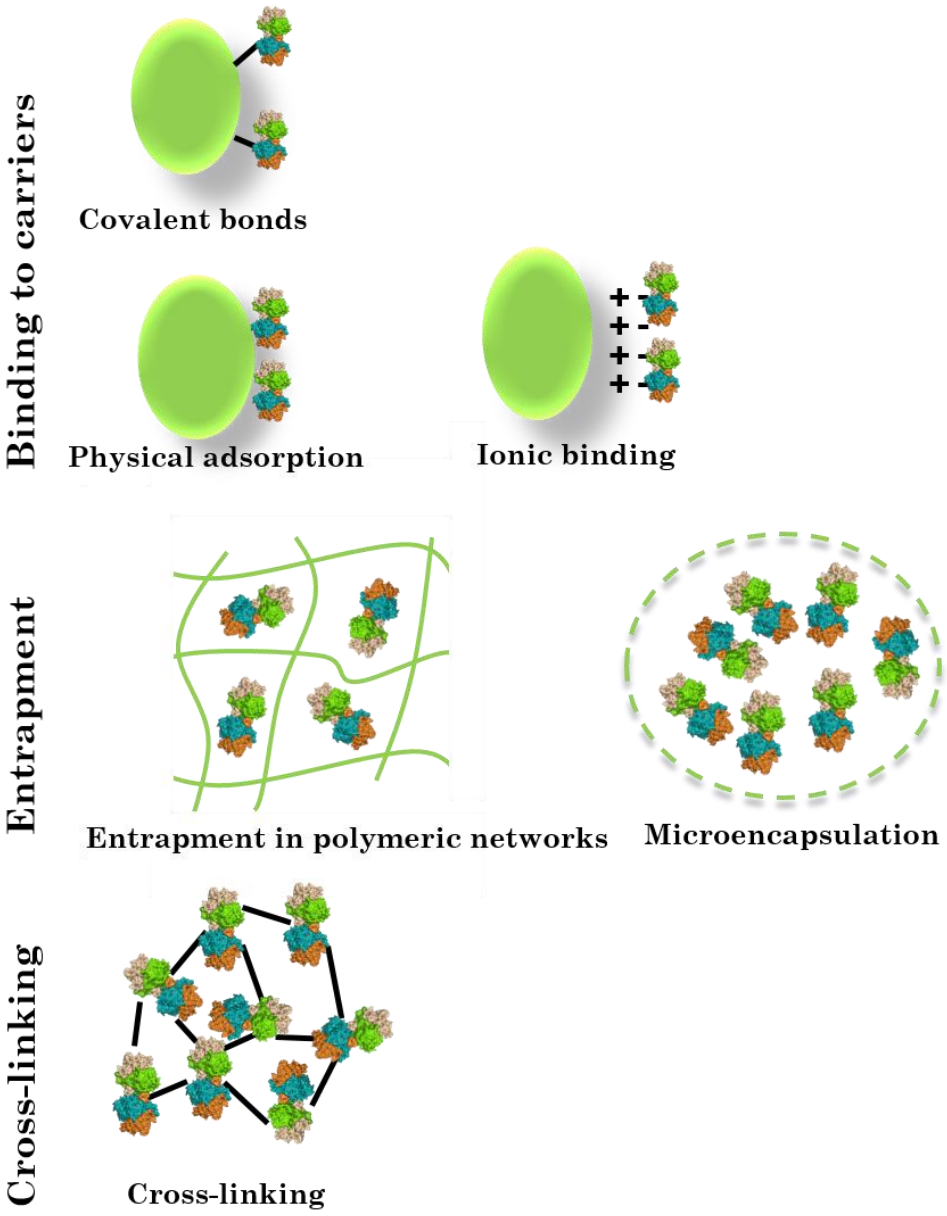

Figure 1.5 Scheme of enzyme immobilization methodologies.

Entrapment involves the inclusion of the enzyme in polymeric networks (polyvinyl-alcohol, alginate, polyacrylamide, etc.) or the micro-encapsulation in semipermeable membranes. Generally, this physical restraint cannot prevent enzyme leakage and is often combined with cross-linking techniques.

Cross-linking is based on the formation of covalent bonds between enzyme molecules without employing a carrier. The preparation of cross-linked enzyme crystals (CLECs) and cross-linked enzyme aggregates (CLEAs) requires the utilization of bifunctional reagents like glutaraldehyde, dextran polyaldehyde or

galactose dialdehyde. In particular, CLEAS have attracted great interest because they offer several advantages, including highly concentrated activity, high stability and low production costs due to the elimination of a probably expensive carrier (Sheldon et al., 2005).

OBJECTIVES

Nowadays, there is a growing demand for healthier foods, which increases the need for new bioactive compounds, such as oligosaccharides or glycoconjugates. Specifically, bioactive molecules obtained from renewable and natural sources have aroused great interest. In addition, a considerable effort should be made for the scale-up preparation, characterization and purification of complex oligosaccharides mixtures and glycoconjugates to further the understanding of their properties, and enable their application in the food, cosmetic or pharmaceutical industries.

The main objectives of this Thesis are:

- Immobilization of the *β*-fructofuranosidase from *Xanthophyllomyces dendrorhous* (pXd-INV) for the production of neo-fructooligosaccharides, new prebiotics with enhanced physico-chemical and biological properties.
- Evaluate the enzymatic fructosylation of hydroxytyrosol employing the enzyme pXd-INV and correlate the experimental results with the structural information.
- Design a methodology for the production and purification of acidic xylooligosaccharides, xylooligosaccharides decorated with uronic acid ramifications that had previously shown improved antioxidant, antimicrobial or anti-inflammatory activity.
- Development of a procedure for the large-scale production of several COS types, as well as their chemical characterization.

MATERIALS AND METHODS

3.1 Materials

3.1.1 Enzymes

The *β*-fructofuranosidase from *Xanthophyllomyces dendrorhous,* expressed in *Pichia pastoris* (pXd-INV), its mutagenic variants W105F, Q341S and N342Q, and chitinase CHIT42 from *Trichoderma harzianum* were produced and kindly provided by the laboratory of Dr. María Fernández Lobato (Centro de Biología Molecular Severo Ochoa, UAM-CSIC, Madrid, Spain).

Depol™ 670L (D670L), a blend of fungal enzymes, was purchased from Biocatalysts Ltd. (Chicago, IL, USA). Neutrase 0.8L, a preparation of neutral proteases from *Bacillus amyloliquefaciens,* was donated by Novozymes (Bagsvaerd, Denmark).

3.1.2 Reagents

Glucose, D-glucosamine (GlcN), N-acetyl-glucosamine (GlcNAc), 2,2'-azino-bis(3-ethylbenzothiazoline-6-sulphonic acid) (ABTS), polyvinyl alcohol (PVA) (99% hydrolyzed, average MW 130,000), *p*-nitrophenol, catechol, and bovine serum albumin (BSA) were purchased from Sigma-Aldrich (St. Louis, MO, USA). 1-Kestose, nystose and xylobiose were from TCI Europe (Zwijndrecht, Belgium). Fructose and xylose were from Merck (Darmstadt, Germany). Sucrose was from Panreac (Madrid, Spain). Beechwood xylan and XOS with DP from 3 to 6 were purchased from Megazyme (Wicklow, Ireland). Hydroquinone and Trolox were from Acros Organics (Geel, Belgium) and Fluka™ (Waltham, MA, USA), respectively. Hydroxytyrosol was acquired from Seprox (Murcia, Spain) and epigallocatequin gallate (EGCG) was purchased from Zhejiang Yixin Pharmaceutical Co. Ltd. (Zhejiang, China). Fully acetylated and deacetylated COS with degrees of polymerization from 2 to 4 and 2 to 5, respectively, were from Carbosynth Ltd. (Berkshire, UK). Chitosans QS1 and CHIT600 were purchased from InFiQuS (Madrid, Spain) and Acros Organics (Geel, Belgium), respectively; and chitosans CHIT1 and CHIT2 were kindly donated by Anfaco-Cecopesca (Vigo, Spain) (**Table 3.1**). XOS standard mixture was from Wako Pure Chemical Industries Ltd. (Osaka, Japan) and COS standard (MW ≤ 2000, DD ≥ 90%) was from Qingdao BZ Oligo Biotech Co. Ltd. (China). Neokestose, 6-kestose, neonystose and blastose were synthetized as described in previous works (Alvaro-

Benito et al., 2007, Linde et al., 2012, Zambelli et al., 2014). All other reagents and solvents were of the highest purity available.

Dialysis membranes MWCO 0.1-0.5 kDa and 3.5 kDa were from VWR (Radnor, PA, USA) and Sep-Pak Accell Plus QMA Plus Short Cartridges (360 mg and 37-55 μm particle size) were purchased from Waters (Milford, MA, USA).

Table 3.1 Chitosans used in this Thesis.

Chitosan	MM (kDa)	DD	Supplier
QS1	98	81%	InFiQus
CHIT600	600-800	≥ 90%	Acros Organics
CHIT1	4	94.7%	Anfaco-Cecopesca
CHIT2	56	79.4%	Anfaco-Cecopesca

3.1.3 Immobilization carriers

Sepabeads® FP-Series EC-EA and EC-HA (spherical, 150-300 μm diameter, 0.8 $meq_{ethylene\ or\ hexamethylenediamino}\ mL_{gel}^{-1}$ minimum) were kindly donated by Resindion S. R. L. (Binasco, MI, Italy).

3.1.4 Buffer solutions

The buffer solutions used in this Thesis are listed in **Table 3.2**.

Table 3.2 Buffer solutions employed in this Thesis.

Buffer	Salt	Concentration	pH
pXd-INV reaction buffer	Sodium acetate	100 mM	5.0
Neutrase and CHIT42 reaction buffer	Sodium acetate	250 mM	5.0
Depol 670L reaction buffer	Sodium acetate	10 mM	4.6
PVA immobilization buffer	Sodium acetate	100 mM	5.0
Sepabeads EC-EA and EC-HA immobilization buffer	Sodium phosphate	300 mM	7.0
XOS separation buffer	Ammonium acetate	10 mM	7.4

3.2 Enzyme characterization

3.2.1 β-Fructofuranosidase activity

The *β*-fructofuranosidase activity was determined using the 3,5-dinitrosalicylic acid (DNS) assay adapted to a 96-well microplate (Ghazi et al., 2007). Briefly, 45 µL of a 100 mg/mL sucrose solution in 100 mM sodium acetate buffer (pH 5.0) and 5 µL of a suitable enzyme dilution were incubated at 60 ºC for 20 min. Then, we added 50 µL of DNS solution and incubated another 20 min at 80 ºC. The quantification of reducing sugars was done with a glucose calibration curve. One unit of activity (U) was defined as that corresponding to the release of one µmol of reducing sugars per minute.

3.2.2 Endoxylanase activity

The endoxylanase activity was also measured by detection of reducing sugars using a modified DNS method. In this case, a 1% (w/v) xylan solution in 10 mM sodium acetate buffer (pH 4.6) and an enzyme solution, conveniently diluted to fit into the xylose calibration curve, were incubated for 30 min at 60 ºC. DNS solution was added and incubated as explained above. One unit of activity (U) also corresponded to the release of one µmol of reducing sugars per minute.

3.2.3 Protein concentration

Protein concentration was determined by the Bradford assay (Bradford, 1976) adapted to 96-well microplates. Bovine serum albumin (BSA) was employed as standard for the calibration curve and samples were measured in triplicate.

3.3 Analytical methods

3.3.1 TLC

Thin Layer Chromatography (TLC) analysis was performed on silica gel plates with fluorescent indicator (Polygram SIL G/UV$_{254}$, Macherey-Nagel, Düren, Germany). Several phenolic compounds were screened by TLC as possible acceptors in transglycosylation reactions with pXd-INV. This was done using a mixture of ethyl acetate and methanol (3:1, v/v) as eluent. Phenolic compounds were observed under UV light (UVP, Upland, CA, USA) and sugars were revealed submerging plates in a general staining solution ($(NH_4)_6Mo_7O_{21}.4H_2O$ + $Ce(SO_4)_2$ in 10% H_2SO_4 in water (v/v)), drying, and then heating for a few minutes.

3.3.2 HPLC

High Performance Chromatography (HPLC) was performed using a quaternary pump (Agilent Technologies model 1100, Santa Clara, CA, USA) coupled to a Waters Spherisorb amino column (4.6 x 250 mm) from Waters (Milford, MA, USA) for the transfructosylation of phenolic compounds (acceptors screening) with pXd-INV, or a Phenomenex Luna-NH2 column (4.6 x 250 mm) from Phenomenex (Terrace, CA, USA) for the production of fructosyl-hydroxytyrosol (Fru-HT) also with pXd-INV. Both columns were kept at 30 ºC and samples were automatically injected with a Hitachi L-2200 autosampler (Hitachi, Tokyo, Japan). Injection volume was 10 µL. Phenolic compounds were analyzed with a photodiode array detector (PDA, Varian ProStar, Palo Alto, CA, USA) and sugars were detected by an evaporative light scattering detector (ELSD 2000ES, Alltech, Lexington, KY, USA). ELSD conditions were set at 83.5 ºC and a nitrogen flow of 2.2 L/min. Mobile phases are detailed in **Table 3.3**. Chromatograms were analyzed employing the Varian Star LC workstation 6.41 (Varian, Palo Alto, CA, USA).

Table 3.3 HPLC methods for transfructosylation of polyphenols and production of Fru-HT with pXd-INV. A: CH_3CN and B: H_2O.

		Method			
Experiment	**Column**	**Time (min)**	**A**	**B**	**Flow rate (mL/min)**
Screening of phenolic compounds as acceptors	Waters Spherisorb amino column (4.6 x 250 mm)	0	82	18	1
		6	82	18	1
		7	70	30	1
		17	70	30	1
		18	82	18	1
		32	82	18	1
Production of Fru-HT	Phenomenex Luna-NH2 column (4.6 x 250 mm)	0	82	18	1
		45	82	18	1

3.3.3 HPAEC-PAD

Mixtures of carbohydrates were analyzed by High Performance Anion Exchange Chromatography with Pulsed Amperometric Detection (HPAEC-PAD) with a Dionex ICS3000 system (Dionex, Thermo Fischer Scientific Inc., Waltham, MA, USA) consisting of an SP gradient pump, an electrochemical detector with a gold working electrode and Ag/AgCl reference electrode, and an AS-HV autosampler. Column temperature was always kept at 30 ºC and eluents were degassed by flushing with helium. Peak analysis was done with Chromeleon software (Dionex, Thermo Fischer Scientific Inc., Waltham, MA, USA), and identification and quantification of sugars was done according to commercially available standards. Two columns were used depending on the oligosaccharides analyzed: CarboPack PA1 column (4 x 250 mm) and its guard column were employed for FOS separation in the fructosylation of HT and in the production of neo-FOS with immobilized pXd-INV, while XOS and COS were analyzed using a CarboPack PA200 column (4 x 250 mm) with the corresponding guard column. Mobile phases for each goal are described in **Table 3.4** and **Table 3.5**.

HPAEC-PAD has been extensively used for the analysis of FOS mixtures (Rodriguez-Gomez et al., 2015, Zambelli et al., 2014). In our case, both methods were developed on the basis of the method designed by Campbell and cols. (Campbell et al., 1997).

The method for analysis of neutral XOS, was previously developed by our group (Nieto-Domínguez et al., 2017). On the basis of this method, we designed another one to specifically improve the separation of acidic XOS.

In addition, chitooligosaccharides were analyzed with two methods developed in our laboratory. For the first one, we employed a CarboPack PA200 column (4 x 250 mm) and a post-column delivery system (PC10) that allowed us to pump 200 mM NaOH to enhance the detector response. This system enabled us to use very unusual eluting conditions (1mM NaOH) that enhanced separation. The second method employed a CarboPack PA100 column (4x 250 mm) and 30 mM NaOH as mobile phase. The interaction of the chitooligosaccharides with the CarboPack PA100 column was stronger, increasing retention times and enabling the use of higher concentrations of NaOH, where the detector response is higher.

Table 3.4 HPAEC-PAD methods for FOS analysis. A: 100 mM NaOH. B: H_2O. D: 100 mM NaOH, 600 mM CH_3COONa.

		Method				
Sugars	**Column**	Time (min)	A	B	D	Flow rate (mL/min)
FOS (Fru-HT)	CarboPack PA1 (4 x 250 mm) + CarboPack PA1 guard (4 × 50 mm)	0	30	70	0	1
		20	100	0	0	1
		26	88	0	12	1
		30	88	0	12	1
		31	50	0	50	1
		37	50	0	50	1
FOS (immobilized pXd-INV)	CarboPack PA1 (4 x 250 mm) + CarboPack PA1 guard (4 × 50 mm)	0	100	0	0	1
		8	100	0	0	1
		30	88	0	12	1
		36	88	0	12	1
		37	50	0	50	1
		42	50	0	50	1

Table 3.5 HPAEC-PAD methods for XOS and COS analysis. A: 200 mM NaOH. B: H_2O. C: 200 mM CH_3COONa. D: 100 mM NaOH, 320 mM CH_3COONa.

		Method					
Sugars	**Column**	Time (min)	A	B	C	D	Flow rate (mL/min)
XOS (neutral)	CarboPack PA200 (4 x 250 mm) + CarboPack PA200 guard (4 × 50 mm)	0	7.5	92.5	0	0	0.5
		12	50	45	5	0	0.5
		20	25	50	0	25	0.5
		25	0	0	0	100	0.5
		30	0	0	0	100	0.5
XOS (acidic XOS)	CarboPack PA200 (4 x 250 mm) + CarboPack PA200 guard (4 × 50 mm)	0	10	90	0	0	0.5
		80	10	60	30	0	0.5
		100	10	10	80	0	0.5
COS (large-scale production)	CarboPack PA200 (4 x 250 mm) + CarboPack PA200 guard (4 × 50 mm)	0	0.5	99.5	0	0	0.3
		20	0.5	99.5	0	0	0.3
		30	0	0	0	100	0.5
COS (large-scale production)	CarboPack PA100 (4 x 250 mm) + CarboPack PA200 guard (4 × 50 mm)	0	15	85	0	0	0.4
		60	15	85	0	0	0.4

3.3.4 Semipreparative HPLC

Fructosyl-hydroxytyrosol (Fru-HT) was purified by semipreparative HPLC using the same equipment employed in analytic chromatography with the addition of a three-way flow splitter (Accurate, LC Packings, Amsterdam, Netherlands), only

the column was changed for a Kromasil amino column (10 x 250 mm, Analisis Vinicos, Tomelloso, Spain) or a Liquid Purple amino column (10 x 250 mm, Analisis Vinicos, Tomelloso, Spain). Injection volume was increased to 50 µL. Mobile phase was modified to optimize purification and is detailed in **Table 3.6**.

Table 3.6 Semipreparative HPLC. A: CH_3CN and B: H_2O.

		Method			
Experiment	**Column**	**Time (min)**	**A**	**B**	**Flow rate (mL/min)**
Purification of Fru-HT	Kromasil amino column (10 x 250 mm)	0	82	18	5
		6	82	18	5
		7	60	40	5
		13	60	40	5
		14	82	18	5
		25	82	18	5
Purification of Fru-HQ	Liquid Purple amino column (10 x 250 mm)	0	75	25	5
		6	75	25	5
		7	70	30	5
		13	70	30	5
		14	75	25	5
		25	75	25	5

3.3.5 Mass spectrometry (MS)

Mass spectrometry of carbohydrates, phenolic derivatives and transfructosylation products was carried out in the Servicio Interdepartamental de Investigación (SIdI, UAM).

The molecular weight of fructosylated derivatives was assessed using a mass spectrometer with hybrid QTOF (quadrupole time of flying) analyzer (model QSTAR, Pulsar i, AB Sciex, Framingham, MA, USA). Samples were analyzed by direct

infusion and ionized by electrospray (with methanol as ionizing phase) both in positive and negative reflector modes.

XOS and COS mixtures were analyzed by MALDI-TOF using a Ultraflex III TOF/TOF (Bruker, Billerica, MA, USA) with a NdYAG laser in positive reflector mode. Registers were taken within the 40-5000 Da mass interval, with external calibration and a 20 mg/mL 2,5-dihydroxybenzoic acid (DHB) solution in acetonitrile (3:7, v/v) as matrix.

3.3.6 Nuclear magnetic resonance (NMR)

The structure of the purified compounds (Fru-HT and X2_MeGlcA) was elucidated by NMR in collaboration with Dr. Jesús Jiménez Barbero and Dr. Ana Poveda (CIC Biogune, Basque Country, Spain). A combination of 1D (1H, 1D-selective NOESY experiments) and 2D (COSY, NOESY, DEPT-HSQC, HSQC-TOCSY, HMBC) techniques was employed. The spectra of the samples, dissolved in deuterated water (ca. 10 mM), were recorded on a Bruker AVIII 800 spectrometer (Billerica, MA, USA) equipped with a TCI cryoprobe with gradients in the Z axis, at a temperature of 25 ^{o}C. Chemical shifts were expressed in ppm with respect to the 0 ppm point of DDS (4-dimethyl-4-silapentane-1-sulfonic acid), used as internal standard. All the pulse sequences were provided by Bruker. For the DEPT-HSQC and HSQC-TOCSY experiments, values of 7 ppm and 2 K points, for the 1H dimension, and 120 ppm and 256 points for the 13 C dimension were employed. For the HMBC experiments, values of 7 ppm and 2 K points, for the 1H dimension, and 170 ppm and 384 points for the 13C dimension were used. For the homonuclear experiments COSY and NOESY, 7 ppm windows were utilized with a 2 K x 256 point matrix. For the NOESY and 1D-selective NOESY experiments, mixing times of 500-600 ms were employed.

3.3.7 Elemental analysis

The percentage of salt (ammonium acetate) in purified samples (acidic XOS) was indirectly estimated by elemental analysis, measuring the amount of nitrogen in the sample. Elemental analysis was carried out in the Servicio Interdepartamental de Investigación (SIdI, UAM), using a Leco CHS-932 analyzer (Leco Corporation, St. Joseph, MI, USA).

3.4 Transfructosylation assays with pXd-INV

3.4.1 Acceptor/Inhibitor screening

Several phenolic compounds (EGCG, HQ, Catechol, *p*-nitrophenol, HT and quercetin) were tested as acceptors in transglycosylation reactions with pXd-INV. Transfructosylation reactions were carried out at 60 ºC for 2 h. Reaction mixtures contained 0.72 U/mL of *β*-fructofuranosidase, 100 mg/mL of sucrose and 20 mg/mL of the screened phenol in 100 mM sodium acetate buffer (pH 5.0). Aliquots were taken out at different times (15 min, 30 min, 45 min, 60 min, 90 min and 120 min), inactivated with 2 volumes of 400 mM sodium carbonate (pH 11) and analyzed by HPLC. Also, a control reaction was performed in the same conditions, but without adding phenolic compounds. Results were employed to calculate hydrolysis and transfructosylation ratios with the following equations. In addition, we estimated the hydrolysis/transfructosylation ratio for all reactions.

$$Hydrolysis\,rate\ = \frac{\Delta[Fructose]}{time}$$

$$Transfructosylation\,rate = \frac{\Delta[Glucose]}{time} - \frac{\Delta[Fructose]}{time}$$

3.4.2 Enzymatic synthesis of fructosylated phenols

The positive acceptors (HQ and HT) found in the previous screening (**Section 3.4.1**) were further assayed to obtain fructosylated products. Reaction parameters were modified to increase fructosides production and facilitate purification. Sucrose concentration, reaction temperature and buffer were the same as before, but phenol concentration was increased to 50 mg/mL and 100 mg/mL for HQ and HT, respectively. Samples were analyzed by TLC.

3.4.3 Fructosylation of HT and reaction optimization

Since HT was the best acceptor in the conditions assayed and aroused great interest for its biological activities, we decided to thoroughly investigate this reaction. The production of Fru-HT with pXd-INV was studied under several conditions but enzyme units and temperature were fixed at 0.14 U/mL and 60 ºC, respectively. Donor and acceptor concentrations were optimized in a series of experiments using different concentrations of sucrose and HT prepared in 100 mM sodium acetate buffer (pH 5.0). First, sucrose concentration was kept at 100 mg/mL and HT was employed in the 10-100 mg/mL range. Secondly, HT concentration was

set at 25 mg/mL and sucrose was varied from 100 to 600 mg/mL. Aliquots were taken out at several times, inactivated by enzyme denaturation (16 min at 96 ºC), and analyzed by HPLC.

The production of HT fructosides was also evaluated (in optimal conditions) with the mutants W105F, Q341S and N342Q.

3.4.4 Purification of Fru-HQ and Fru-HT

Probable HQ and HT fructosides obtained as described above (section 3.4.2) were purified by semipreparative HPLC as previously explained (section 3.3.4). Finally, the chosen fractions were desiccated with an R-210 rotavapor (Büchi, Germany) and characterized by mass spectrometry and NMR.

3.4.5 Crystallization and X-Ray structure determination

Soaking experiments were carried out with pXd-INV and several phenolic compounds by Dr. Mercedes Ramírez Escudero and Dr. Julia Sanz Aparicio (Instituto de Química-Física Rocasolano, CSIC, Madrid, Spain) in the context of GLICOENZ project (http://www.glicoenz.org). Diffraction data were collected using synchrotron radiation on the XALOC beamline at ALBA (Cerdanyola del Vallés, Spain). Diffraction images were processed with XDS and merged using AIMLESS from the CCP4 package.

3.5 β-Fructofuranosidase immobilization

3.5.1 Entrapment in PVA lenses

These experiments were carried out at the University of Lisbon, in collaboration with the group of Prof. Maria Ribeiro. A 10% PVA solution (w/v) was prepared in 100 mM sodium acetate buffer (pH 5.0) at 90 ºC under magnetic stirring for 45 min. The entrapment of pXd-INV was assayed with different enzyme loadings (7.1 and 16.9 U/mL of PVA) by directly adding the convenient enzyme solution to the previously prepared PVA at room temperature and under intense magnetic stirring. Lenses were made using a NE-300 syringe pump (NewERA Pump Systems Inc., Farmingdale, NY, USA) to pump the mixture into a 96-well microplate. Each lens was produced by dripping 4 drops of the PVA + enzyme solution into a well and drying it overnight at 50 ºC. This immobilization methodology is detailed in **Figure 3.1**.

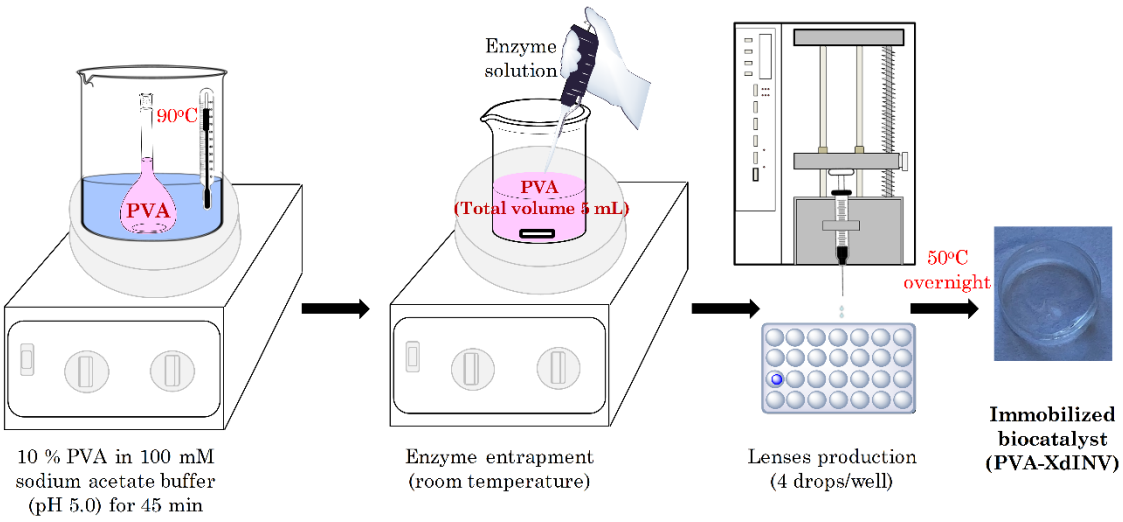

Figure 3.1. Immobilization of pXd-INV by entrapment in PVA.

3.5.2 Binding to carriers

Ionic adsorption was studied employing two different carriers, but in this case, they were both amino-activated resins (Sepabeads EC-EA and Sepabeads EC-HA) that only varied in the length of the spacer arm.

The immobilization methodology was based on the micro-scale immobilization assay (Fernández-Arrojo et al., 2015) and it was performed similarly for all the evaluated carriers. A determined amount of carrier was placed inside a micro-centrifuge filter tube (Spin-X, 0,45 µm, Costar, Corning Inc., Corning, NY, USA) and washed twice with 500 µL of immobilization buffer to achieve carrier equilibration. After centrifugation (2000 x g, 2 min), carriers were mixed with the convenient enzyme solution and the appropriate immobilization buffer. Then, immobilization blends were incubated for a predetermined time at room temperature in a roller mixer (J.P. Selecta, Barcelona, Spain). After incubation, micro-filter tubes were centrifuged (2000 x g, 2 min) and the flow-through was stored at 4 ºC. The obtained biocatalysts were washed 3-times with reaction buffer (500 µL), and washing solutions were also collected and preserved at 4 ºC. Theoretical activity was calculated after measuring activity in the flow-through and washing solutions, previously collected. Specific conditions for each carrier are detailed in **Table 3.7**.

Table 3.7 pXd-INV immobilization conditions for the different carriers.

Carrier		Immobilization conditions		
Type	**Weight (mg)**	**Buffer (250 µL)**	**Enzyme (µL)**	**Incubation time (h)**
Sepabeads EC-EA (amino-activated)	200-250	300 mM sodium phosphate (pH 7.0)	250	24
Sepabeads EC-HA (amino-activated)	200-250	300 mM sodium phosphate (pH 7.0)	250	24

3.5.3 Apparent activity

The effective activity of the immobilized biocatalysts was calculated incubating a known amount of biocatalyst (250 mg or one PVA lens) in a micro-centrifuge filter tube with 500 µL of a 100 mg/mL sucrose solution in 100 mM sodium acetate buffer (pH 5.0). The mixture was incubated at 50 ºC and 900 rpm in a TS-100 Thermo-Shaker (bioSan, Riga, Latvia) for 20 min, and then the reaction mixture and the biocatalyst were separated by centrifugation at 2000 x g for 2 min (**Figure 3.2**). One volume of a 400 mM sodium carbonate solution (pH 11) was added to the supernatant to inactivate the possible lixiviated enzyme. Finally, reducing sugars were measured using the DNS method as described above.

3.5.4 Operational stability of immobilized biocatalysts

The operational stability of the obtained biocatalysts was studied employing a micro-scale assay that was previously developed in our group (Fernandez-Arrojo et al., 2015). This methodology permits to make successive reaction cycles in a rapid manner and is easily adjusted to different immobilizations and reactions. Each cycle includes the measurement of the biocatalyst apparent activity and three washing steps of the solid with 500 µL of reaction buffer (100 mM sodium acetate pH 5.0). The procedure is represented in detail in **Figure 3.2**. Residual activities were referred to the first reaction cycle.

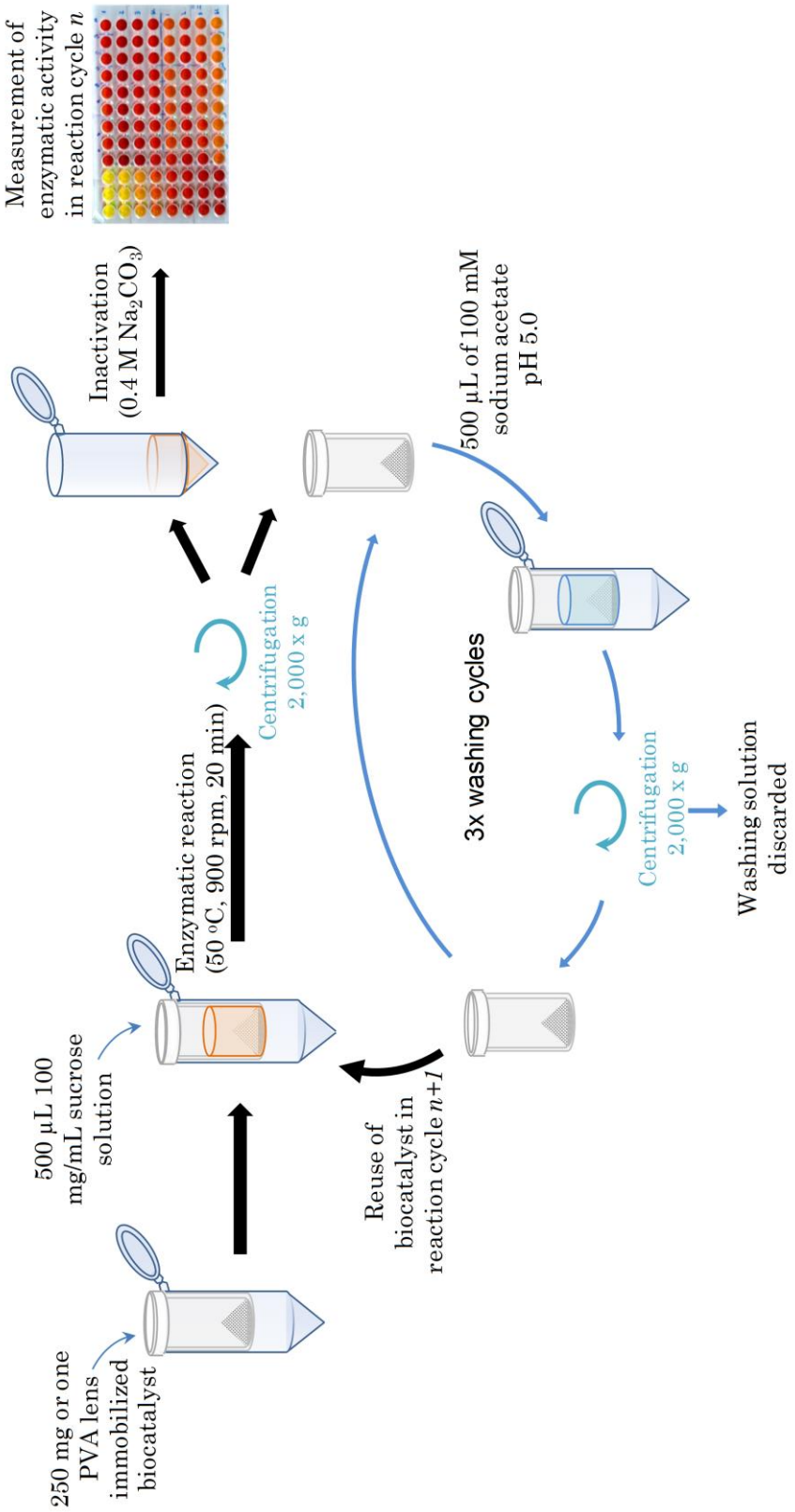

Figure 3.2. Micro-scale assay for the determination of apparent activity and operational stability of immobilized biocatalysts.

3.5.5 Thermostability of PVA hydrogels

The thermostability of the PVA biocatalysts was evaluated by incubating lenses at different temperatures (4-60 ºC) for 24 h in reaction buffer. Then, the residual activity of the PVA lenses was determined employing the DNS method under the same conditions as before.

3.5.6 Large-scale immobilization in Sepabeads EC-HA

The biocatalyst obtained using the amino-activated resin (Sepabeads EC-HA) was produced at a larger scale using 15 mL tubes instead of micro-centrifuge filter tubes. Immobilization conditions were the same but the incubation took place in a Rotoflex R-2001 overhead rotator at 18 rpm (Argos Technologies Inc., Vernon Hills, IL, USA). Also, the biocatalyst was separated from the immobilization and washing solutions by filtration with acetate/nitrate cellulose filters (0.45 µm, Merck Millipore, Billerica, MA, USA).

3.6 Neo-FOS production in reactors with immobilized pXd-INV

3.6.1 Batch reactor

A batch reactor was set up with the pXd-INV entrapped in PVA using one lens-shaped particle (0.3 U) and 340 µL of a 600 mg/mL sucrose solution in reaction buffer. The lens and reaction mixture were placed in a micro-centrifuge tube and incubated at 30 ºC and 900 rpm for 26 h. Then, the tube was centrifuged (2000 x g, 2 min) to collect the supernatant and the possible lixiviated enzyme was inactivated adding 400 mM sodium carbonate. Several successive reaction cycles were performed and, in between them, the lens-shaped biocatalyst was washed thrice with 100 mM sodium acetate buffer (pH 5.0). Neo-FOS production was analyzed in each cycle by HPAEC-PAD as described earlier.

3.6.2 Packed-bed reactor

A packed-bed reactor was assembled using 1 mL empty cartridges (Agarose Bead Technologies, Miami, FL, USA) and the pXd-INV immobilized in Sepabeads EC-HA. Biocatalyst (23 U) was packed following provider instructions. Column and substrate (600 mg/mL sucrose solution in reaction buffer) were kept at 50 ºC in a heater (MOD. MFE-01, Analisis Vinicos, Tomelloso, Spain). Substrate was pumped into the column at 0.03 mL/min with a 515 HPLC pump (Waters, Milford, MA, USA). Once the system was in a steady state, samples were collected and neo-FOS

production was evaluated by HPAEC-PAD. Also, we determined the productivity and conversion yield.

3.7 Production of acidic XOS

3.7.1 Enzymatic hydrolysis of beechwood xylan

Hydrolysis reactions were performed with a 2% (w/v) xylan solution in distilled water and 3 U/mL of Depol 670L. Incubation at 60 ºC and under orbital stirring took place in a Stuart Orbital Incubator S-150 (Cole-Parmer, Staffordshire, UK). Aliquots were taken out at different times and mixed with absolute ethanol until the final ethanol concentration was 70%. This allowed the precipitation of the remaining xylan and the inactivation of the enzyme. Samples were centrifuged (1200 x g, 10 min) and analyzed by HPAEC-PAD as described above.

3.7.2 Acidic XOS purification

XOS were separated in neutral and acidic fractions using anion-exchange Sep-Pak Accell Plus QMA Plus Short Cartridges (Waters, Milford, MA, USA). Firstly, cartridges were equilibrated with distilled water (8 mL). Then, the reaction mixture (neutral and acidic XOS) was loaded (4 mL). Neutral XOS were obtained after washing with distilled water (4 mL) and acidic XOS were eluted with 4 mL of a 10 mM ammonium acetate solution (pH 7.4). Neutral and acidic XOS were analyzed by HPAEC-PAD using a previously described method that focuses on the separation of acidic XOS.

3.7.3 Large-scale production and purification of acidic XOS

A xylan hydrolysis reaction (100 mL) was set in the same conditions as before, choosing 72 h as the optimum reaction time. Enzyme inactivation and xylan precipitation were carried out as previously explained. Then, the reaction mixture was concentrated 3-times using a R-210 rotavapor (Büchi, Germany).

The anion-exchange procedure for the purification of acidic XOS, previously reported, was slightly adjusted to fit better the larger scale. For this, five Sep-Pak Cartridges were connected in series and equilibrated with 10 mL of distilled water. Then, the reaction mixture (1 mL) was loaded into the cartridges and neutral XOS were eluted in a washing step with distilled water (10 mL). Finally, the acidic fraction was attained after washing with 10 mL of 10 mM ammonium acetate (pH

7.4). Each lot of five cartridges was reused five times, employing a total of 30 anion-exchangers for the whole purification. This purification methodology is described in **Figure 3.3**.

The obtained acidic XOS were concentrated by rotary evaporation, subjected to dialysis using 100-500 Da tubing to remove salts and freeze-dried with a Freezone 2.5^{PLUS} lyophilizer (Labconco Corporation, Kansas City, MO, USA). Acidic XOS were then characterized by elemental analysis, HPAEC-PAD, MS and NMR.

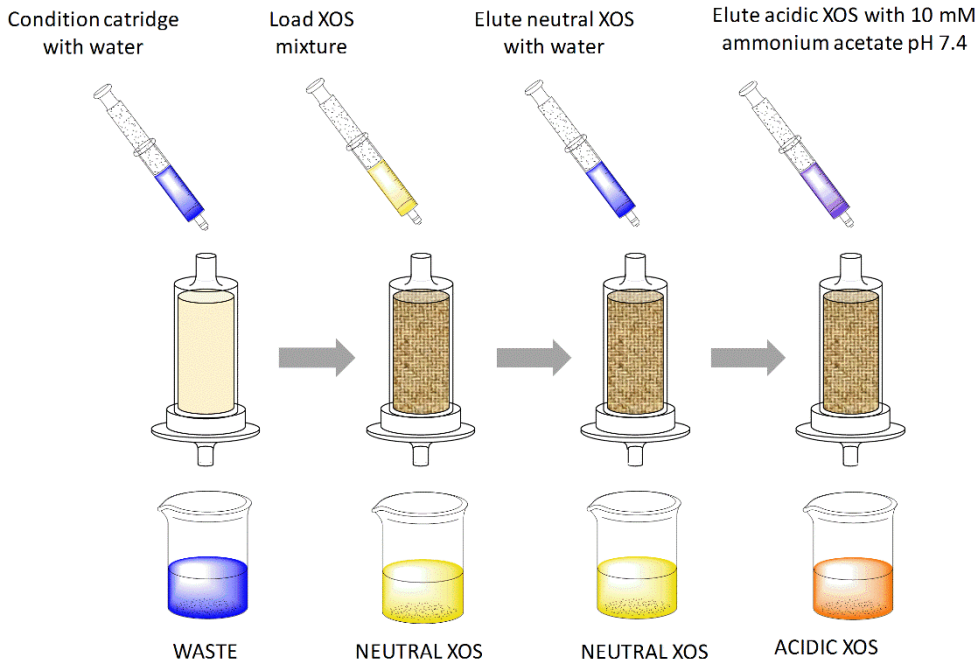

Figure 3.3. Anion-exchange purification of acidic XOS.

3.7.4 Scavenging of ABTS radical

The antioxidant activity of acidic XOS was evaluated applying the ABTS radical cation decolorization assay (Re et al., 1999) with slight modifications. The radical was produced reacting a stock ABTS solution (7 mM in water) with a 2.45 mM (final concentration) potassium persulfate solution and keeping it in the dark at room temperature overnight. Afterwards, the reaction was diluted with water until a final absorbance of 0.7 at 734 nm.

Beechwood xylan and XOS mixtures (neutral and acidic) were tested at several concentrations (0-8 mg/mL) by mixing 20 µL of these compounds stock solutions with 230 µL of ABTS radical. The absorbance was followed at 734 nm after a 10 min

incubation at room temperature in the dark. Samples were measured in triplicates and xylan and XOS concentration was represented *vs.* the decrease in absorbance (in percentage).

The half maximal scavenging concentration (SC_{50}) was defined as the concentration of antioxidant, in mg/mL, that is able to diminish the absorbance of the ABTS radical cation in a 50% in 10 min. (R)-Trolox was used as reference.

3.8 Large-scale production of COS

A procedure was developed for the production of several COS mixtures at a large-scale. Chitosans with different deacetylation degrees (**Table 3.1**) and various enzymes were employed. Chitosan solutions were always prepared at 1% (w/v) in sodium acetate buffer (pH 5.0). Hydrolysis was performed with Neutrase (10% v/v) or CHIT42 (3-10% v/v) as biocatalysts. Neutrase was previously dialyzed with 3.5 kDa tubing to remove sorbitol and other possible contaminants. Incubation was done at 50 ºC and 150 rpm for 48-72 h. Reaction mixtures (1 L) were then concentrated by rotary evaporation and filtrated with paper filters, glass microfiber filters (Whatman™, GE Healthcare, Chicago, IL, USA) and acetate/nitrate cellulose filters (0.45 μm). Later on, enzymes and non-hydrolyzed chitosan were removed by ultrafiltration with an Amicon® system (10 kDa membrane). In this way, we obtained high molecular weight (< 10 kDa) COS. Eventually, some COS mixtures were ultrafiltrated a second time with a 1 kDa membrane to obtain low (< 1 kDa) molecular weight COS. Finally, COS were concentrated again by rotary evaporation, dialyzed to eliminate salts (100-500 Da tubing) and lyophilized. COS mixtures were characterized by HPAEC-PAD, as described before, and mass spectrometry.

RESULTS AND DISCUSSION

4.1 Production of neo-FOS by immobilized pXd-INV

The *β*-fructofuranosidase from *Xanthophyllomyces dendrorhous* (pXd-INV) is an extracellular glycoprotein that synthesizes neo-FOS, mainly neokestose and neonystose (Linde et al., 2009). Under optimum conditions (600 g/L of sucrose), pXd-INV produces 118 g/L of neo-FOS, which is the largest yield of this kind of FOS reported for a microbial enzyme (Gimeno-Pérez et al., 2015). Besides synthesizing neo-FOS, the invertase pXd-INV is able to fructosylate several carbohydrates such as maltose (Gimeno-Pérez et al., 2014). These features make pXd-INV an interesting enzyme for its application in the food, pharmaceutical or cosmetic industries.

Enzyme immobilization promotes industrial application by enabling biocatalyst separation and reuse, facilitating product processing and enhancing enzyme stability. Thus, we studied several strategies for the immobilization of pXd-INV and evaluated the biocatalysts obtained in terms of recovered activity and operational stability.

4.1.1 Immobilization of pXd-INV in PVA hydrogels

The *β*-fructofuranosidase Xd-INV is a notably large dimeric enzyme with a molecular mass of 360 kDa (Ramirez-Escudero et al., 2016). This considerable size should restrict enzyme leakage through matrix pores, making entrapment a suitable technique for its immobilization. Polyvinyl alcohol (PVA) is a cheap, non-toxic and mechanically robust polymer that can form highly stable and elastic hydrogels. Gelation is achieved by the formation of hydrogen bonds between the numerous hydroxyl groups of PVA, resulting in a complex three-dimensional network (Lozinsky and Plieva., 1998). PVA hydrogels have been used successfully for several applications, including the immobilization of enzymes, controlled drug release, artificial tissues or biosensors (Nuneslentik et al., 2016, Durieux et al., 2000, Ariga et al., 1994, Cao et al., 2017). Moreover, PVA-based biocatalysts have shown excellent mechanical and operational stability in different kinds of bioreactors such as shaken microtiter plates, batch stirred tanks and packed-bed reactors (Nunes et al., 2014). Taking this into consideration, pXd-INV was immobilized by entrapment in PVA lenses as explained in **Section 3.5.1**. The enzyme was mixed with a PVA solution, and PVA lenses were formed by dripping the mixture onto 96-well microplates and promoting gelation by partial drying at 50 ºC (Schlieker and Vorlop,

2006). The gelatinization process can be facilitated by other means like freezing, thawing (Gomez de Segura et al., 2003) or UV radiation (Imai et al., 1986).

The immobilization assays were carried out with 10% (w/v) PVA in the enzyme optimum buffer and two different pXd-INV loadings. The main immobilization parameters obtained with both biocatalysts are summarized in **Table 4.1**. The volumetric activity of the biocatalyst did not increase with higher enzyme loadings, resulting in a decrease of the recovered activity. We performed several successive washings and corroborated that pXd-INV was not leaked from the PVA matrix. Taking this into account and considering the high stability of the enzyme under the immobilization conditions, we presume that diffusional limitations caused by high enzyme concentration inside the lenses could explain the results obtained when the initial activity was increased.

Table 4.1 Immobilization parameters of pXd-INV in PVA lenses with two enzyme loadings.

Total initial activity (U)[a]	Volume of biocatalyst (mL)	Lens volume (µL)[b]	Activity of the biocatalyst (U/lens)[a]	Activity of the biocatalyst (U/ml)[a]	Recovered activity (%)[c]
35.5	4.8	56.3	0.34	5.96	80.4
84.5	4.7	52.6	0.33	6.20	34.7

[a] Measured by the DNS assay; [b] Lens volume = (volume dispensed/number of drops dispensed) x number of drops in each lens; [c] (Activity of the biocatalyst x Volume of biocatalyst obtained x 100)/Total activity introduced.

4.1.2 Immobilization of pXd-INV by ionic binding

The immobilization of the *β*-fructofuranosidase pXd-INV was assayed by binding to different carriers. Generally, covalent binding is preferred since it forms strong linkages that avoid enzyme leakage (Sheldon, 2007). However, covalent binding usually requires incubating the enzyme in alkaline conditions, and most commercial activated carriers are quite expensive. Taking this into account, we decided to attempt the pXd-INV immobilization with two polymethacrylate amino activated resins (Sepabeads). Besides being rather cheap, these carriers are easily arranged into packed-bed bioreactors, are non-compressible, and the enzyme immobilization occurs at neutral pH. We chose two kinds of Sepabeads, EC-EA (ethylamine) and EC-HA (hexamethylamine), which only differ on the length of the spacer arm.

The immobilization of pXd-INV was performed with 200-250 mg of carrier at pH 7.0 and, as in the previous case, two different enzyme loadings were evaluated.

Increasing the activity offered to the support resulted in a significant increment of activity for both biocatalysts. In contrast, the percentage of recovered activity was slightly lower in both cases (**Table 4.2**). The activity yield shows that enzymatic activity is always lost in the immobilization process. This loss could be explained by an inefficient binding of the protein and/or mass transfer restrictions within the carriers that limit substrate accessibility (Bolivar et al., 2014). The glycosylation degree of pXd-INV is quite high, approximately 50% (Gimeno-Pérez et al., 2015), which could restrict the interaction between the protein and the amino groups, preventing a more effective immobilization. In addition, low initial activities showed better yields indicating that the enzyme was bound in a more efficient manner when protein concentration was lower.

Comparing both resins, Sepabeads EC-HA showed better results in terms of activity and yield at both enzyme loadings. This may be explained by the superior length of its spacer arm that could reduce mass transfer limitations, improving both ionic binding and diffusion of substrate and products.

Table 4.2 Immobilization parameters of pXd-INV in Sepabeads EC-EA and EC-HA with two different enzyme loadings.

Carrier	Initial Activity (U)[a]	Biocatalyst Activity	
		Activity (U/g)[b]	Yield (%)[c]
Sepabeads EC-EA	41.8	59.4	15.6
	4.18	7.87	20.7
Sepabeads EC-HA	41.8	114.0	29.9
	4.18	16.1	42.3

[a] Activity of the enzyme solution measured by DNS; [b] Experimental (apparent) activity; [c] (Total experimental activity x 100)/ Initial activity.

4.1.3 Operational stability of the immobilized biocatalysts

The operational stability of all the biocatalysts obtained by ionic binding and the PVA biocatalyst obtained with the lowest enzyme loading was assayed following a micro-scale protocol developed in our laboratory (**Section 3.5.4)** (Fernandez-Arrojo et al., 2015). Biocatalysts were used in a series of batch reactions with 100 mg/mL of

sucrose as substrate at 50 ºC. After each cycle (20 min), reducing sugars were measured by the DNS method and biocatalysts were thoroughly washed to remove any remaining substrate and/or products, along with any desorbed enzyme. **Figure 4.1** represents the residual activity of each biocatalyst after ten short reaction cycles. As shown, the operational stability was satisfactory for all the biocatalysts evaluated.

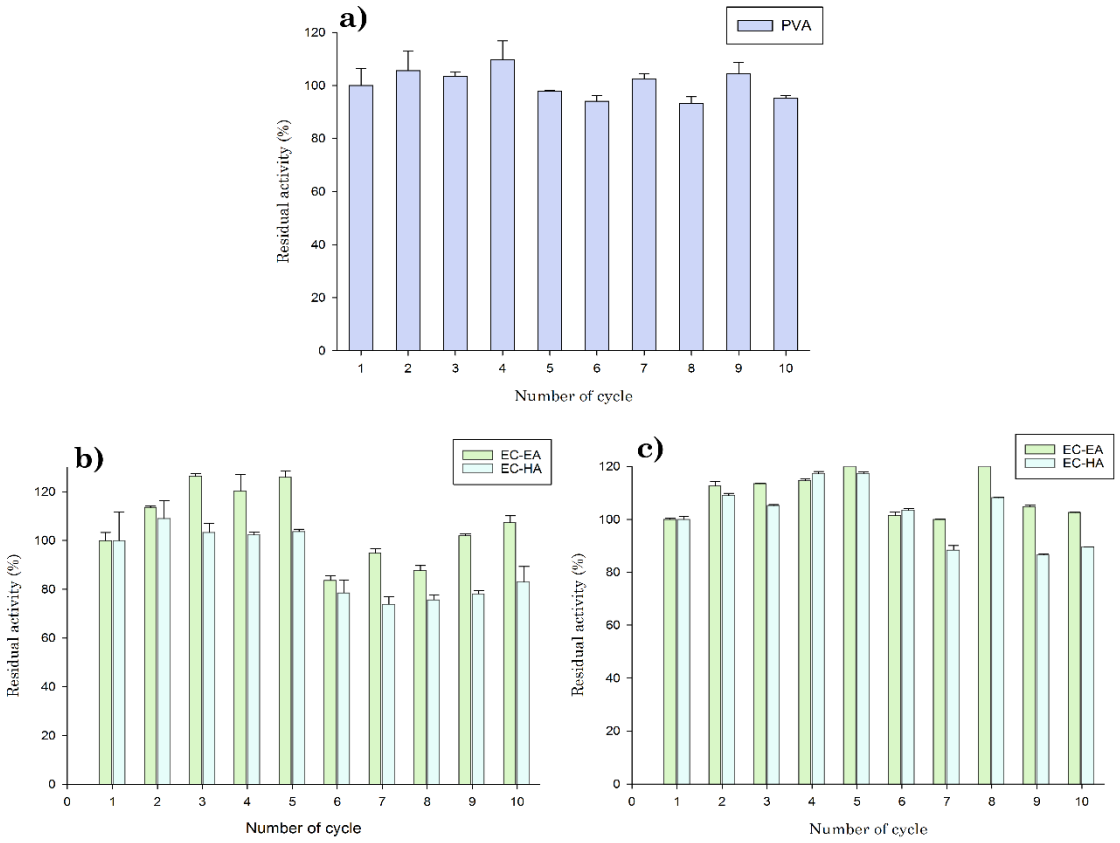

Figure 4.1. Operational stability of pXd-INV biocatalysts: a) PVA (Initial activity 35.5 U); b) EC-EA and EC-HA (Initial activity 41.8 U); c) EC-EA and EC-HA (Initial activity 4.18 U). Reaction conditions: 100 g/L of sucrose in 100 mM sodium acetate buffer (pH 5.0) at 50 ºC for 20 min. Values are referred to the activity of the biocatalyst in the first cycle.

4.1.4 Thermal stability of PVA-based biocatalyst

The optimum temperature for pXd-INV is between 50 and 60 ºC (Gimeno-Perez et al., 2015). Even though PVA-lens shaped particles showed satisfactory operational stability in short reaction cycles (**Figure 4.1**), we analyzed the thermostability of the biocatalyst in long-term operation. Thus, the PVA biocatalyst was incubated at different temperatures (4-60 ºC) for 24 h in reaction buffer, and the residual activity

was measured by the DNS assay (**Figure 4.2**). As shown, the activity of the immobilized enzyme was maintained up to nearly 40 ºC. On the other hand, more than half of the activity was lost at higher temperatures. The instability of PVA hydrogels at temperatures over 50 ºC is well reported (Alves et al., 2011, Rescignano et al., 2014). Hence, enzyme leakage could be facilitated by the loss of the PVA lenses 3D structure, resulting in a decay of activity. Based on this, we chose 30 ºC to evaluate the operational stability of the PVA biocatalyst for neo-FOS production, as a compromise between stability and activity.

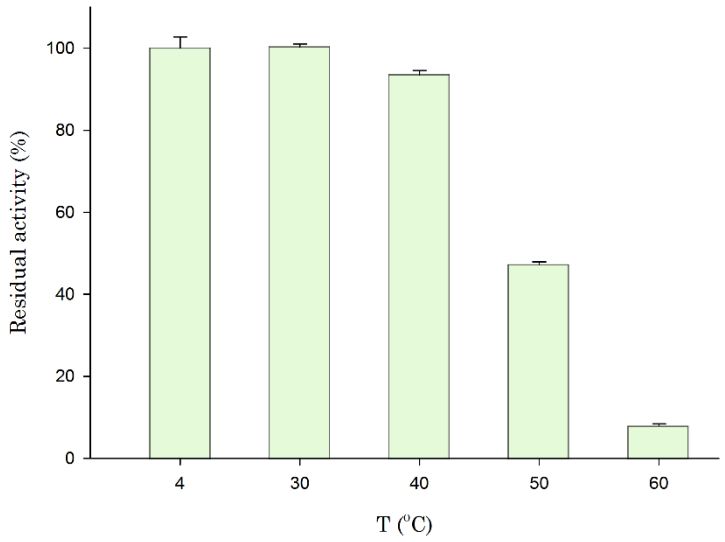

Figure 4.2. Thermostability of pXd-INV entrapped in PVA lenses after incubating at 4-60 ºC for 24 h in 100 mM sodium acetate buffer (pH 5.0).

4.1.5 Production of FOS by PVA-entrapped pXd-INV

The production of fructooligosaccharides with immobilized pXd-INV was assessed using 600 g/L of sucrose. Substrate concentration was previously optimized with the soluble enzyme (Linde et al., 2012). In addition, high concentrations of sucrose promote transglycosylation reactions instead of substrate hydrolysis (Ghazi et al., 2007). The profile of FOS synthesized by the PVA-entrapped enzyme was characterized by HPAEC-PAD (**Figure 4.3**) and compared with the soluble enzyme. The products pattern was very similar to the one obtained with free enzyme (Gimeno-Pérez et al., 2015). Employing neo-FOS standards previously purified and characterized by our group (Linde et al., 2012, Zambelli et al., 2014), we managed to

identify neokestose (the main product), 1-kestose, neonystose and blastose. Blastose is a sucrose isomer synthesized by neokestose hydrolysis since Xd-INV cannot transfer fructose to free glucose (Linde et al., 2012, Gimeno-Pérez et al., 2015). The structure of the FOS produced is illustrated in **Figure 4.3**.

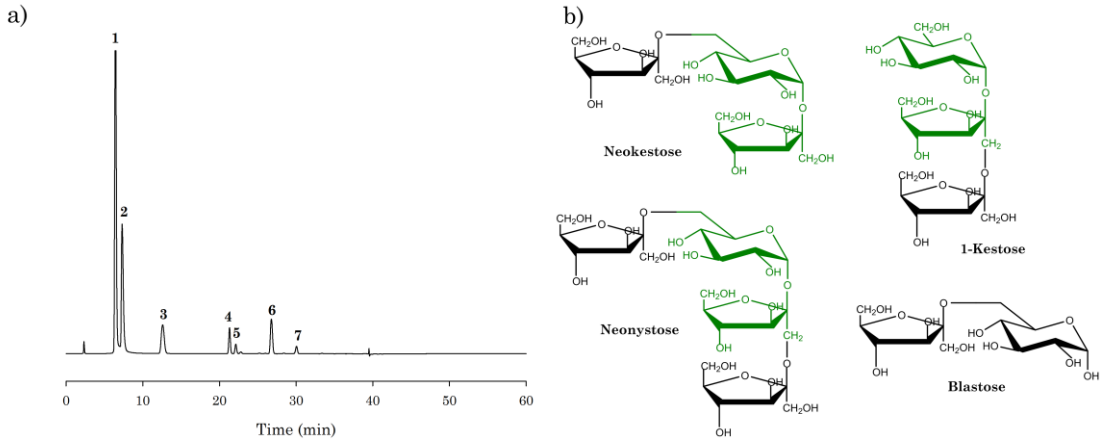

Figure 4.3. a) HPAEC-PAD chromatogram of the reaction of 600 g/L of sucrose at 30 ºC with pXd-INV immobilized in PVA lenses. (1) Glucose; (2) Fructose; (3) Sucrose; (4) 1-Kestose; (5) Blastose; (6) Neokestose; (7) Neonystose. b) Structure of the FOS synthesized by the PVA-entrapped enzyme. The sucrose skeleton is represented in green.

FOS production with the entrapped enzyme was analyzed employing 600 g/L of sucrose as substrate. As previously explained, the reaction temperature was set at 30 ºC. The formation of the different FOS was represented as a function of sucrose consumption (**Figure 4.4**). As shown, the highest FOS concentration was achieved when almost 86% of the initial sucrose was transformed, as occurred with the soluble enzyme. The immobilized enzyme yielded a maximum of 18.9% (w/w) of FOS (113.5 g/L), of which 59.1 g/L were neokestose, 30.2 g/L 1-kestose, 11.6 g/L neonystose and 12.6 g/L blastose.

We confirmed that blastose was obtained by neokestose hydrolysis since blastose concentration increased significantly (30.5 g/L) at the end of the reaction, while neokestose concentration rapidly declined. This value is quite relevant since 34 g/L is the largest amount reported for the production of this disaccharide (Zambelli et al., 2014). In addition, the acute decrease of FOS concentration after 85-90% hydrolysis of sucrose occurred similarly with the free native enzyme (Gimeno-

Pérez et al., 2015), and is quite common in FOS production with β-fructofuranosidases (Gutierrez-Alonso et al., 2009).

It is worth mentioning that the highest FOS concentration obtained (18.9%) was considerably lower than the reported with the soluble enzyme (29%) (Gimeno-Pérez et al., 2015). Moreover, the concentration of blastose produced by the immobilized enzyme was significantly higher (30 g/L vs. 8 g/L). A possible explanation could be that the hydrophilic environment inside the PVA lenses favors hydrolysis instead of transfructosylation. Several studies have reported that carrier environment can alter the hydrolysis to transglycosylation ratio (Imai et al., 1986, Ghazi et al., 2005, Rodrigues et al., 2013, Hill et al., 2016). In addition, changing the reaction temperature from 60 ºC (soluble enzyme) to 30 ºC (immobilized enzyme) could also affect the transferase to hydrolysis rate.

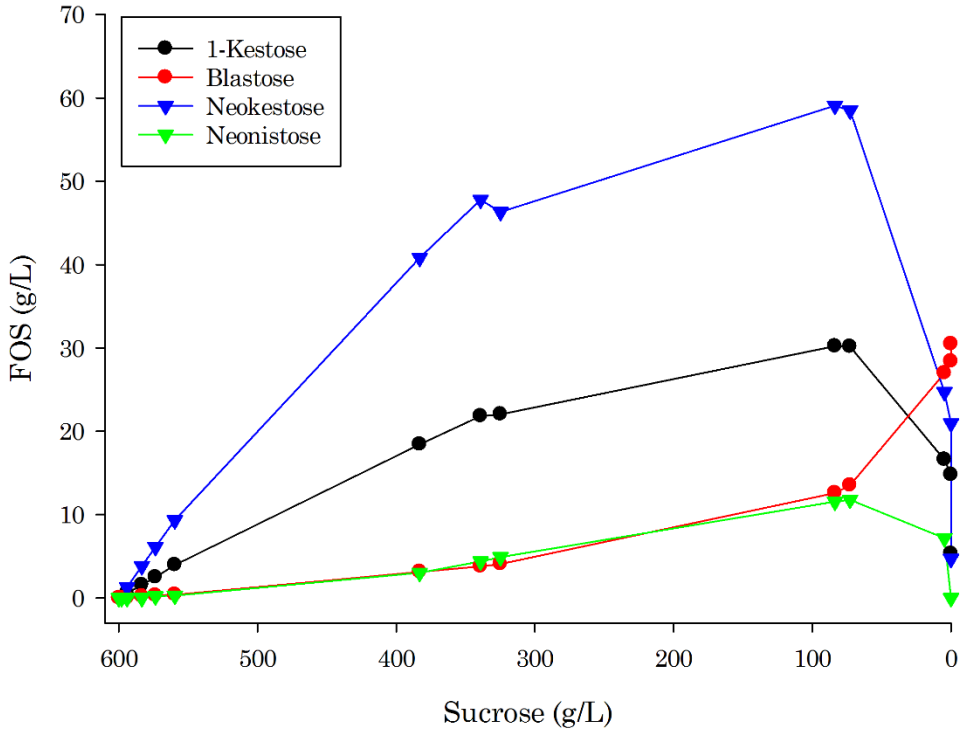

Figure 4.4. Kinetics of FOS formation with PVA-entrapped pXd-INV as a function of sucrose concentration. Reaction conditions: 600 g/L of sucrose in 100 mM sodium acetate buffer (pH 5.0) at 30 ºC.

4.1.6 Batch reactor for neo-FOS production with PVA-based biocatalyst

A batch stirred tank reactor was set up with the PVA-entrapped pXd-INV and FOS production was analyzed by HPAEC-PAD (**Figure 4.5**). We carried out seven reaction cycles of 26 h at 30 ºC, using 600 g/L of sucrose as substrate. PVA lenses were thoroughly washed between cycles to eliminate any residual sugars. The production of FOS in each reaction cycle is represented in **Figure 4.6**. As shown, the conversion of sucrose (23%) was quite far from the optimum for FOS production (86%, see above). Nevertheless, this study was very useful to determine the reusability of the PVA biocatalyst in neo-FOS industrial production. **Figure 4.6** illustrates that FOS concentration was kept constant during the seven cycles. This remarkable operational stability could be dependent on the fact that the original shape of the lenses was preserved during the assay.

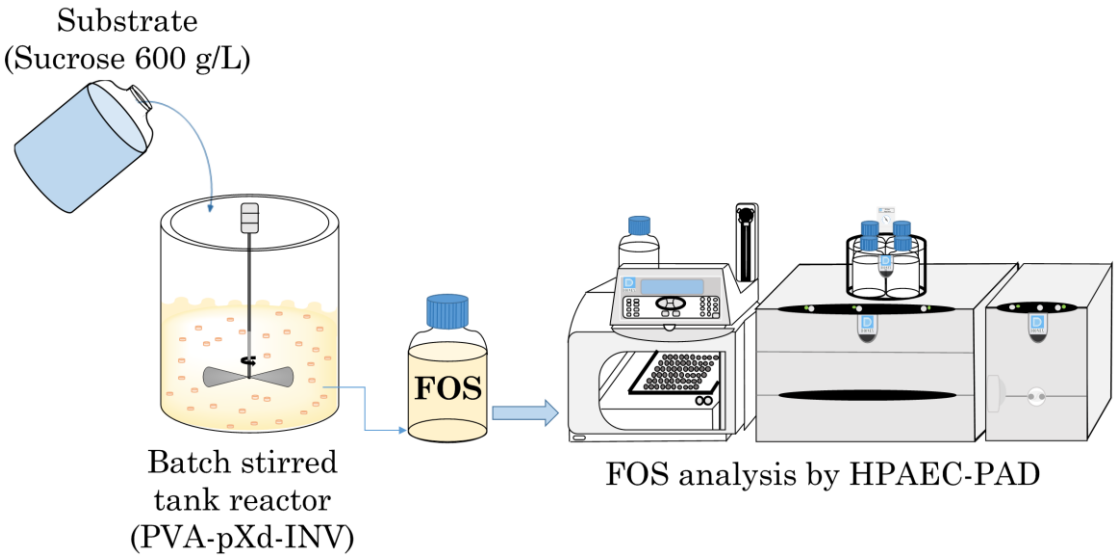

Figure 4.5. Batch stirred tank reactor system for FOS production with PVA-entrapped pXd-INV (PVA-pXd-INV). Reaction conditions: 600 g/L of sucrose in 100 mM sodium acetate buffer (pH 5.0) at 30 ºC.

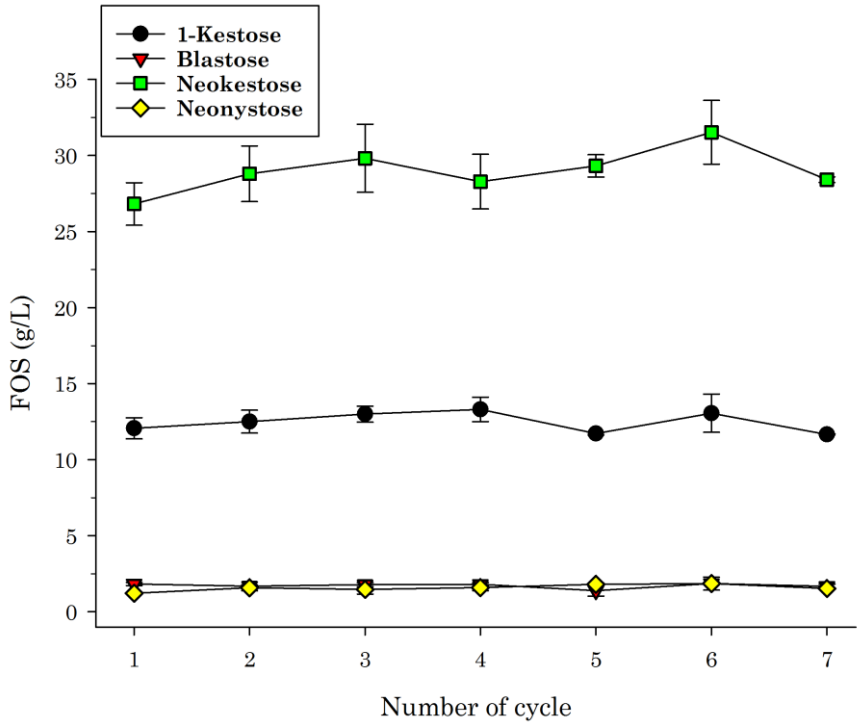

Figure 4.6. Operational stability of the immobilized biocatalyst (PVA-pXd-INV) in a batch reactor. Reaction conditions per cycle: 600 g/L of sucrose in 100 mM sodium acetate buffer (pH 5.0) at 30 ºC for 26 h.

4.1.7 Packed-bed reactor for neo-FOS production with Sepabeads biocatalyst

Continuous packed bed reactors are formed by immobilized enzymes packed into a column where the substrate is continuously fed through the inlet and the product is recovered at the outlet. Their productivity is quite high compared with the obtained with other reactors (Rakmai and Cheirsilp, 2016). As previously mentioned, polymethacrylate carriers are easily packed into columns. Thus, we decided to set up a packed bed reactor with the most active biocatalyst obtained with the amino resins. Hence, the selected biocatalyst was the one produced with Sepabeads EC-HA and the high enzyme loading (HA-pXd-INV). In this work, 410 mg (47 U) of the immobilized enzyme were packed into a 1 mL column and FOS production was analyzed by HPAEC-PAD (**Figure 4.7**).

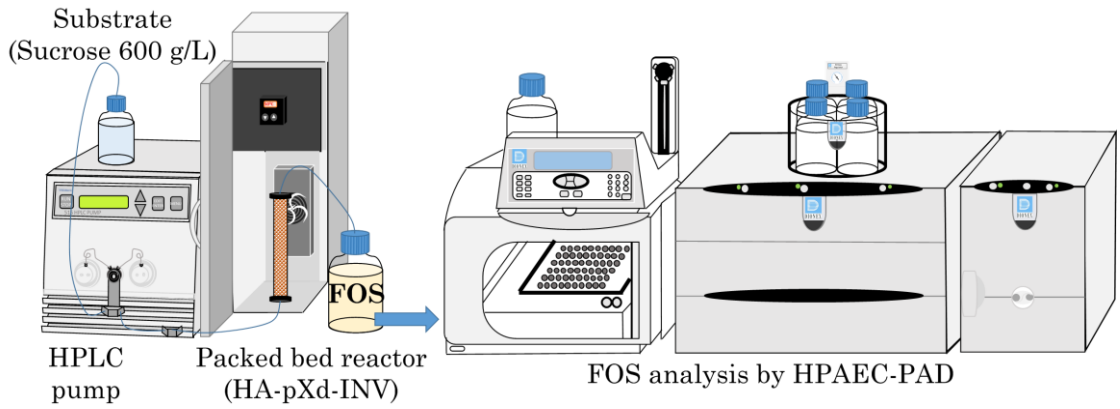

Figure 4.7. Packed bed reactor system for FOS production with pXd-INV immobilized in Sepabeads EC-HA (HA-pXd-INV). Reaction conditions: 600 g/L of sucrose in 100 mM sodium acetate buffer (pH 5.0) at 50 ºC.

A continuous process for FOS synthesis was operated at 0.03 mL/min using 600 g/L sucrose as feed solution. Taking into account that the maximum temperature of operation recommended by the manufacturer for these carriers is 60 ºC, we chose 50 ºC as reaction temperature to minimize damage in a long process. The initial productivity of the reactor was calculated using the following equations:

$$Dilution\ Rate\ (d, h^{-1}) = \frac{Flow\ (mL\ h^{-1})}{Column\ volume\ (mL)}$$

$$Initial\ Productivity\ (g_{FOS}\ L^{-1}\ day^{-1}) = [FOS] \times d$$

The dilution rate of the bioreactor was 1.8 h^{-1}, giving an initial productivity of 218 g_{FOS} L^{-1} day^{-1}, which was more than 4-times the FOS obtained in each PVA batch reactor cycle (approximately 45 g_{FOS} L^{-1} in 26 h). The bioreactor was continuously operated for 12 days and samples were taken out at different times and analyzed by HPAEC-PAD to determine the operational stability (**Figure 4.8**). As shown, FOS production decreased steadily with time but the enzyme seemed to keep its activity since it could still hydrolyze sucrose. On the other hand, fructose and glucose concentration grew with time, probably due to an enzyme conformational change that favored hydrolysis over fructose transference.

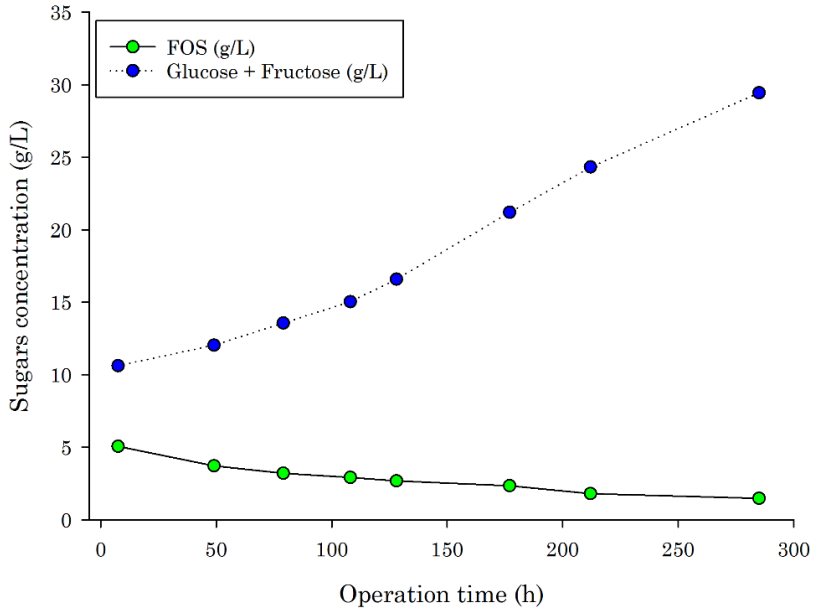

Figure 4.8. Operational stability of the immobilized biocatalyst (HA-pXd-INV) in a packed bed reactor. Reaction conditions: 600 g/L of sucrose in 100 mM sodium acetate buffer (pH 5.0) was fed at 0.03 mL/min and the column was kept at 50 ºC.

The operational stability of immobilized biocatalysts for FOS production has been investigated several times (Plou et al., 2014). Satisfying results has been accomplished with different methodologies, including entrapment in alginate and subsequent drying (Fernández-Arrojo et al., 2013), crosslinking in presence of chitosan (Mouelhi et al., 2016), glutaraldehyde-activated chitosan (Lorezoni et al., 2014) or adsorption onto niobium ore (Aguiar-Oliveira and Maugeri, 2010).

4.2 Fructosylation of phenolic compounds with pXd-INV

As mentioned before, glycosyl hydrolases catalyze the cleavage of glycosidic bonds and, under the proper conditions, can produce different oligosaccharides and glycoconjugates. A great number of glycosidases (α- and *β*-glucosidases, *β*-galactosidases, *β*-xylosidases, *β*-fructofuranosidases, etc.) have been successfully employed for the glycosylation of different organic compounds (Ono et al., 2006, Saiki et al., 2007, Park et al., 2008, Lu et al., 2015, Nieto-Dominguez et al., 2017). Besides catalyzing the hydrolysis of sucrose and the synthesis of neo-FOS, the recombinant *β*-fructofuranosidase pXd-INV can also accomplish the fructosylation of several carbohydrates (maltose, maltotriose, maltotetraose and isomaltulose) and sugar

alcohols (erythritol, xylitol, sorbitol and dulcitol) (Gimeno-Perez et al., 2014, Gimeno-Perez, 2019).

Interestingly, a previous crystallographic study of pXd-INV revealed that the organic molecule HEPES could be accommodated in the active site alongside a fructose residue. Considering this fact, we decided to attempt the fructosylation of non-sugar compounds such as polyphenols, whose structure resembled that of HEPES (Ramirez-Escudero et al., 2016).

Several transfructosylation assays were carried out with a variety of phenolic compounds (hydroquinone, hydroxytyrosol, epigallocatechin gallate, catechol and *p*-nitrophenol) and pXd-INV. Reactions were performed with 100 g/L of sucrose as fructosyl donor, 20 g/L of the putative acceptor and 0.72 U/mL of the *β*-fructofuranosidase pXd-INV at 60 ºC. In addition, control reactions in absence of acceptor or sucrose were carried out under the same conditions. Reaction mixtures were analyzed by HPLC and, as example, chromatograms with HQ, catechol, EGCG and *p*-nitrophenol are represented in **Figure 4.9**.

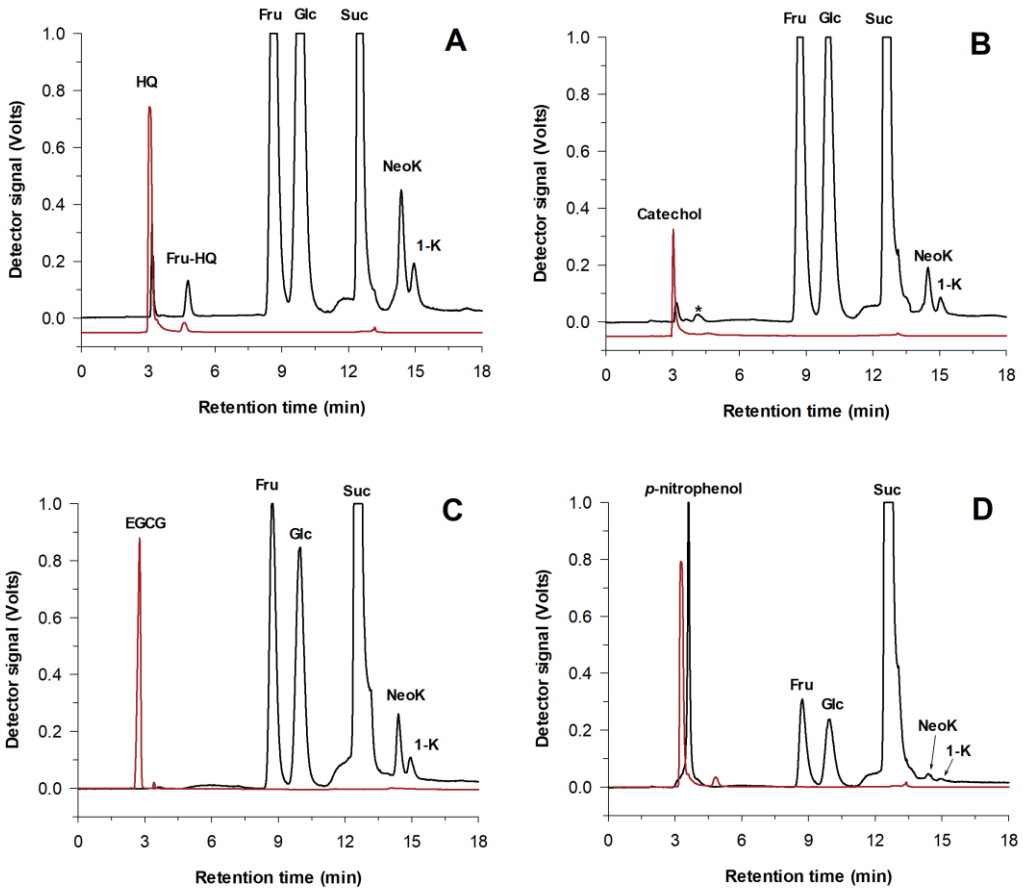

Figure 4.9. HPLC analysis of the assays with (A) hydroquinone (HQ); (B) catechol; (C) EGCG and (D) *p*-nitrophenol. Reaction conditions: 100 g/L of sucrose and 20 g/L of phenolic compound in 100 mM sodium acetate buffer (pH 5.0) at 60 ºC. Red: PDA detector; Black: ELSD detector. HQ: hydroquinone; Fru-HQ: fructosyl hydroquinone; Fru: fructose; Glc: glucose; Suc: sucrose; NeoK: neokestose; 1-K: 1-kestose.

As shown, the presence of *p*-nitrophenol and EGCG considerably inhibited both hydrolysis and transfructosylation. On the other hand, the hydrolysis rate with hydroquinone and catechol was similar to the observed for the control reaction (data not shown). In addition, two peaks that could correspond to fructosides of both HQ and catechol were detected. Based on the results above, fructosylation of HT and HQ was furtherly investigated. The analysis of the TLC plates revealed the presence of new spots that could correspond to fructosylated derivatives of HQ and HT. However, catechol fructosylation could not be confirmed by TLC. Hydroxytyrosol (HT) gave rise to the most transfructosylation spot in TLC analysis (**Figure 4.10**).

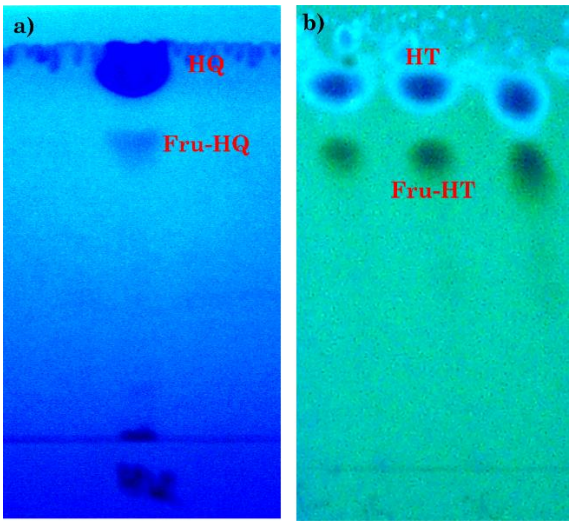

Figure 4.10. TLC analysis of reactions in presence of a) Hydroquinone (HQ) and b) Hydroxytyrosol (HT) observed at UV light. Reaction conditions: 100 g/L of sucrose and 20 g/L of phenolic compound in 100 mM sodium acetate buffer (pH 5.0) at 60 ºC.

Figure 4.11 represents FOS production by pXd-INV in the presence and absence of the investigated polyphenols. As shown, FOS production decreases with all the investigated phenolic compounds in different degrees depending on the nature of the compound.

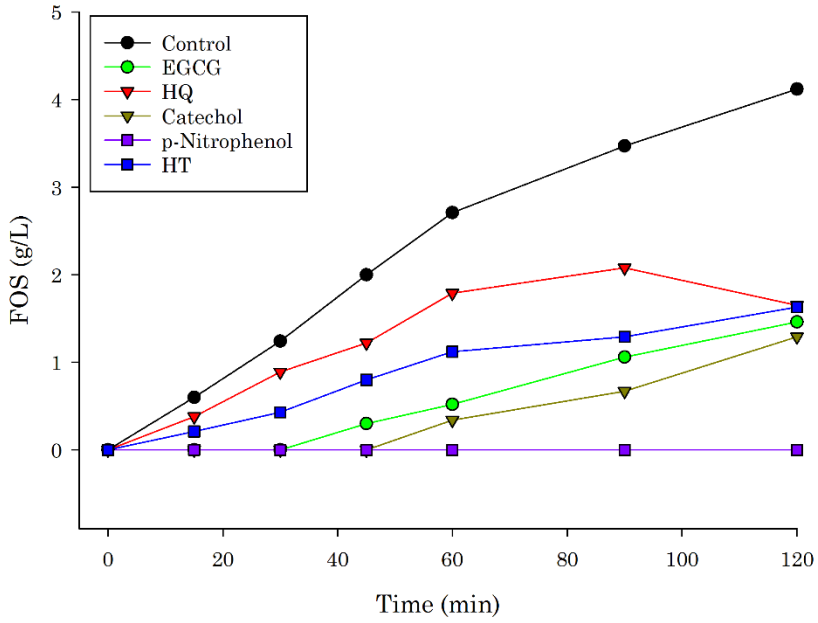

Figure 4.11. FOS production in absence and presence of various phenolic compounds. Reaction conditions: 100 g/L of sucrose and 20 g/L of phenolic compound in 100 mM sodium acetate buffer (pH 5.0) at 60 ºC.

HPLC analysis revealed that most of the polyphenols exert an inhibiting effect in both sucrose hydrolysis and FOS formation. Considering this, the hydrolysis and transfructosylation rates of each assay were calculated with the following equations:

$$Hydrolysis\,rate\ = \frac{\Delta[Fructose]}{time}$$

$$Transfructosylation\,rate = \frac{\Delta[Glucose]}{time} - \frac{\Delta[Fructose]}{time}$$

In addition, the ratio between the hydrolysis and transfructosylation rates was estimated, and they are all portrayed in **Table 4.3**.

Table 4.3 Effect of the assayed phenolic compounds on the hydrolytic and transfructosylation activity of pXd-INV.

	Structure	Hydrolysis rate (mM min^{-1})	Transfructosylation rate (mM min^{-1})	Hydrolysis / Transfructosylation ratio
Control	---------	1.545	0.482	**3.2**
Hydroxytyrosol	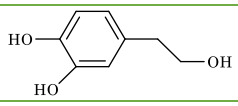	1.040	0.329	**3.2**
Hydroquinone	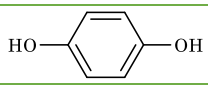	2.110	0.474	**4.5**
Catechol	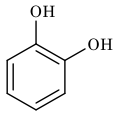	0.764	0.100	**7.7**
EGCG	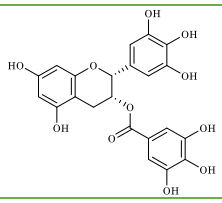	0.668	0.062	**10.8**
p-Nitrophenol	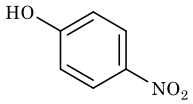	0.199	0.003	**67.1**

The majority of the phenolic compounds investigated (catechol, EGCG and *p*-nitrophenol) hindered hydrolysis as much as transfructosylation, and no new polyphenol conjugates were observed. Nevertheless, the hydrolysis and transfructosylation rates obtained with HT and HQ were similar to the ones estimated for the control assay, and they were both positive acceptors. After purifying the new HQ derivative by semipreparative HPLC, HQ fructosylation was demonstrated by mass spectrometry (Supplementary Material, **Figure S1**), which showed a peak of 295.08 Da ($M + Na^+$). As the two phenolic groups in HQ are equivalent, the synthesized derivative must be 4-hydroxyphenyl-β-D-fructofuranoside (**Figure 4.12**). Hydroquinone is mainly employed in the cosmetic industry as a tyrosinase inhibitor; however, it has some undesired side effects (skin irritation and inflammation). Lately, cosmetic companies had been substituting hydroquinone for α- and β-arbutin (HQ glucosides) that do not present these side effects (Desmet et al., 2012). The fructosylation of HT was furtherly studied and it will be described in the next section (**Section 4.3**).

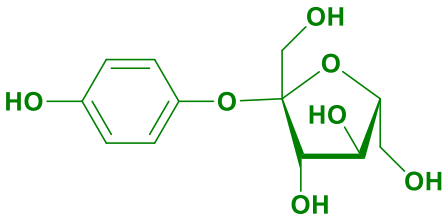

Figure 4.12. Predicted structure of the obtained HQ derivative (4-hydroxyphenyl-*β*-D-fructofuranoside).

Furthermore, crystallographic ternary complexes with the inactive mutant D80A-pXdINV, fructose and an acceptor (HQ) or an inhibitor (EGCG) were obtained. In all cases, fructose was situated in the -1 subsite and polyphenols were located in the active site by hydrophobic interactions (**Figure 4.13**). EGCG was additionally stabilized on the active site by numerous polar interactions, probably blocking substrate access and explaining the inhibitory effect. On the other hand, hydroquinone seemed to have some mobility in the active site, which could enable transfructosylation.

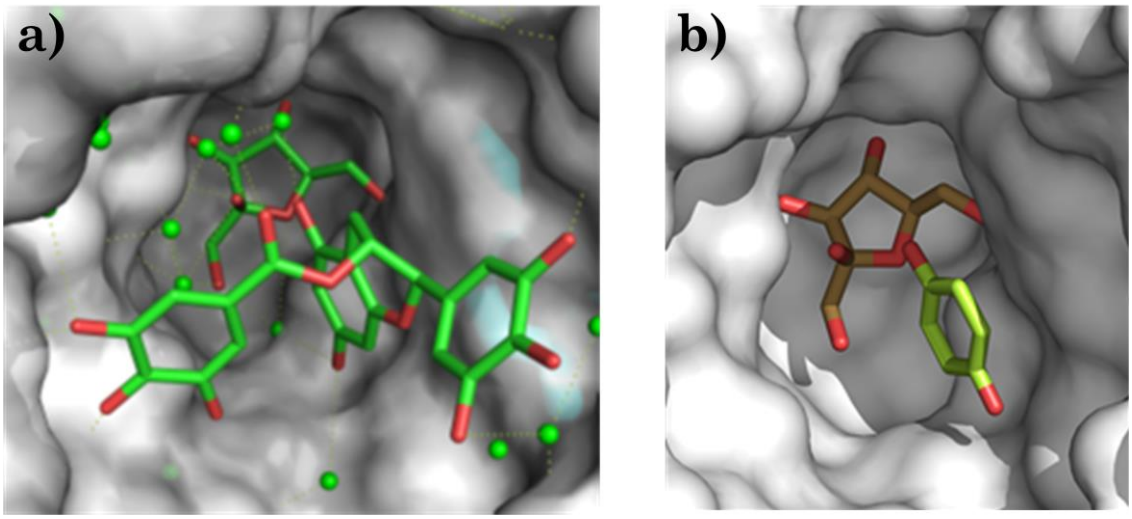

Figure 4.13. Surface depiction of D80A-pXdINV with fructose and two phenolic compounds in the active site. a) Crystals soaked with fructose and EGCG (both in green) and b) Crystals soaked with fructose (orange) and HQ (light green).

4.3 Production of fructosylated hydroxytyrosol conjugates by pXd-INV

4.3.1 Fructosylation of HT by pXd-INV

Out of the positive acceptors found in the previous experiments, hydroxytyrosol (HT) was the most interesting due to its strong biological activities (antioxidant,

anticancer, neuroprotective, etc.). Hence, we decided to further explore the ability of the enzyme pXd-INV to fructosylate this phenolic compound. Several assays were carried out employing sucrose as donor and HT as acceptor. HPLC analysis using an amino column and a photodiode array detector revealed the presence of two possible fructosylated HT conjugates (Fru-HT1 and Fru-HT2) (**Figure 4.14a**). Both products showed a higher retention time than HT, supporting the hypothesis that they were, in fact, fructosylated derivatives of HT. Fru-HT1 was found in a larger proportion, indicating that it was the major HT conjugate (**Figure 4.14a**). Moreover, FOS production was analyzed by anion exchange chromatography with an amperometric detector (HPAEC-PAD) to check that HT did not influence the FOS profile (**Figure 4.14b**). As shown, product selectivity was not changed since neokestose and 1-kestose were still the main transglycosylation products.

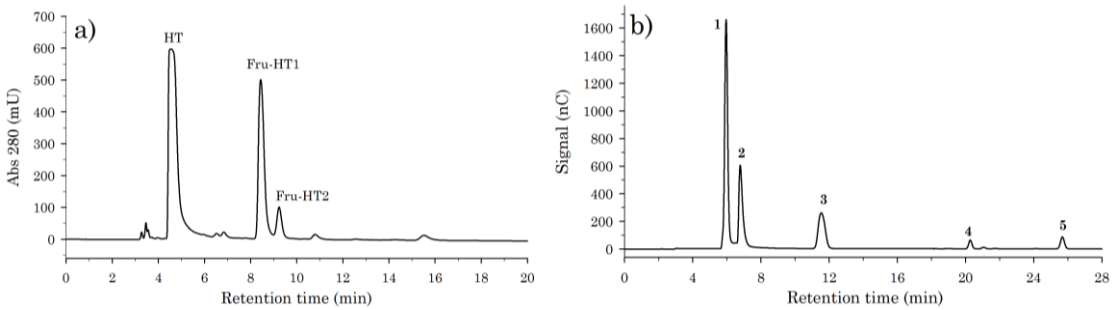

Figure 4.14. HPLC analysis of the HT fructosylation assay catalyzed by pXd-INV. Reaction conditions: 300 g/L of sucrose and 25 g/L of HT in 100 mM sodium acetate buffer (pH 5.0) at 60 ºC. a) Chromatogram employing a NH2 column and PDA detector. (HT) Hydroxytyrosol; (Fru-HT1 and Fru-HT2) Hydroxytyrosol fructosides. b) HPAEC-PAD chromatogram with a PA1 column. Peaks: (1) Glucose; (2) Fructose; (3) Sucrose; (4) 1-Kestose; (5) Neokestose.

The production of the fructosylated HT derivatives, Fru-HT1 and Fru-HT2, was optimized by evaluating different donor and acceptor concentrations (**Figure 4.15**). First, sucrose concentration was kept at 100 g/L while HT concentration was varied in the 10-100 g/L range. The yield of fructosylated derivatives increased with HT concentration (**Figure 4.15a**); however, this growth was quite modest when changing from 25 g/L to 100 g/L of HT. Taking into account the product yield and HT cost, we selected 25 g/L as the optimum HT concentration.

In order to furtherly improve product yield, sucrose concentration was also investigated in the 100-600 g/L range (**Figure 4.15b**). The highest product

concentration (11.7 g/L) was achieved after 6 h with 300 g/L of sucrose. Higher sucrose concentrations did not improve Fru-HT yield probably due to pXd-INV favoring sucrose as acceptor and consequently FOS production.

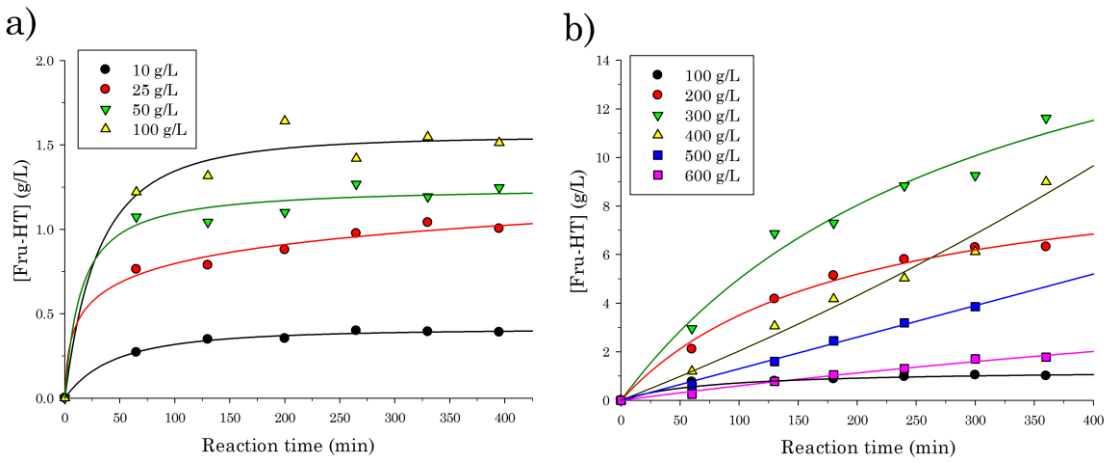

Figure 4.15. Production of fructosylated hydroxytyrosol derivatives (Fru-HT1 and Fru-HT2) with pXd-INV. a) Effect of HT concentration with sucrose concentration fixed at 100 g/L. b) Effect of sucrose concentration with HT concentration set at 25 g/L. The different sucrose and HT assayed concentrations are displayed on each panel.

Considering the previous experiments, the kinetics of Fru-HT and FOS production were studied under the chosen optimal conditions (25 g/L of HT and 300 g/L of sucrose). **Figure 4.16** represents the synthesis of Fru-HT1 and Fru-HT2 as a function of sucrose consumption. The maximum yield of fructosylated HT conjugates was 45.6% with 11.1 g/L of Fru-HT1 and 0.2 g/L of Fru-HT2, and it was obtained after almost 80% of the initial sucrose had been consumed. The main product (Fru-HT1) was only hydrolyzed when sucrose decreased below 5% of the initial concentration, and by the end of the reaction Fru-HT1 was practically inexistent. Thus, the reaction profile was the typically observed for glycosidase-catalyzed synthesis, where the product ends up hydrolyzed when the substrate is nearly consumed (Potocka et al., 2015, Piedrabuena et al., 2016). In contrast, Fru-HT2 was more resistant to hydrolysis, even though its concentration was significantly lower. As shown, Fru-HT1 and FOS formation profiles were quite similar, and FOS production was in agreement with the results obtained in this Thesis (**Figure 4.4**) and previous works (Gimeno-Pérez et al., 2015)

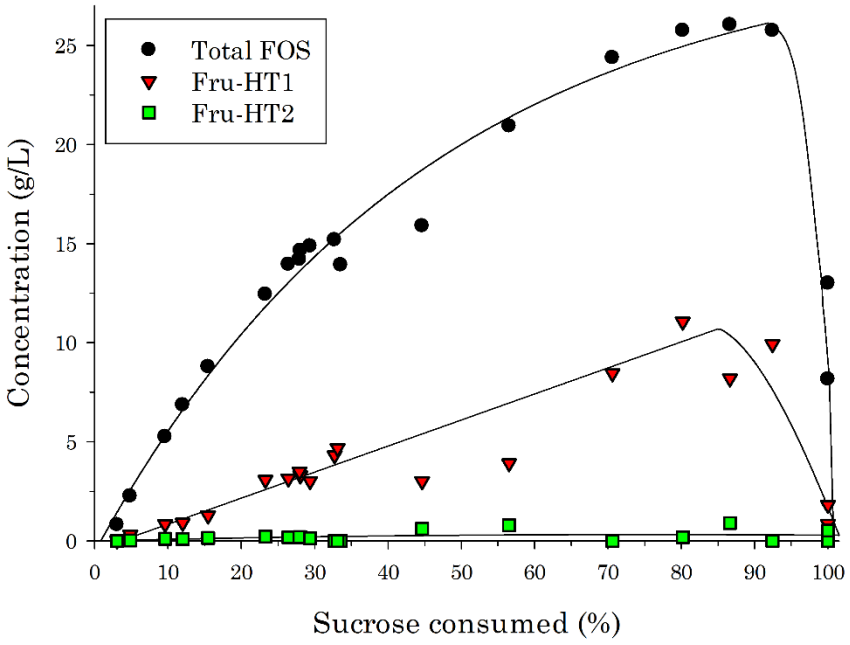

Figure 4.16. Production of fructosylated hydroxytyrosol conjugates (Fru-HT1 and Fru-HT2) and FOS by pXd-INV represented as a function of sucrose consumption under optimum reaction conditions (300 g/L of sucrose as donor and 25 g/L of HT as acceptor in 100 mM sodium acetate buffer, pH 5.0, at 60 ºC).

The major fructosylated conjugate (Fru-HT1) was purified by semipreparative HPLC and characterized by mass spectrometry (Supplementary Material, **Figure S2**), which showed a peak of 339.10 Da ($M + Na^+$). The structure of the compound was determined by 1D and 2D NMR techniques in collaboration with Dr. Jesús Jiménez Barbero and Dr. Ana Poveda (CIC Biogune, Basque Country, Spain). The synthesized product was identified as 3,4-dihydroxyphenyl ethyl β-D-fructofuranoside (Supplementary Material, **Figure S3**), and its structure is depicted in **Figure 4.17**.

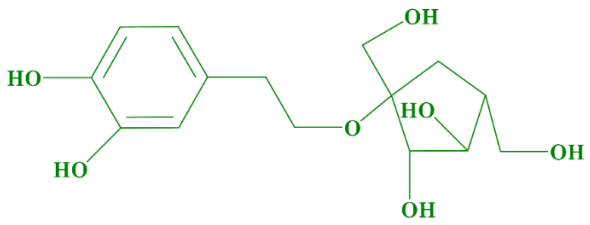

Figure 4.17. Structure of Fru-HT1 (3,4-dihydroxyphenyl ethyl *β*-D-fructofuranoside) determined by NMR.

4.3.2 Structural and molecular analysis of HT fructosylation by pXd-INV

The structural and molecular determinants of the reaction were investigated by crystallographic studies in collaboration with Dr. Julia Sanz Aparicio (IQFR, CSIC, Madrid, Spain). Thus, crystals from the inactive mutant pXd-INV-D80A were soaked with both substrates, fructose and HT, and the purified product (Fru-HT1), to obtain the ternary intermediate complexes. The obtained crystals displayed clear electron density at the active site, enabling unambiguous modelling of the confined molecules (**Figure 4.18**).

The ternary intermediate complex with both substrates displays fructose on the −1 subsite, as described in previous studies (Ramirez-Escudero et al., 2016). On the other hand, HT can be located in several positions in the active site (HT1, HT2 and HT3) (**Figure 4.18a**). Two of these positions (HT1 and HT2) are compatible with fructosylation since both substrates show OH groups in the vicinity of fructose C2, allowing the formation of the glycosidic bond. In this manner, HT2 exhibits one phenolic hydroxyl placed 3.5 Å from fructose C2, which is an appropriate distance for the nucleophilic attack to occur. On the contrary, the primary OH of HT1 is the closest to fructose C2, albeit the distance is a bit higher. Thus, the location of HT1 is in accordance with the major product (Fru-HT1) whereas the position of HT2 indicates a different binding manner that could result on another fructosylated product, which could be related with the minor product detected by HPLC. The last location (HT3) is at a considerable distance from the fructose molecule, preventing fructosylation.

Regarding the soakings obtained with the product (**Figure 4.18b**), we observed a fructosylated HT compound positioned in the active site with the fructose unit on the −1 subsite. This compound was identified as the main product and fructosylation

occurred in the primary OH. In addition, a second molecule was surprisingly found in the active site that clearly corresponded to another fructosylated conjugate. In this case, fructosylation took place in the phenolic OH, which is in agreement with the second binding manner (HT2), and probably corresponds to the secondary product (Fru-HT2).

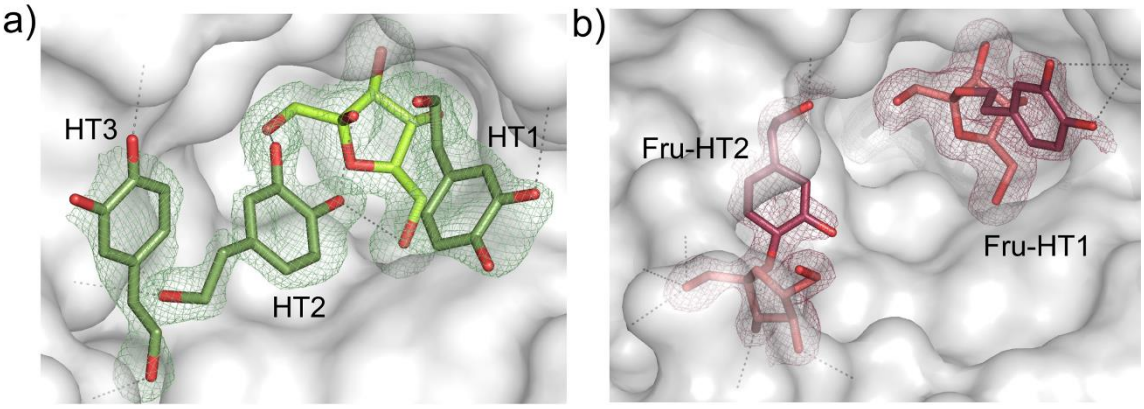

Figure 4.18. Surface depiction of pXd-INV-D80A with both substrates and product bound in the active site. a) Crystals soaked with fructose (light green) and HT (dark green). HT was located in three positions labelled as HT1, HT2 and HT3. b) Crystals soaked with the fructosylated product (fructose in light red and HT in dark red) purified by HPLC. Fru-HT1 is the main product characterized by NMR, and it will be formed when HT is located at HT1 binding site. Fru-HT2 is produced when HT fructosylation occurs at the HT2 position. The 2Fo-Fc electron density maps are contoured at 1 σ.

Therefore, pXd-INV is able to fructosylate hydroxytyrosol in two different manners, giving rise to two fructosylated conjugates (Fru-HT1 and Fru-HT2). **Figure 4.19** illustrates the reaction scheme.

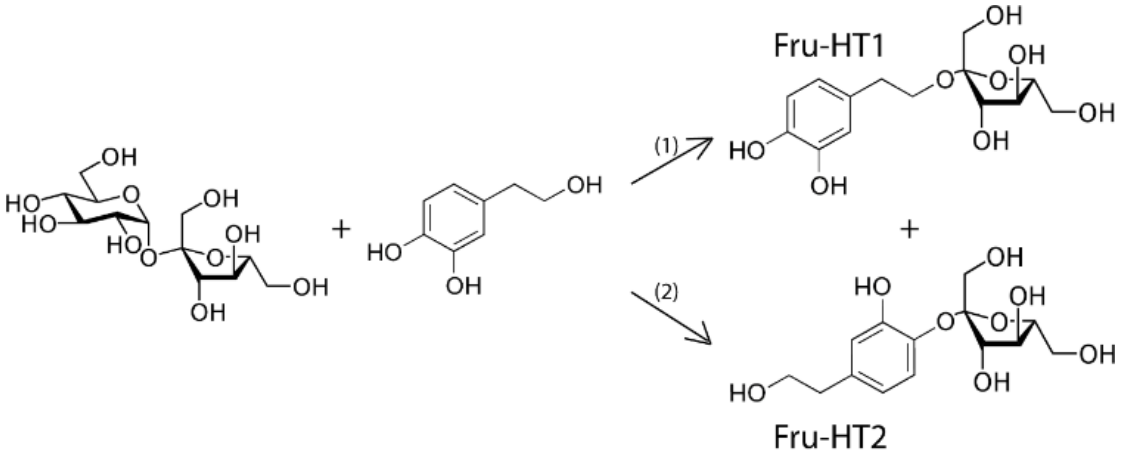

Figure 4.19. Reaction scheme of HT fructosylation by pXd-INV. Fru-HT1 is the main product characterized by NMR and Fru-HT2 is a secondary product identified by crystallography.

4.3.3 Site-Directed mutagenesis of pXd-INV

As previously explained, HT can be bound in two different manners at the active site of pXd-INV-D80A. A more detailed study of these binding modes revealed that they are mostly determined by packing to Trp105 or polar interaction with the loop Glu334-Asn342 (Míguez et al., 2018). Hence, specific mutagenesis at any of these residues could alter both transfructosylation activity and product selectivity.

Taking this into account, we decided to investigate the residues that belong to the Glu334-Asn342 loop, aiming to modulate product selectivity. Specifically, we chose to study changes in Gln341 and Asn342. Two pXd-INV mutants (Q341S and N342Q) were obtained by site-directed mutagenesis in the laboratory of Prof. Maria Fernández Lobato (Centro de Biología Molecular Severo Ochoa, UAM-CSIC, Madrid, Spain). The production of FOS and fructosylated derivatives of hydroxytyrosol (Fru-HT1 and Fru-HT2) was investigated with both mutants under optimum conditions (**Figure 4.20**).

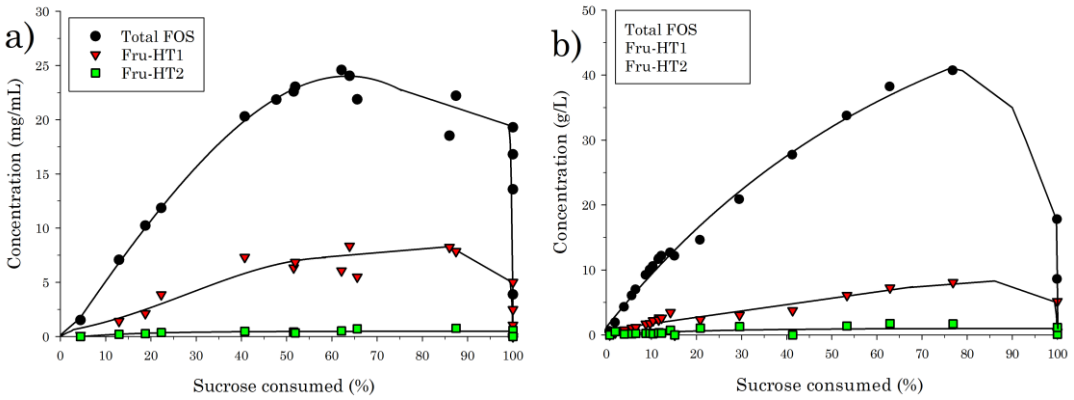

Figure 4.20. Production of fructosylated hydroxytyrosol conjugates (Fru-HT1 and Fru-HT2) and FOS under optimum reaction conditions (300 g/L of sucrose as donor and 25 g/L of HT as acceptor in 100 mM sodium acetate buffer, pH 5.0, at 60 ºC), represented as a function of sucrose consumption, employing the mutants. a) pXd-INV-Q341S and b) pXd-INV-N342Q.

In the same way as in the wild type reaction, the maximum yield of fructosylated conjugates was achieved when more than 80% of the initial sucrose was consumed. Nevertheless, the ratio between Fru-HT1 and Fru-HT2 was significantly different than the obtained for the wild type (**Table 4.4**).

Table 4.4 Maximum production of the fructosylated HT conjugates (FOS concentration at this time) by pXd-INV and its mutants.

Enzyme	**[Fru-HT1] (g/L)**	**[Fru-HT2] (g/L)**	**HT1/HT2**	**[FOS] (g/L)**
Wild-type	11.1	0.18	61.7	25.7
Q341S	7.9	0.76	10.4	22.2
N342Q	8.1	1.70	4.8	40.7

As shown, Fru-HT1 production was higher with the wild-type, but both mutants synthesized more Fru-HT2. The mutant N342Q was the most specific for the fructosylation at the phenolic OH. The function of these residues is still not clear, although these results confirm that the Glu334-Asn342 loop has a key role in the enzymatic mechanism.

Moreover, it is worth mentioning that the mutant N342Q exhibits a higher FOS yield compared with Q341S and the wild-type, probably due to favoring sucrose as acceptor.

4.4 Enzymatic production of acidic XOS

Another objective of this Thesis was the preparation of xylooligosaccharides (XOS) containing acidic ramifications such as glucuronic acid or related moieties (acidic XOS), Acidic XOS have very interesting biological properties (antioxidant, antimicrobial, anti-inflammatory or prebiotic, among other) that can be enhanced with respect to neutral XOS. We selected a glucurunoxylan such as that from beechwood as starting material. Among the different enzymes screened for the production of this kind of glycoderivatives, the commercial preparation Depol 670L gave rise to the highest concentration of acidic XOS as inspected by HPAEC-PAD (data not shown). Depol 670L is described by the manufacturer as a broad-spectrum carbohydrase blend that includes a wide range of activities such as cellulase, pectinase, ferulic acid esterase and exo-glycosidase. It is commercialized for the rupture of botanical tissue and the release of bound flavors.

Although endo-xylanase activity is not described in the manufacturer guidelines, xylanase activity was assayed by the DNS method, as described in the **Experimental Section 3.2.2**, and 960 U/mL were obtained. We considered this value high enough to attempt the efficient production of acidic XOS with this preparation.

4.4.1 Production of neutral and acidic XOS

XOS production was carried out with 2% (w/v) beechwood xylan and 3 U/mL of Depol 670L in distilled water at 60 ^{o}C. The synthesis of XOS was analyzed by HPAEC-PAD at different time points. **Figure 4.21** presents the chromatographic analysis of the XOS produced at 3 and 48 h. Neutral XOS were identified with commercial standards; however, acidic XOS characterization was not possible due to the lack of available standards. Nevertheless, acidic XOS should display high retention times in anion-exchange chromatography due to the presence of uronic acid residues that bind tightly to the column. Thus, we assumed that the peaks with higher retention times (right area of the chromatogram) were majorly acidic XOS.

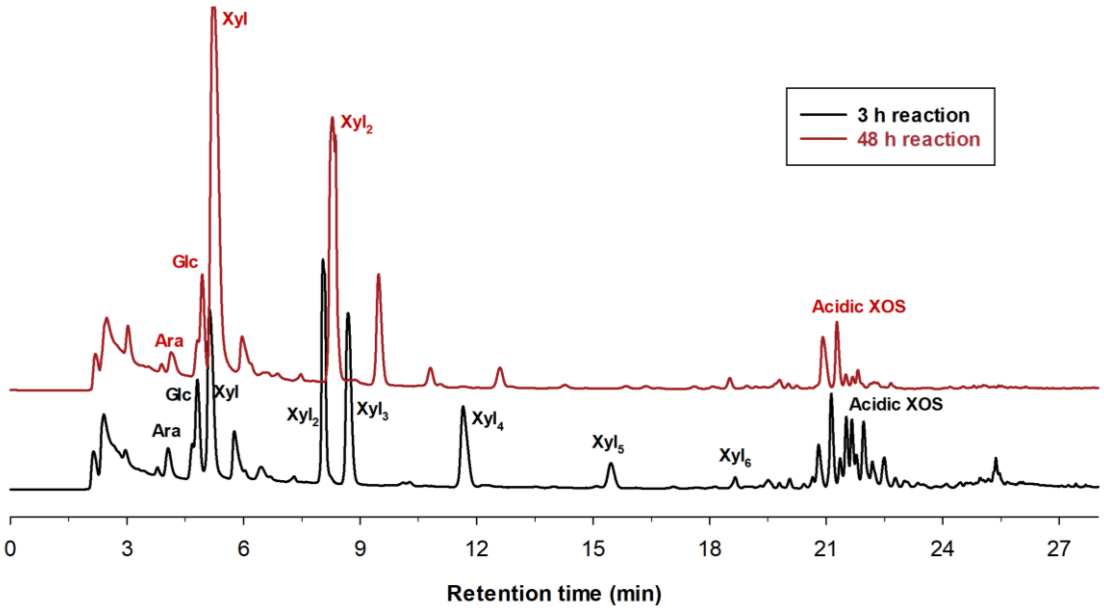

Figure 4.21. HPAEC-PAD chromatogram of the hydrolysis of 2% xylan at 3 and 48 h with Depol 670L. (Ara) Arabinose; (Glc) Glucose; (Xyl) Xylose; (Xyl_2) Xylobiose; (Xyl_3) Xylotriose; (Xyl_4) Xylotetraose; (Xyl_5) Xylopentaose; (Xyl_6) Xylohexaose.

As shown, the reaction mixture at 3 h presented a wide variety of peaks, including neutral xylooligosaccharides from X2 to X6, as well as numerous peaks that could correspond to acidic XOS (high retention time). On the other hand, XOS production at 48 h showed less diversity. The neutral fraction fundamentally consisted of xylose and xylobiose, while the acidic one was significantly enriched in two peaks.

Bearing in mind that our objective was the purification of acidic XOS, we selected 72 h as the optimum reaction time, seeking to facilitate the purification process.

4.4.2 Anion-exchange purification of acidic XOS

Neutral and acidic XOS were separated by anion-exchange chromatography employing Sep-Pak cartridges, as explained in **Section 3.7.2**. Two different fractions were obtained: the neutral fraction and the acidic fraction. Both fractions were analyzed by HPAEC-PAD to check the effectiveness of the separation (**Figure 4.22**).

As shown, the separation was quite efficient, although the neutral fraction was slightly contaminated with acidic XOS. As previously observed, the neutral fraction

was majorly composed by xylose and xylobiose, and the acidic fraction was enriched in one unidentified product.

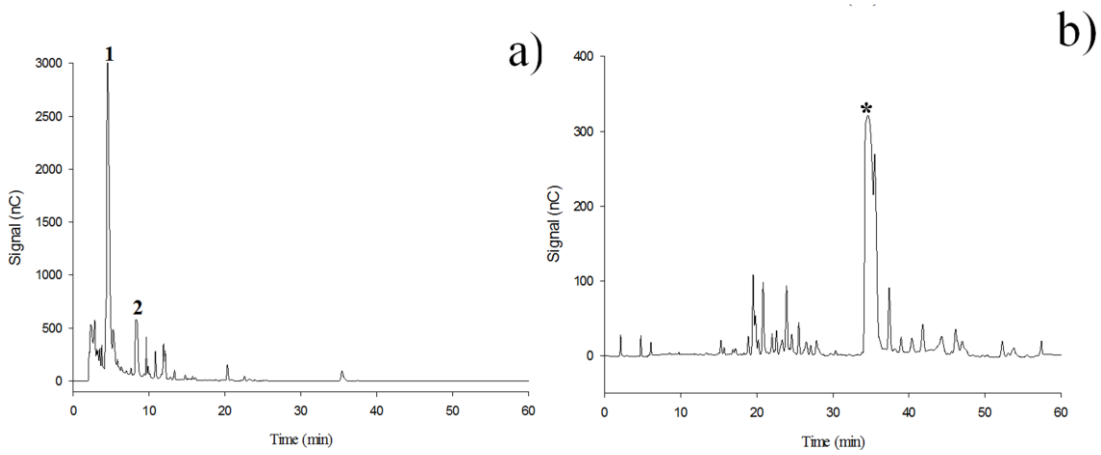

Figure 4.22. HPAEC-PAD analysis of the a) Neutral fraction and b) Acidic fraction. Identified peaks: (1) Xylose; (2) Xylobiose. (*) Main peak of the acidic fraction.

Considering the enrichment of the acidic fraction in one main product, we decided to scale both the reaction and the purification methodology to attempt the identification and characterization of this product.

Thus, xylan hydrolysis was carried out at a larger scale (100 mL) and reaction conditions were kept as before, excluding reaction time that was increased to 72 h. Taking into account the loss of product diversity from 3 h to 48 h, we expected that the acidic fraction would be additionally enriched in this main product.

As described in **Section 3.7.3**, the purification was adapted to the larger scale, employing several Sep-Pak cartridges in series. Moreover, we added a desalinization step to improve the purification process. The removal of the remaining salts was done by dialysis in 100-500 Da tubing. After freeze-drying, the product was characterized by HPAEC-PAD, mass spectrometry and NMR. In addition, salt content was determined by elemental analysis (measuring the amount of nitrogen in the sample).

In agreement with HPAEC-PAD analysis, mass spectrometry (MALDI-TOF) showed a majoritarian product with a mass of 495.2 Da, which could correspond to methyl-glucuronosyl xylobiose ($M + Na^+$) and an additional peak of 511.1 Da that could correspond to the same product ($M + K^+$) (**Figure 4.23**). In addition, some

minor peaks were observed that corresponded to methyl-glucuronosyl xylosides (X3-X6).

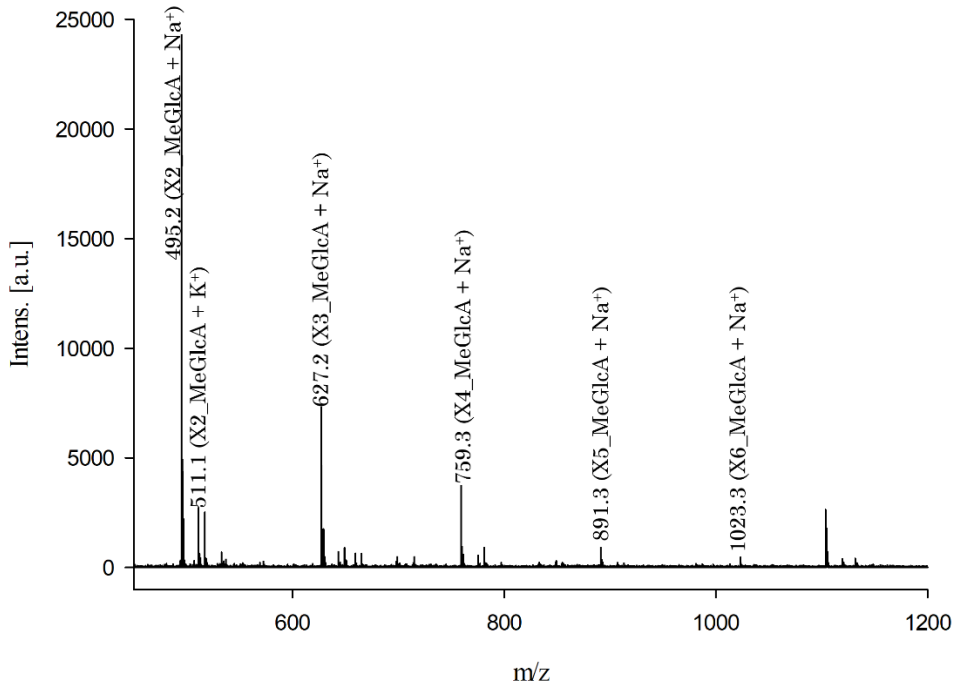

Figure 4.23. Characterization of the acidic fraction by mass spectrometry (MALDI-TOF). Peaks: X2_MeGlcA (methyl-glucuronic xylobiose); X3_MeGlcA (methyl-glucuronic xylotriose); X4_MeGlcA (methyl-glucuronic xylotetraose); X5_MeGlcA (methyl-glucuronic xylopentaose); X6_MeGlcA (methyl-glucuronic xylohexaose).

The structure of the main compound was determined by 1D and 2D NMR techniques (Supplementary Material, **Table S1**) and is depicted in **Figure 4.24**. The purified acidic XOS was 2'-O-α-(4-O-methyl-α-D-glucuronosyl)-xylobiose (MeGlcA-*α*-1,2-Xyl*β*-1,4-Xyl). The acidic XOS yield was approximately 5%, meaning that we obtained about 100 mg of this acidic fraction from 2 g of beechwood xylan. Also, salt percentage (ammonium acetate) was estimated to be almost 20% of the final product.

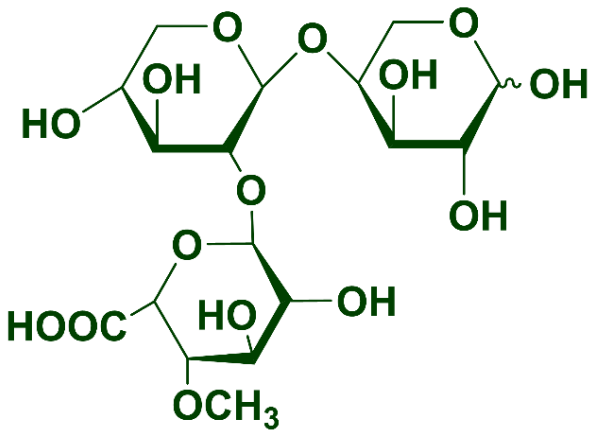

Figure 4.24. Structure of 2'-O-α-(4-O-methyl-α-D-glucuronosyl)-xylobiose elucidated by NMR.

4.4.3 Antioxidant activity of acidic XOS

The antioxidant activity of the purified product was investigated by measuring the $ABTS^{\cdot+}$ radical discoloration. This assay was previously validated for determining XOS antioxidant activity (Valls et al., 2018). Trolox was used as a reference but TEAC values were not calculated, since the molar concentration of the acidic fraction could not be determined. Considering this, the half-maximum scavenging concentration (SC_{50}) was defined as the concentration (mg/mL) necessary to decrease 50% of the absorbance of the $ABTS^{\cdot+}$ radical in ten minutes.

Thus, we assayed the antioxidant activity of the purified product at several concentrations in the 0-8 mg/mL range. In addition, the antioxidant activities of both neutral XOS and beechwood xylan were investigated and compared with our product activity (**Figure 4.25**). Moreover, half-maximum scavenging concentrations were calculated for all the compounds assayed (**Table 4.5**).

As shown, X2_MeGlcA has the highest antioxidant activity of the assayed compounds, with the exception of Trolox, which is in a different scale. Unexpectedly, neutral XOS had no activity, suggesting that the activity found in XOS mixtures is strongly related to the degree and nature of the ramifications. This result is in agreement with the obtained in previous works (Valls et al., 2018). Valls and cols. measured the antioxidant activity of several XOS mixtures (acidic XOS, neutral and acidic XOS and neutral XOS), xylose and methyl-glucuronic acid; they found that only the mixtures containing acidic XOS showed antioxidant activity. In addition,

they measured the antioxidant capacity of two acidic XOS mixtures (low and high molecular weight) and glucuronoxylan, determining that xylan had the lowest activity, while the high molecular weight fraction of acidic XOS showed the highest activity. This is also in accordance with our results, where glucuronoxylan showed less activity than the obtained acidic XOS (low molecular weight), indicating that polymerization degree also influences antioxidant activity. The lower activity of xylan may be due to the smaller proportion of uronic residues per molecule compared with the acidic XOS.

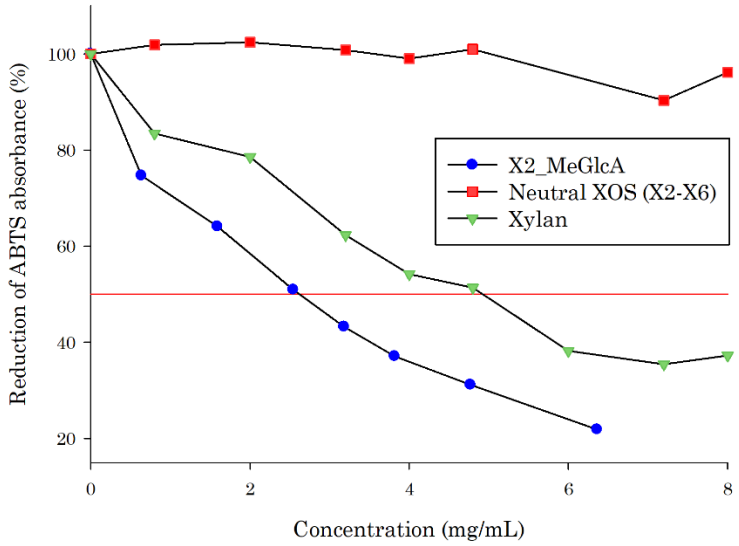

Figure 4.25. Antioxidant activity of neutral XOS, beechwood xylan and acidic XOS (X2_MeGlcA).

Table 4.5 Half-maximal scavenging activity of beechwood xylan, neutral XOS and X2_MeGlcA, compared with Trolox

Compound	SC_{50} (mg/mL)
Neutral XOS	-
Xylan	4.71
X2_MeGlcA	2.55
Trolox	0.004

4.5 Large-scale production of COS

Chitooligosaccharides (COS) are produced by hydrolysis of chitosan or chitin. Depending on the substrate source and the enzyme employed, a wide diversity of products can be obtained. As previously mentioned, COS can be classified in three different groups: fully deacetylated COS (fdCOS), fully acetylated COS (faCOS), and partially acetylated COS (paCOS). Several biological activities have been reported for the three families (Liaqat et al., 2018), and these properties are strongly influenced by their degree of polymerization (MW), pattern of acetylation (PA) and degree of deacetylation (DD) (Hamer et al., 2015). The preparation and characterization of well-defined COS mixtures is quite difficult and scarcely reported (Li et al., 2016). In this work, we developed a single methodology for the large-scale production of several COS mixtures with different sizes and deacetylation degrees. In addition, products were characterized by HPAEC-PAD and mass spectrometry.

4.5.1 Large-scale procedure for COS synthesis

On the basis of previous works (Santos-Moriano et al., 2018a, Kidibule et al., 2018), we selected the commercial proteolytic preparation Neutrase 0.8L and the chitinase Chit42 from *Trichoderma harzianum* to scale-up the synthesis of several COS mixtures. Neutrase 0.8L is a proteolytic preparation from *Bacillus amyloliquefaciens* that had previously shown moderate activity towards chitosan (Santos-Moriano et al., 2016). Chitinase CHIT 42 belongs to the GH18 family and mainly catalyzes the production of $(GlcNAc)_2$ with chitin as substrate (Kidibule et

al., 2018).Various commercial and non-commercial chitosans were hydrolyzed with one or both enzymes. A common procedure was designed for the large-scale production of diverse COS mixtures (**Figure 4.26**). Chitosan (1% w/v) was dissolved in sodium acetate buffer (pH 5.0) and hydrolysis was carried out at 35-50 ^{o}C for 48-72 h. Afterwards, enzymes and the remaining chitosan were removed by ultrafiltration with a 10 kDa membrane. Then, ultrafiltration with a 1 kDa membrane was only applied to some mixtures, producing high or low molecular weight COS. Finally, salts and small contaminants were eliminated by dialysis with 100-500 Da tubing, and COS fraction were freeze-dried.

Fully-deacetylated COS (fdCOS) were produced by hydrolysis of chitosan (CHIT600), which is more than 90% deacetylated, with the commercial preparation Neutrase 0.8L. In addition, ultrafiltration (1kDa) was employed to obtain a low molecular weight mixture of fdCOS.

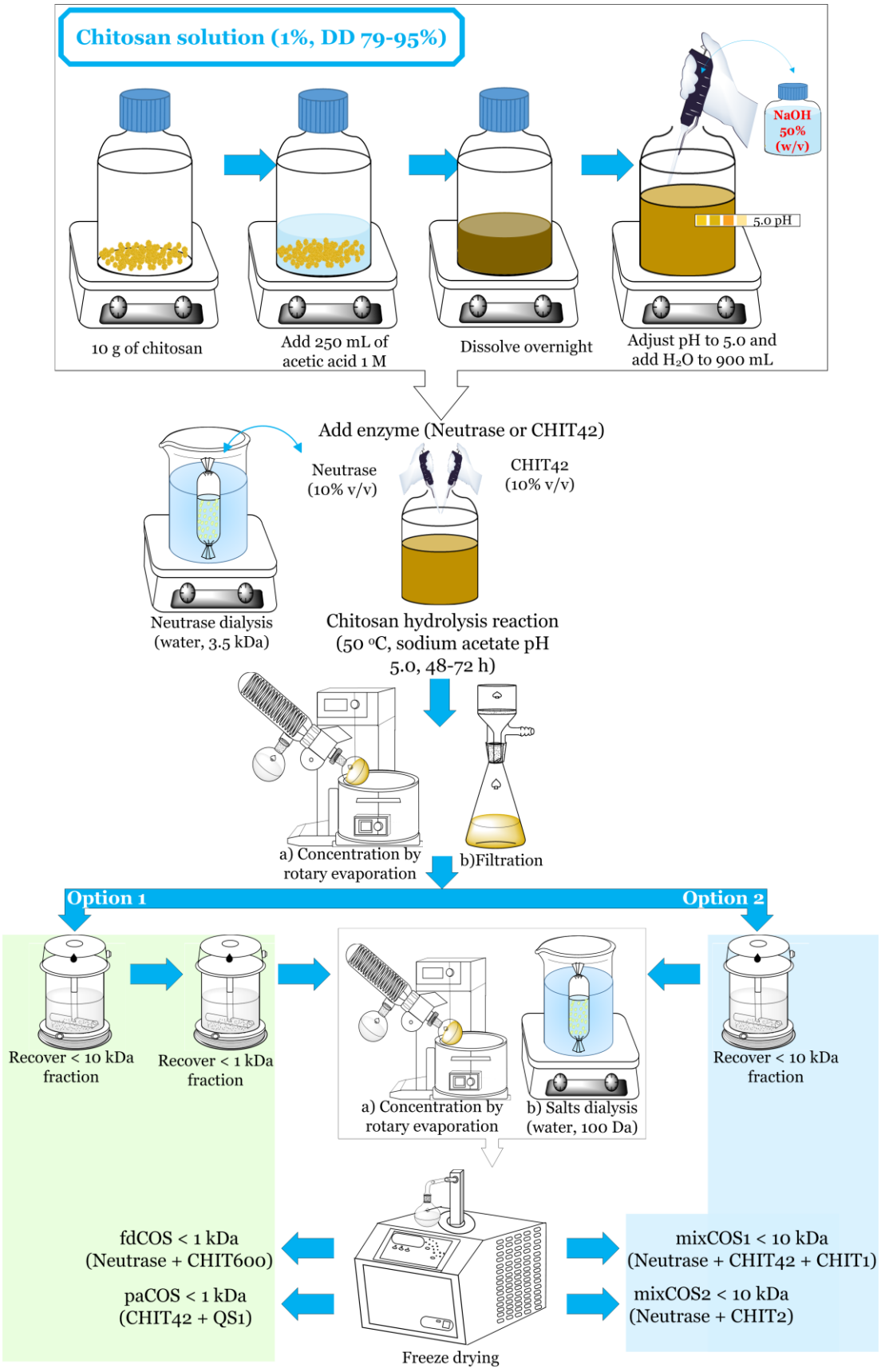

Figure 4.26. Large-scale procedure for COS production.

Partially acetylated chitooligosaccharides (paCOS) were synthesized employing chitosan QS1, with about 80% deacetylation degree, and chitinase CHIT42 at 35 ºC. This enzyme requires an N-acetyl-glucosamine residue in the -1 substrate position to achieve hydrolysis. Ultrafiltration with a 1 kDa membrane was also applied to obtain low molecular weight paCOS.

For the preparation of COS mixtures with higher molecular weight, two chitosans provided by the company Anfaco-Cecopesca were employed. They were less pure and their deacetylation degree varied between 79.4% and 94.7%. Chitosans CHIT1 and CHIT2 were both hydrolyzed with 10% of Neutrase 0.8L. For these mixtures, the 1 kDa cut-off was not used, hence, high molecular weight COS mixtures could be obtained. The deacetylation degree of CHIT2 (79.4%) and the use of Neutrase 0.8L, which only cleaves GlcN-GlcN bonds, resulted in a COS fraction enriched in both fdCOS and paCOS. On the other hand, CHIT1 had a higher deacetylation degree (94.7%), but we still detected several paCOS.

Figure 4.27 represents the reactions carried out and the products obtained. COS production with CHIT42 was done at 35 ºC, while reactions with Neutrase 0.8L were incubated at 60 ºC.

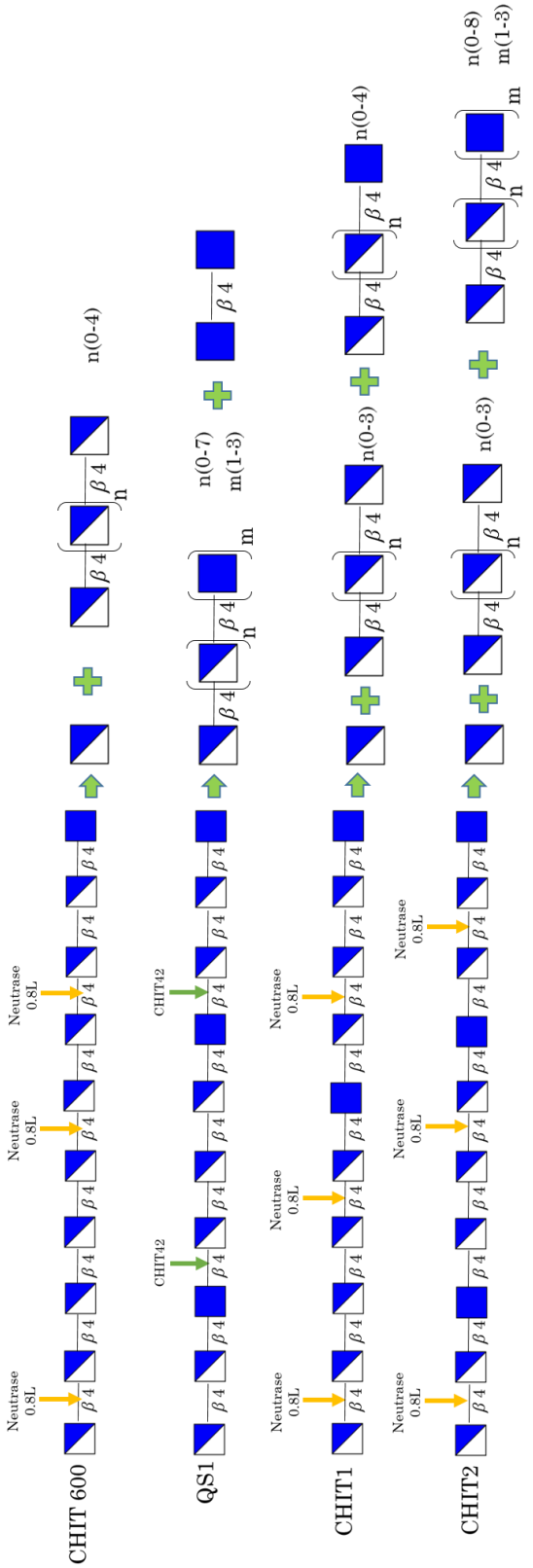

Figure 4.27. Schematic representation of the reactions carried out to hydrolyze chitosan by the different enzymes and the products obtained for each of them.

4.5.2 Characterization of COS mixtures

The different COS fractions were analyzed by HPAEC-PAD chromatography and MALDI-TOF mass spectrometry.

a) fdCOS with MW < 1 kDa

The HPAEC-PAD chromatogram of the fdCOS fraction of low molecular weight (< 1 kDa), obtained with CHIT600 and Neutrase 0.8L, is illustrated in **Figure 4.28**. As shown, four main peaks were identified as fdCOS, with the corresponding standards. Chitobiose ($(GlcN)_2$) and chitotriose ($(GlcN)_3$) were the major products. The characterization of some peaks was not possible due to the lack of standards. The MALDI-TOF spectrum of the COS mixture is shown in the Supplementary Material, **Figure S4**. HPAEC-PAD and MALDI-TOF were in agreement, since the main *m/z* peaks matched the molecular weight of the fdCOS previously identified by chromatographic analysis.

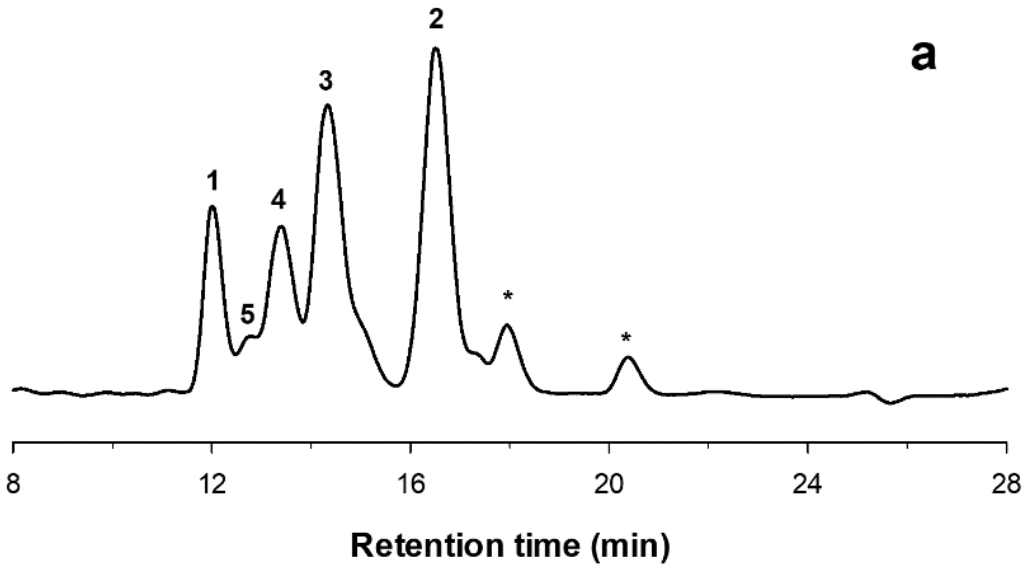

Figure 4.28. HPAEC-PAD chromatogram of the COS produced with CHIT600 and Neutrase 0.8L. Reaction conditions: 1% (w/v) chitosan, 10% (v/v) Neutrase 0.8L in sodium acetate buffer (pH 5.0) at 50 ºC for 48 h. Peaks: (1) GlcN; (2) $(GlcN)_2$; (3) $(GlcN)_3$; (4) $(GlcN)_4$; (5) $(GlcN)_5$.

Table 4.6 compiles the main *m/z* signals and their composition. Some masses corresponding to partially acetylated COS (paCOS) were detected by mass spectrometry, but with notably lower intensity than the observed for peaks

corresponding to fdCOS. These paCOS probably corresponded to the unidentified peaks in the HPAEC-PAD chromatogram (**Figure 4.28**). Nevertheless, their chemical structure could not be determined with the available data.

Table 4.6 Main identified signals in the MALDI-TOF mass spectrum of the reaction between chitosan CHIT600 and Neutrase 0.8L.

m/z	**Assignation**
180.0	GlcN + H^+
363.1	$(GlcN)_2$ + Na^+
524.2 / 540.2	$(GlcN)_3$ + Na^+ (K^+)
566.2 / 582.2	$(GlcN)_2$-GlcNAc + Na^+ (K^+)
685.3 / 701.3	$(GlcN)_4$ + Na^+ (K^+)
727.3 / 743.3	$(GlcN)_3$-GlcNAc + Na^+ (K^+)
846.3 / 862.2	$(GlcN)_5$ + Na^+ (K^+)
888.3 / 904.3	$(GlcN)_4$-GlcNAc + Na^+ (K^+)
1023.3	$(GlcN)_6$ + K^+
1049.4	$(GlcN)_5$-GlcNAc + Na^+
1210.4	$(GlcN)_6$-GlcNAc + Na^+

b) paCOS with MW < 1 kDa

The identification of peaks in the chromatographic analysis of partially acetylated COS (paCOS) was not possible due to the lack of commercial standards. **Figure 4.29** illustrates this fact with the presence of up to 11 unidentified peaks in the HPAEC-PAD analysis of the mixture. Hence, mass spectrometry analysis was of the utmost importance. The MALDI-TOF spectrum is represented in the Supplementary Material, **Figure S5**.

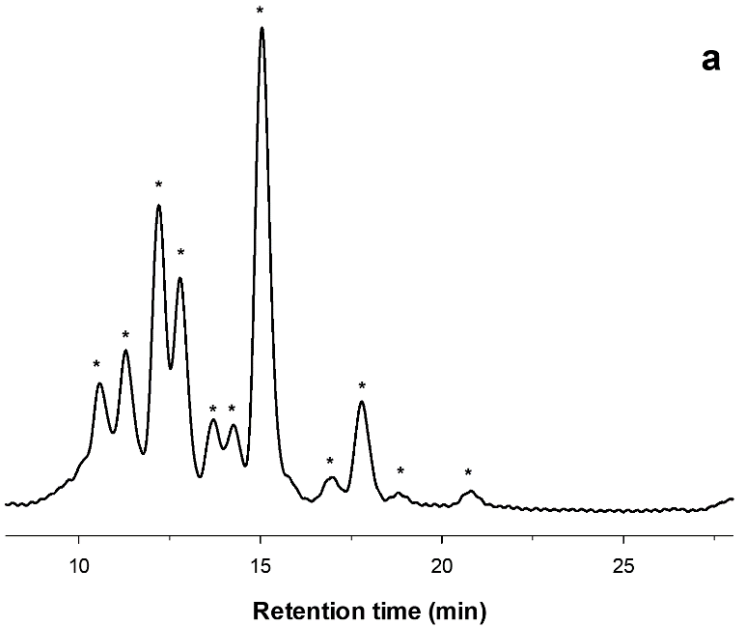

Figure 4.29. HPAEC-PAD chromatogram of the COS produced with QS1 and CHIT42. Reaction conditions: 1% (w/v) chitosan, 10% (v/v) CHIT42 in sodium acetate buffer (pH 5.0) at 35 ºC for 48 h.

Table 4.7 summarizes the main *m/z* peaks and the suggested composition. Nonetheless, the chemical structure of these compounds cannot be assumed with the MALDI-TOF data. Since chitinase Chit42 only hydrolyzes chitosan when a GlcNAc residue is located at the −1 position, the obtained COS should present a GlcNAc at the reducing end. **Table 4.7** includes COS containing up to nine residues, with GlcN being the major constituent, which agrees with the deacetylation degree of chitosan QS1.

Table 4.7 Main identified signals in the MALDI-TOF mass spectrum of the reaction between chitosan QS1 and CHIT42.

m/z	Assignation
405.2/421.2	GlcN-GlcNAc + Na^+ (K^+)
447.2/463.2	$(GlcNAc)_2$ + Na^+ (K^+)
566.3/582.2	$(GlcN)_2$-GlcNAc + Na^+ (K^+)
608.3/624.3	GlcN-$(GlcNAc)_2$ + Na^+ (K^+)
727.3/743.3	$(GlcN)_3$-GlcNAc + Na^+ (K^+)
769.3/785.3	$(GlcN)_2$-$(GlcNAc)_2$ + Na^+ (K^+)
811.3/827.3	GlcN-$(GlcNAc)_3$ + Na^+ (K^+)
888.4/904.3	$(GlcN)_4$-GlcNAc + Na^+ (K^+)
930.4/946.3	$(GlcN)_3$-$(GlcNAc)_2$ + Na^+ (K^+)
1049.4/1065.4	$(GlcN)_5$-GlcNAc + Na^+ (K^+)
1091.4/1107.4	$(GlcN)_4$-$(GlcNAc)_2$ + Na^+ (K^+)
1133.4/1149.4	$(GlcN)_3$-$(GlcNAc)_3$ + Na^+ (K^+)
1210.4/1226.4	$(GlcN)_6$-GlcNAc + Na^+ (K^+)
1252.5/1268.4	$(GlcN)_5$-$(GlcNAc)_2$ + Na^+ (K^+)
1294.5/1310.4	$(GlcN)_4$-$(GlcNAc)_3$ + Na^+ (K^+)
1413.5/1429.5	$(GlcN)_6$-$(GlcNAc)_2$ + Na^+ (K^+)
1532.6/1548.5	$(GlcN)_8$-GlcNAc + Na^+ (K^+)
1574.6/1590.5	$(GlcN)_7$-$(GlcNAc)_2$ + Na^+ (K^+)

c) COS mixtures < 10 kDa

COS mixtures prepared by hydrolysis of the chitosans provided by ANFACO-CECOPESCA, were also characterized by HPAEC-PAD and mass spectrometry (MALDI-TOF), although, the chromatographic analysis was complicated due to the complexity of the mixtures. Considering this, the HPAEC-PAD method was optimized employing a PA100 column to enable an improved separation (**Section 3.3.3**).

In the first case, the chromatographic analysis of the fdCOS and paCOS mixture was quite complex due to the lack of standards for paCOS and the overlapping of several peaks (**Figure 4.30**). As in the previous case, mass spectrometry was very important, since it enabled product identification. **Figure 4.30** shows the analysis by HPAEC-PAD that allowed the identification of glucosamine (GlcN), chitobiose ($(GlcN)_2$), chitotriose ($(GlcN)_3$) and chitotetraose ($(GlcN)_4$).

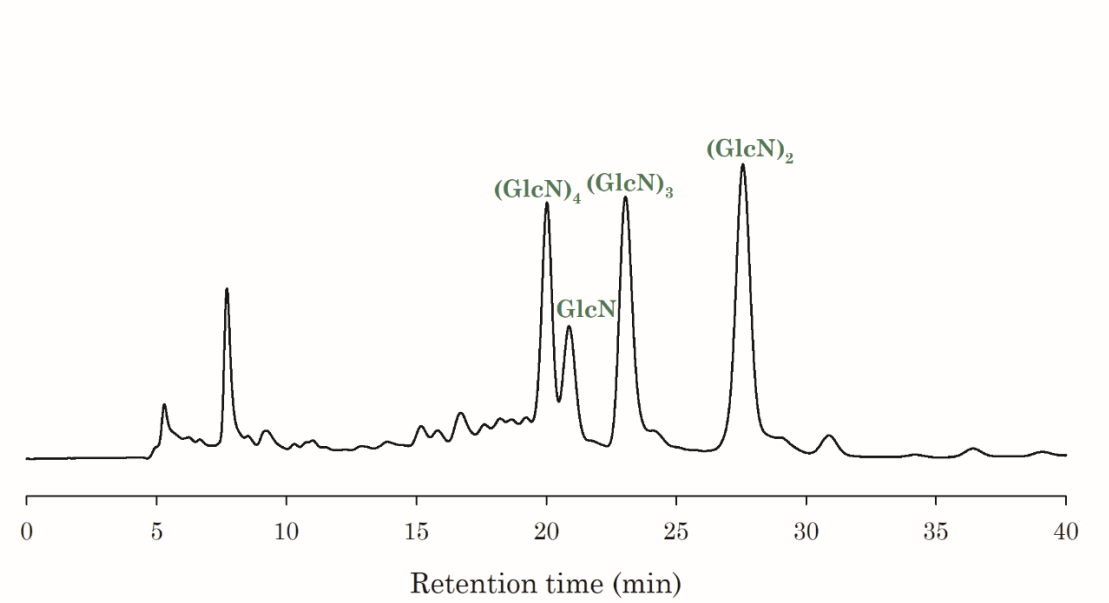

Figure 4.30. HPAEC-PAD chromatogram of the COS produced with CHIT1 and Neutrase 0.8L. Reaction conditions: 1% (w/v) chitosan, 10% (v/v) Neutrase 0.8L in 250 mM ammoniun acetate buffer (pH 5.0) at 60 ºC for 48 h.

As in the previous case, numerous peaks could not be identified due to the lack of standards. Thus, mass spectrometry analysis (MALDI-TOF) was carried out (Supplementary Material, **Figure S6**), and **Table 4.8** lists the main *m/z* signals detected and their composition. Considering the high deacetylation degree of CHIT1 (94.7%), fdCOS should be the main product, but several signal corresponding to paCOS were also detected.

Table 4.8 Main identified signals in the MALDI-TOF mass spectrum of the reaction with chitosan CHIT1 and Neutrase 0.8L.

m/z	Assignation
180.0/202.0	GlcN + H^+ (Na^+)
341.1/363.1	$(GlcN)_2$ + H^+ (Na^+)
405.2	GlcN-GlcNAc + Na^+
502.2/524.2	$(GlcN)_3$ + H^+ (Na^+)
566.2	$(GlcN)_2$-GlcNAc + Na^+ (K^+)
685.3	$(GlcN)_4$ + Na^+
727.3	$(GlcN)_3$-GlcNAc + Na^+
846.3	$(GlcN)_5$ + Na^+
888.3	$(GlcN)_4$-GlcNAc + Na^+
1049.4	$(GlcN)_5$-GlcNAc + Na^+

The fdCOS and paCOS mixture obtained with CHIT2 and Neutrase 0.8L was characterized by HPAEC-PAD (**Figure 4.31**) and MALDI-TOF (Supplementary Material, **Figure S7**).

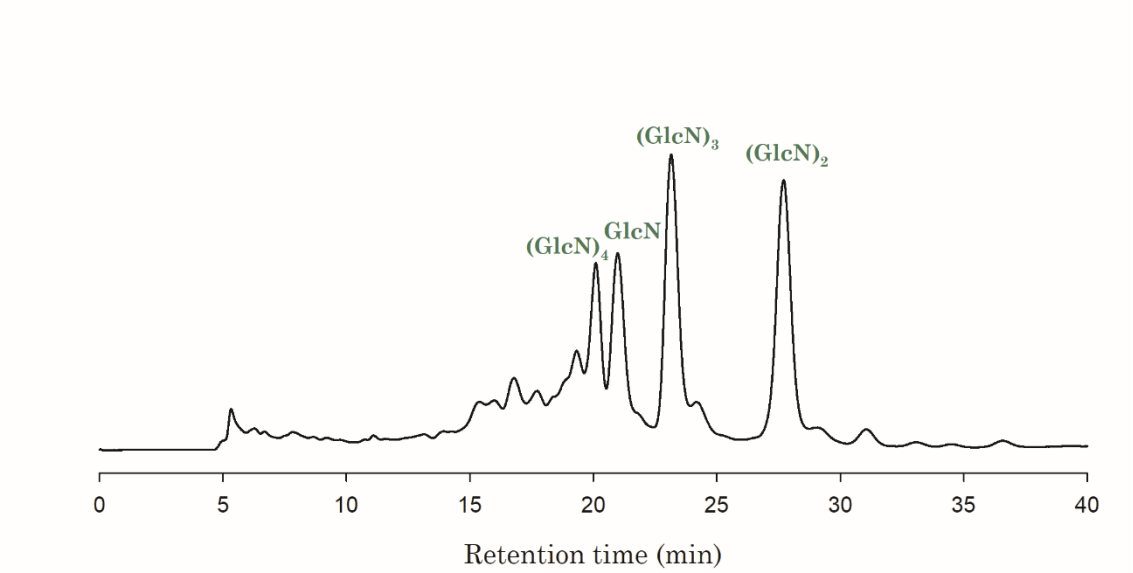

Figure 4.31. HPAEC-PAD chromatogram of the COS produced with CHIT2 and Neutrase 0.8L. Reaction conditions: 1% (w/v) chitosan, 10% (v/v) Neutrase 0.8L in ammoniun acetate buffer (pH 5.0) at 60 ºC for 48 h.

As shown, only a few peaks could be identified by HPAEC-PAD. The identified peaks were glucosamine (GlcN), chitobiose ($(GlcN)_2$), chitotriose ($(GlcN)_3$) and chitotetraose ($(GlcN)_4$). Moreover, the number of unidentified peaks was higher than in the previous case, making the analysis by mass spectrometry even more impotant.

Table 4.9 summarizes the main m/z signals obtained by mass spectrometry (MALDI-TOF) and their composition. In contrast with the previous case, the number of signals corresponding to paCOS was much higher, which is in accordance with the lower deacetylation degree of CHIT2 (79.4%). In addition, paCOS with more than one N-acetylated residue were observed.

Table 4.9 Main identified signals in the MALDI-TOF mass spectrum of the reaction with chitosan CHIT2 and Neutrase 0.8L.

m/z	Assignation
202.0	GlcN + Na^+
363.1	$(GlcN)_2$ + Na^+
447.1	$(GlcNAc)_2$ + Na^+
524.2	$(GlcN)_3$ + Na^+
566.2	$(GlcN)_2$-GlcNAc + Na^+
608.2	GlcN-$(GlcNAc)_2$ + Na^+
685.3	$(GlcN)_4$ + Na^+
769.3	$(GlcN)_2$-$(GlcNAc)_2$ + Na^+
846.3	$(GlcN)_5$ + Na^+
930.3	$(GlcN)_3$-$(GlcNAc)_2$ + Na^+
1049.4	$(GlcN)_5$-GlcNAc + Na^+
1133.4	$(GlcN)_3$-$(GlcNAc)_3$ + Na^+
1210.4	$(GlcN)_6$-GlcNAc + Na^+
1413.5	$(GlcN)_6$-$(GlcNAc)_2$ + Na^+
1574.5	$(GlcN)_7$-$(GlcNAc)_2$ + Na^+
1896.7	$(GlcN)_9$-$(GlcNAc)_2$ + Na^+

In summary, one common procedure (with slight modifications) was applied for the hydrolysis of chitosan, and products of different nature were obtained, depending on the characteristics of the chitosan (DD, PA, DP) and the enzyme employed. Thus, we were able to synthesize a mixture of mainly <1 kDa fdCOS, a mixture mainly composed of <1 kDa paCOS and two mixtures containing both fdCOS and paCOS. Although both mixtures contained fdCOS and paCOS, they could be clearly differentiated by the number and composition of their paCOS.

GENERAL DISCUSSION

5.1 Neo-FOS production by immobilized pXd-INV

Besides their prebiotic properties, fructooligosaccharides have interesting physico-chemical and organoleptic properties, including high stability (thermal and pH), low caloric value (50-75% less than fructose, glucose or sucrose) and moderate sweetness. In addition, FOS show very useful technological properties since they can decrease microbial growth, enable fiber inclusion into liquids and control browning due to Maillard reactions (Gibson and Roberfroid, 1995, Yun, 1996, Critteden and Playne, 1996). These great features make fructooligosaccharides a very interesting ingredient for functional foods; in fact, they are the most commonly used in the European Food Market (alongside GOS) and they are added to several functional foods in varying amounts (2-50%) (Franck, 2002). However, most commercial FOS are unpurified mixtures with diminished properties due to low yield production processes and/or expensive purification techniques (Nobre et al., 2015).

A few studies have reported that neo-fructooligosaccharides present better physico-chemical and prebiotic properties than commercialized FOS (inulin-type FOS) (Kilian et al., 2002, Lim et al., 2007). Despite their enhanced properties, neo-FOS have not been implemented in the food industry because of their low production yields and scarce study of their functionality and biological activities. Neo-FOS production has only been reported for a few microbial enzymes (β-fructofuranosidases and levansucrases), and only a handful of works have investigated neo-FOS production (**Table 1.3**). Among the enzymes producing neo-FOS, the β-fructofuranosidase pXd-INV gives rise to the largest yield reported for neo-FOS production with 118 g/L of neo-FOS obtained under optimum conditions (600 g/L sucrose) (Gimeno-Perez et al., 2015). Efficient enzyme immobilization and the implementation of these biocatalysts in bioreactors provide several advantages (improved volumetric activity, simplification of the biocatalyst separation and reuse, chance to operate a continuous process, easier product purification and enhanced stability of the biocatalyst, among others) that could promote large-scale production and industrial application (Flores-Maltos et al., 2016).

Hence, we have investigated several methodologies for the immobilization of pXd-INV, as well as their application in two kinds of bioreactors. Two strategies were evaluated: entrapment in PVA and ionic binding.

Entrapment in PVA hydrogels was selected due to the large size of the enzyme (360 kDa) (Ramirez-Escudero et al., 2016) that could prevent enzyme leakage, as well as the successful application of PVA-based biocatalysts in several bioreactors (Nunes et al., 2013, Nunes et al., 2014). A couple of enzyme loadings were assayed and the recovered activity was quite high for the lowest one (**Table 4.1**). In addition, the operational stability in short-term operation was remarkable (**Figure 4.1**). Hence, we decided to investigate long-term thermal stability and neo-FOS production. Unfortunately, the thermal stability of the PVA based biocatalyst was quite low (**Figure 4.2**), requiring a decrease in the reaction temperature for long-term operation. Thus, temperature was changed to 30 ºC, which was below the optimum reaction temperature for pXd-INV (60 ºC). Nevertheless, neo-FOS production was evaluated at 30 ºC (**Figure 4.4**); as expected, the yield (18.9%) was lower than the obtained with the free enzyme (29%) probably due to the change in temperature favoring hydrolysis over transfructosylation. Despite the lower yield, a batch stirred tank reactor system was set up and its productivity and operational stability were investigated (**Figure 4.6**). Although operational stability was satisfactory (≥ 7 cycles of 26 h), productivity was quite low (42 $g_{FOS}\,L^{-1}\,day^{-1}$) probably because of the low activity of the biocatalyst (0.34 U/lens) and the decrease in reaction temperature.

In order to improve neo-FOS production, ionic binding was assessed since it enables the set-up of continuous processes (packed-bed bioreactors) and was successfully employed in previous studies (Yun et al., 1995, Mayer et al., 2010). We evaluated two different amino-activated carriers (Sepabeads EC-EA and Sepabeads EC-HA) and two different enzyme loadings. In contrast with the PVA based biocatalysts, the recovered activity was lower but the apparent activity was quite high (**Table 4.2**). Moreover, the operational stability of the biocatalysts in short-term operation was satisfactory and similar to the obtained with the PVA-based biocatalysts (**Figure 4.1**). Hence, neo-FOS production in a packed-bed reactor was investigated with the most active biocatalyst (HA-pXd-INV). The initial productivity (218 $g_{FOS}\,L^{-1}\,day^{-1}$) was higher than the obtained in the batch stirred tank reactor (42 $g_{FOS}\,L^{-1}\,day^{-1}$). However, neo-FOS production decreased with time while glucose and fructose increased (**Figure 4.8**).

Table 5.1 summarizes the strategies evaluated in this Thesis for neo-FOS production with immobilized pXd-INV. In both cases the sucrose hydrolysis was favored, increasing the hydrolysis to transfructosylation ratio. In fact, the biocatalyst prepared by ionic binding changed product selectivity, increasingly favoring glucose and fructose production. Considering the FOS profile, both biocatalysts maintained a product pattern similar to the obtained with the free enzyme. The only exception was the significant increase in blastose production (synthesized by neo-kestose hydrolysis) probably due to the increased hydrolysis/transfructosylation ratio.

Table 5.1 Production of neo-FOS with immobilized pXd-INV.

Biocatalyst	T (°C)	Type of bioreactor	Main products	Productivity (g_{FOS} L^{-1} day^{-1})	Time assayed (days)
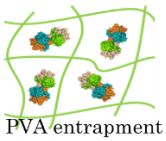 PVA entrapment	30	Batch stirred tank	Glucose and fructose +++ Neo-FOS ++ Inulin-FOS +	42	7.6
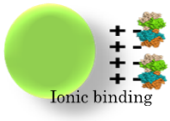 Ionic binding	50	Continuous packed-bed	Glucose and fructose +++* Neo-FOS ++# Inulin-FOS +	218	12

+ low production; ++ moderate production; +++ high production; * production increased with time; # production decreased with time.

Several processes for FOS production employing different enzymes, immobilization techniques and bioreactors have been described. It is worth noting that some companies (e.g. Meiji Seika; Cheil Food and Chemicals) have developed industrial procedures for FOS production with immobilized cells in packed bed reactors (Flores-Maltos et al., 2016). In contrast, to our knowledge, this is the first work reported attempting neo-FOS production with immobilized enzymes in bioreactors. Only a couple of studies have reported neo-FOS production using bioreactors and, in both cases, the biocatalysts were immobilized whole cells (Park et al., 2005, Ning et al., 2010). Although industrial application is still far, these

procedures were valuable as a first approach to the industrial production of neo-FOS employing bioreactors with immobilized enzymes.

5.2 Fructosylation of phenolic compounds by pXd-INV

Glycosylation provides structural diversity to numerous natural molecules, such as proteins, lipids, alkaloids, steroids, flavonoids or antibiotics. Besides contributing to structural diversity, glycosylation can improve the physico-chemical and biological properties of natural compounds. Hence, the transfer of a sugar moiety can be used for several applications, including increasing water solubility and/or stability, decreasing toxicity or side effects, controlling flavor and fragrances, improving pharmacokinetics or modulating the activity of antibiotics (Desmet et al., 2012, Xu et al., 2016).

Phenolic compounds display very interesting biological activities, such as antioxidant, anticancer, antimicrobial, cardio-protective or neuroprotective. However, their use is often hampered by low solubility, stability or bioavailability. Glycosylation has been extensively employed for the improvement of these or other properties and some glucosides are already being used in the pharmaceutical or cosmetic industries (Yamamoto et al., 1990, Kurosu et al., 2002, Murota et al., 2010, Xu et al., 2016).

There are several reports about glycosylation of phenolic compounds but only a few of them deal specifically with fructosylation (Herrera-González et al., 2017). Nonetheless, new phenolic compounds with potential application in the industry have been produced by enzymatic fructosylation (Herrera-González et al., 2017).

The *β*-fructofuranosidase pXd-INV from *Xanthophyllomyces dendrorhous* showed great flexibility for transfructosylation, since it was able to fructosylate other carbohydrates (besides sucrose) and non-sugar molecules (alditols) (Gimeno-Perez et al., 2014, Gimeno-Perez, 2019). In addition, a HEPES molecule was located alongside fructose on the active site (crystallographic studies), indicating the potential of pXd-INV for the fructosylation of similar compounds like polyphenols (Ramirez-Escudero et al., 2016).

In this Thesis, we evaluated the capacity of pXd-INV to fructosylate several phenolic compounds of diverse complexity, and the effect these have in the hydrolysis

and transfructosylation rates. Fructosylated derivatives were only obtained with hydroxytyrosol and hydroquinone as acceptors (**Figure 4.9**). Nonetheless, most of the assayed compounds exerted an inhibitory effect on the activity of pXd-INV (**Table 4.3)**, indicating that they were located on the active site. **Table 5.2** summarizes the evaluated phenolic compounds, their behavior (acceptor/inhibitor) and their effect in the hydrolysis transfructosylation ratio.

Table 5.2 Fructosylation of phenolic compounds with pXd-INV.

Compound	Structure	Acceptor/Inhibitor	Hydrolysis / Transfructosylation ratio
Control	---------	------	**3.2**
Hydroxytyrosol	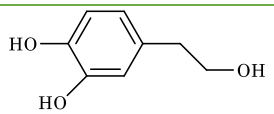	Acceptor	**3.2**
Hydroquinone	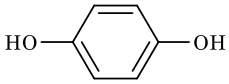	Acceptor	**4.5**
Catechol	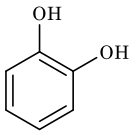	Inhibitor	**7.7**
EGCG	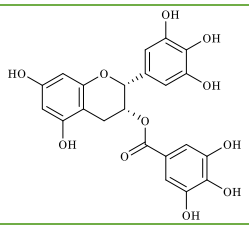	Inhibitor	**10.8**
p-Nitrophenol	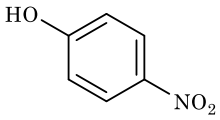	Inhibitor	**67.1**

Crystallographic studies showed that fructose was always situated in the -1 subsite and the phenolic compounds were located on the active site by stacking to Trp105 (**Figure 4.11**). Hydroquinone and hydroxytyrosol behavior as acceptors could be explained by higher mobility and flexibility.

The fructosylated conjugate of HQ was purified and characterized by mass spectrometry (**Figure S1**). The obtained product was 4-hydroxyphenyl-β-D-fructofuranoside. This compound was previously synthesized employing levansucrases and inulosucrases (Kang et al., 2009, Mena-Arizmendi et al., 2011),

but, to our knowledge, this is the first report on HQ fructosylation by a *β*-fructofuranosidase. Hydroquinone has a skin whitening effect that was used for the treatment of pigmentation disorders; however, it has side-effects like skin irritation and inflammation (Nordlund et al., 2006). Hydroquinone glucosides (α- and *β*-arbutin) are replacing hydroquinone in the cosmetic industry, since the transfer of a glucosyl moiety eliminates the undesired side-effects (Funayama et al., 1995, Desmet et al., 2012). According to Kang and *cols*. the HQ fructoside showed higher activities (antioxidant, inhibition of tyrosinase and lipid peroxidation) than *β*-arbutin, making this product a better functional ingredient for cosmetics (Kang et al., 2009).

Hydroxytyrosol possess strong biological activities (antioxidant, antimicrobial, anti-inflammatory, neuroprotective) and low bioavailability, making its fructosylation very interesting. Hence, we chose to study the production of HT fructosylated derivatives in greater detail. Two fructosylated conjugates (Fru-HT1 and Fru-HT2) were observed by HPLC analysis (**Figure 4.12a**), and the production yield was optimized after performing a series of experiments with different sucrose and HT concentrations (**Figure 4.13**). Optimum sucrose and HT concentrations were stablished at 300 g/L and 25 g/L, respectively; and the maximum yield of HT fructosides was observed at 6 h (11.7 g/L). After optimizing the reaction conditions, the production of both derivatives (Fru-HT1 and Fru-HT2) was studied as a function of sucrose consumption (**Figure 4.14**). In addition, FOS production profile was investigated simultaneously. Maximum production of Fru-HT1 (11.1 g/L) and Fru-HT2 (0.2 g/L) was observed after sucrose consumption was nearly 80%. Similarly, FOS maximum yield was obtained after about 85% sucrose hydrolysis. Moreover, Fru-HT1 and FOS concentration decreased rapidly when sucrose consumption reached 95%, which was in agreement with the profile observed for other synthesis catalyzed by glycosidases (Potocka et al., 2015, Piedrabuena et al., 2016). After purification, Fru-HT1 was characterized as 3,4-dihydroxyphenyl ethyl *β*-D-fructofuranoside by a combination of 1D and 2D NMR techniques (**Figure 4.15**).

Crystallographic studies were performed with fructose, HT and Fru-HT; revealing that HT can be located in three positions on the active site (HT1, HT2 and HT3); but only two of them (HT1 and HT2) were appropriate for fructosylation (**Figure 4.16a**). In addition, the location of HT1 was in agreement with the

characterized product (Fru-HT1) and HT2 suggested a different binding mode, which correlates perfectly with the secondary product detected by HPLC (Fru-HT2). Product soaking confirmed fructosylation in the primary OH for the major product; and revealed a secondary derivative fructosylated in the phenolic OH, which probably corresponds to Fru-HT2 (**Figure 4.16b**).

Site directed mutagenesis was carried out in the Glu334-Asn342 loop, responsible for the binding of HT2 (Miguez et al., 2018), aiming to modulate product selectivity. Thus, two residues were chosen (Gln341 and Asn342) and mutated, obtaining two mutants pXd-INV-Q341S and pXd-INV-N342Q. The production of fructosylated HT conjugates and FOS was investigated for both mutants, under optimum conditions (**Figure 4.18**). Product profile was the same as for the wild-type reaction, and maximum yield of fructosylated derivatives was observed after sucrose consumption was higher than 80%. On the other hand, the product yield and the Fru-HT1/Fru-HT2 ratio were significantly different (**Table 4.4**). The wild-type yielded the highest amount of Fru-HT1, but both mutants synthesized higher amounts of Fru-HT2, being pXd-INV-N342Q the most specific for fructosylation at the phenolic OH. Interestingly, the mutant pXd-INV-N342Q also produces the highest amount of FOS, favoring sucrose as acceptor.

The major product (Fru-HT1) was also synthesized by Potocka et al. (Potocka et al., 2019). On the contrary, HT fructosylation on the phenolic OH had not been reported until now. HT glycosylation has been barely explored, nevertheless, HT glucosides and xylosides have been reported (Trincone et al., 2012, Nieto-Dominguez et al., 2017).

5.3 Production of acidic XOS

Hemicellulose is the second most abundant agro-industrial residue, only after cellulose, and rich in xylan. Xylan is a polysaccharide that can be used as a renewable source for the production of bioethanol or high value-added compounds. Specifically, xylooligosaccharides (XOS), oligosaccharides formed by xylose residues linked by ß-(1→4) bonds, have aroused great interest due to their biological activities (prebiotic, antimicrobial, anti-inflammatory and antitumor) (Aachary and Prapulla, 2011, Azevedo-Carvalho et al., 2012).

Acidic xylooligosaccharides (acidic XOS) or aldouronics are hetero-oligosaccharides formed by xylose residues randomly linked to uronic acid (glucuronic or methyl-glucuronic acids) substitutions. Several studies have reported the health promoting activities of acidic XOS, often superior to the ones observed for neutral XOS (Ohbuchi et al., 2010, Valls et al., 2018). However, only a few reports have determined the activity of pure and structurally characterized acidic XOS (Christakopoulos et al., 2003).

In this Thesis, we investigated the production of acidic XOS with the enzyme cocktail Depol 670L and the purification of single acidic XOS. Production of neutral and acidic XOS was observed by HPAEC-PAD and chromatogram analysis revealed that product diversity decreased with time (**Figure 4.19**). Pursuing a simpler purification procedure, 72 h was chosen as the optimum reaction time.

A large-scale purification methodology was set up employing a series of anion-exchange Sep-Pak cartridges (**Section 3.7.3, Figure 3.3**). The obtained fractions (neutral and acidic XOS) were analyzed by HPAEC-PAD. As described in **Section 3.3.3**, a HPAEC-PAD analytical method was designed for the separation of acidic XOS. Considering that acidic XOS bind strongly to the stationary phase and the high diversity of products, a gradient of 200 mM sodium acetate was applied to slowly elute the acidic fraction and maximize separation. HPAEC-PAD confirmed the separation of both fractions, and one main product was observed in the acidic fraction (**Figure 4.21**). The acidic fraction was also characterized by mass spectrometry (MALDI-TOF), revealing the presence of 5 products: X2-MeGlcA, X3-MeGlcA, X4-MeGlcA, X5-MeGlcA and X6-MeGlcA; but, in agreement with HPAEC-PAD, the fraction appeared to be significantly enriched in X2-MeGlcA (**Figure 4.22**). NMR analysis revealed that the main product was indeed X2-MeGlcA (MeGlcAα-1,2-Xylβ-1,4-Xyl).

The analysis of the obtained hydrolysis products by HPAEC and mass spectrometry (MALDI-TOF) showed the possible cleavage points for Depol 670L. A reaction scheme is represented in **Figure 5.1**.

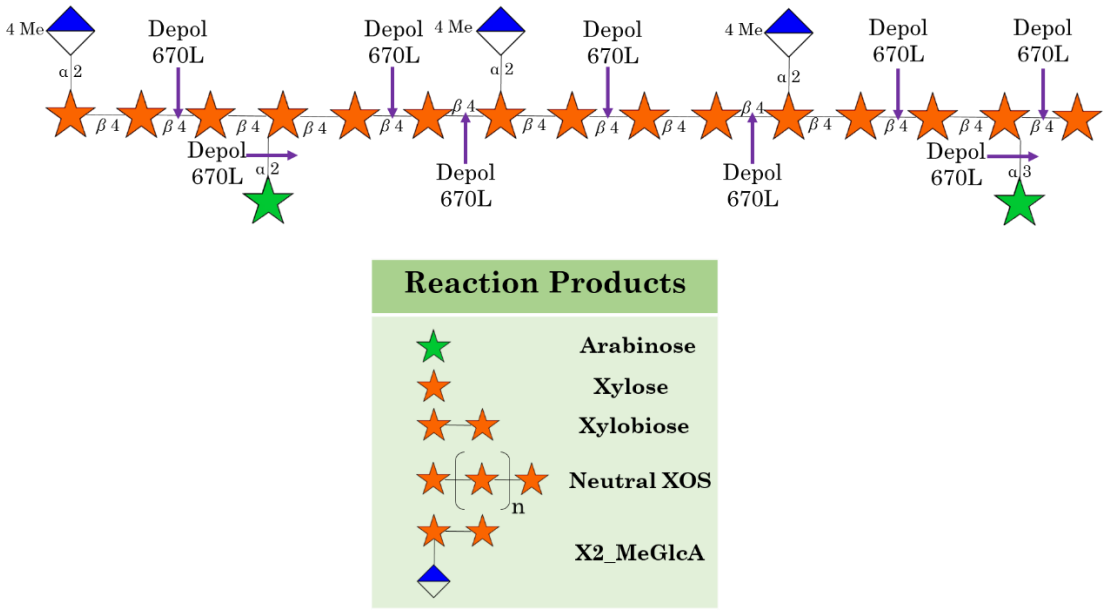

Figure 5.1 Schemed reaction of xylan hydrolysis by Depol 670L.

Finally, the antioxidant activity of the obtained product was evaluated along with the activity of neutral XOS and xylan. Neutral XOS showed no scavenging capacity on the ABTS radical, while X2-MeGlcA showed the highest activity (**Figure 4.24**). Considering these results, it is safe to assume that both uronic acid residues and polymerization degree can influence the antioxidant activity, which is in accordance with previous studies (Valls et al., 2018).

5.4 Large-scale production of COS

Chitooligosaccharides (COS) are homo- or hetero-oligomers of glucosamine and N-acetyl glucosamine that can be prepared by chitosan or chitin hydrolysis. COS display a wide range of biological functions (**Table 1.1**) that make them very interesting for diverse applications in food, medicine, cosmetics or agriculture. However, these bioactivities are strongly dependent on the deacetylation degree, acetylation pattern or polymerization degree (Hamer et al., 2015). For this reason, the synthesis of well characterized COS mixtures is necessary for a better understanding of their properties and application in several industries (Aam et al., 2010).

Chitosan oligomers can be classified in two families depending on their composition: fully deacetylated chitooligosaccharides (fdCOS), exclusively composed by glucosamine residues, and partially acetylated chitooligosaccharides (paCOS),

oligomers containing random moieties of glucosamine and N-acetyl glucosamine (Santos-Moriano et al., 2018). Depending on the nature of the chitosan and the enzyme employed, one or both families can be obtained after hydrolysis.

In this Thesis, a common procedure was designed for the large-scale production of COS mixtures containing one family or a combination of the two. In addition, the synthesized mixtures were characterized by HPAEC-PAD and mass spectrometry (MALDI-TOF).

Several chitosans were hydrolyzed with the proteolytic preparation Neutrase 0.8L or a chitinase from *Trichoderma harzanium* CHIT42, employing the methodology represented in **Figure 4.25**. The nature of the obtained products was strongly influenced by the nature of the chitosan (DD, DP and PA) and the enzyme employed. Thus, the hydrolysis of CHIT600, a highly deacetylated chitosan, with Neutrase 0.8L gave rise to a mixture of fdCOS. On the other hand, paCOS were synthesized by hydrolysis of chitosan QS1 (DD 81%) with CHIT42. In addition, two COS mixtures, containing both fdCOS and paCOS, were prepared after hydrolyzing two chitosans provided by ANFACO-CECOPESCA with Neutrase 0.8L. **Table 5.3** lists the products obtained with the different chitosans, enzymes and reaction conditions

Table 5.3 Description of the production process for each COS mixture (substrate, reaction conditions, product and MW).

Chitosan	(MW, DD)	Enzyme	Reaction conditions	Product
CHIT600 (Acros Organics)	(600-800 kDa, ≥ 90%)	Neutrase 0.8L	50 °C, pH 5.0	fdCOS
QS1 (InFiQus)	(98 kDa, 81%)	CHIT42	35 °C, pH 5.0	paCOS
CHIT1 (Anfaco)	(4 kDa, 94.7%)	Neutrase 0.8L	50 °C, pH 5.0	fdCOS + paCOS
CHIT2 (Anfaco)	(56 kDa, 79,4%)	Neutrase 0.8L	50 °C, pH 5.0	fdCOS + paCOS

CONCLUSIONS

1. The *β*-fructofuranosidase from *Xanthophyllomyces dendrorhous* (pXd-INV) was successfully immobilized by entrapment in PVA lenses and employed for neo-FOS synthesis in a batch stirred-tank reactor with a productivity of 42 g $_{FOS}$ L^{-1} day^{-1}, showing notable reusability.

2. The *β*-fructofuranosidase from *Xanthophyllomyces dendrorhous* (pXd-INV) was successfully immobilized by ionic binding in Sepabeads EC-EA and EC-HA. A packed-bed reactor was set up with the most active biocatalyst (HA-pXd-INV), obtaining an initial productivity of 218 g $_{FOS}$ L^{-1} day^{-1}.

3. The ability of pXd-INV to fructosylate phenolic compounds was tested with hydroquinone, hydroxytyrosol, EGCG, catechol and *p*-nitrophenol. Hydroquinone and hydroxytyrosol were positive acceptors, whilst the rest of the compounds inhibited the enzyme, which was corroborated by crystallographic studies.

4. Two fructosylated hydroxytyrosol derivatives (Fru-HT1 and Fru-HT2) were synthesized. Hydroxytyrosol fructosylation was optimized by investigating different donor and acceptor concentrations. The highest yield of fructosylated conjugates (11.7 g/L) was reached with 300 g/L of sucrose and 25 g/L of hydroxytyrosol.

5. The main product (Fru-HT1) was characterized by mass spectrometry and bidimensional NMR as 3,4-dihydroxyphenyl ethyl *β*-D-fructofuranoside. Crystallographic studies revealed that the secondary product (Fru-HT2) was fructosylated at the phenolic OH.

6. The selective production of acid xylooligosaccharides (decorated with methyl-glucuronic acid ramifications) was achieved with the enzyme Depol 670L. A method of analysis by HPAEC-PAD was developed to charcterize such compounds.

7. A fractionation method based on anion-exchange chromatography was set up to isolate acidic xylooligosaccharides. The main product was 2'-O-α-(4-O-methyl-α-D-glucuronosyl)-xylobiose.

8. The antioxidant capacity of 2'-O-α-(4-O-methyl-α-D-glucuronosyl)-xylobiose (X2_MeGlcA), neutral XOS (X2-X6) and glucuronoxylan was tested. The obtained product showed the highest antioxidant activity with ABTS.

9. A large-scale method was developed for the preparation of several types of chitooligosaccharides (COS), which were characterized by a combination of HPAEC-PAD and MALDI-TOF methods.

10. The enzyme Neutrase 0.8L was useful to obtain fully deacetylated chitooligosaccharides (fdCOS). Chitinase CHIT42 from *Trichoderma harzianum* was employed to produce a mixture of partially acetylated chitooligosaccharides (paCOS).

1. La *β*-fructofuranosidasa de *Xanthophyllomyces dendrorhous* (pXd-INV) se inmovilizó con éxito mediante el atrapamiento en lentes de PVA y se empleó para la síntesis de neo-FOS en un reactor de tanque agitado por lotes con una productividad de 42 g FOS L^{-1} $día^{-1}$, mostrando una reutilización notable.

2. La *β*-fructofuranosidasa de *Xanthophyllomyces dendrorhous* (pXd-INV) se inmovilizó con éxito mediante unión iónica en Sepabeads EC-EA y EC-HA. Se configuró un reactor de lecho fijo con el biocatalizador más activo (HA-pXd-INV), obteniendo una productividad inicial de 218 g FOS L^{-1} $día^{-1}$.

3. La capacidad de pXd-INV para fructosilar compuestos fenólicos se probó con hidroquinona, hidroxitirosol, EGCG, catecol y p-nitrofenol. La hidroquinona y el hidroxitirosol fueron aceptores positivos, mientras que el resto de los compuestos inhibieron la enzima, lo que fue corroborado mediante estudios cristalográficos.

4. Se sintetizaron dos derivados fructosilados del hidroxitirosol (Fru-HT1 y Fru-HT2). Se investigaron diferentes concentraciones de aceptor y donador para optimizar la reacción de fructosilación. El rendimiento máximo de derivados fructosilados (11.7 g/L) se alcanzó con 300 g/L de sacarosa y 25 g/L de hidroxitirosol.

5. El producto principal (Fru-HT1) se caracterizó por espectrometría de masas y RMN bidimensional como 3,4-dihidroxifenil etil ß-D-fructofuranósido. Los estudios cristalográficos revelaron que el producto secundario (Fru-HT2) estaba fructosilado en el OH fenólico.

6. La producción selectiva de xiloligosacáridos ácidos (ramificados con ácido metilglucurónico) se consiguió con la enzima Depol 670L. Se desarrolló un método de análisis por HPAEC-PAD para caracterizar dichos compuestos.

7. Se estableció un método de fraccionamiento basado en cromatografía iónica para aislar xilooligosacáridos ácidos. El producto principal fue 2'-O-α-(4-O-metil-α-D-glucuronosil)-xilobiosa.

8. Se analizó la capacidad antioxidante de 2'-O-α-(4-O-metil-α-D-glucuronosil)-xilobiosa (X2_MeGlcA), los XOS neutros y el glucuronoxilano. El producto obtenido mostró la mayor capacidad antioxidante con ABTS.

9. Se desarrolló un método a gran escala para la preparación de varios tipos de quitooligosacáridos (COS), que se caracterizaron mediante una combinación de métodos de HPAEC-PAD y MALDI-TOF.

10. La enzima Neutrasa 0.8L se utilizó para obtener quitooligosacáridos totalmente desacetilados (fdCOS). La quitinasa CHIT42 de *Trichoderma harzianum* se empleó para producir una mezcla de quitooligosacáridos parcialmente acetilados (paCOS).

REFERENCES

A

AACHARY, A. A. & PRAPULLA, S. G. 2010. Xylooligosaccharides (XOS) as an Emerging Prebiotic: Microbial Synthesis, Utilization, Structural Characterization, Bioactive Properties, and Applications. *Comprehensive Reviews in Food Science and Food Safety,* 10**,** 2-16.

AAM, B. B., HEGGSET, E. B., NORBERG, A. L., SORLIE, M., VARUM, K. M. & EIJSINK, V. G. 2010. Production of chitooligosaccharides and their potential applications in medicine. *Marine Drugs,* 8**,** 1482-517.

AGUIAR-OLIVEIRA, E. & MAUGERI, F. 2010. Characterization of the Immobilized Fructosyltranferase from *Rhodotorula sp. International Journal of Food Engineering*, 6, 3, 9.

ALUKO, R. 2012. Bioactive Carbohydrates. *In:* ALUKO, R. (ed.) *Functional Foods and Nutraceuticals.* New York, NY: Springer New York, pp. 3-22.

ALVES, M.-H., JENSEN, B. E. B., SMITH, A. A. A. & ZELIKIN, A. N. 2011. Poly(Vinyl Alcohol) Physical Hydrogels: New Vista on a Long Serving Biomaterial. *Macromolecular Bioscience,* 11**,** 1293-1313.

AN, Q. D., ZHANG, G. L., WU, H. T., ZHANG, Z. C., ZHENG, G. S., LUAN, L., MURATA, Y. & LI, X. 2009. Alginate-deriving oligosaccharide production by alginase from newly isolated *Flavobacterium* sp. LXA and its potential application in protection against pathogens. *Journal of Applied Microbiology,* 106**,** 161-170.

ARIGA, O., KUBO, T. & SANO, Y. 1994. Effective diffusivity of glucose in PVA hydrogel. *Journal of Fermentation and Bioengineering,* 78**,** 200-201.

ARTAN, M., KARADENIZ, F., KARAGOZLU, M. Z., KIM, M. M. & KIM, S. K. 2010. Anti-HIV-1 activity of low molecular weight sulfated chitooligosaccharides. *Carbohydrate Research,* 345**,** 656-662.

AZUMA, K., OSAKI, T., MINAMI, S. & OKAMOTO, Y. 2015. Anticancer and anti-inflammatory properties of chitin and chitosan oligosaccharides. *Journal of Functional Biomaterials,* 6**,** 33-49.

B

BAHRKE, S. 2008. Mass spectrometric analysis of chitooligosaccharides and their interaction with proteins, Tesis Doctoral, Universitat Potsdam.

BALI, V., PANESAR, P. S., BERA, M. B. & PANESAR, R. 2015. Fructo-oligosaccharides: Production, Purification and Potential Applications. *Critical Reviews in Food Science and Nutrition,* 55**,** 1475-1490.

BEKERS, M., LAUKEVICS, J., UPITE, D., KAMINSKA, E., VIGANTS, A., VIESTURS, U., PANKOVA, L. & DANILEVICS, A. 2002. Fructooligosaccharide and levan producing activity of *Zymomonas mobilis* extracellular levansucrase. *Process Biochemistry,* 38**,** 701-706.

BIELY, P., VRŠANSKÁ, M., TENKANEN, M. & KLUEPFEL, D. 1997. Endo-ß-1,4-xylanase families: Differences in catalytic properties. *Journal of Biotechnology,* 57**,** 151-166.

BIESALSKI, H.-K., DRAGSTED, L. O., ELMADFA, I., GROSSKLAUS, R., MULLER, M., SCHRENK, D., WALTER, P. & WEBER, P. 2009. Bioactive compounds: Definition and assessment of activity. *Nutrition,* 25**,** 1202-1205.

BISSARO, B., MONSAN, P., FAURÉ, R. & O'DONOHUE, M. J. 2015. Glycosynthesis in a waterworld: new insight into the molecular basis of transglycosylation in retaining glycoside hydrolases. *Biochemical Journal,* 467**,** 17.

BOJAROVÁ, P. & KŘEN, V. 2009. Glycosidases: a key to tailored carbohydrates. *Trends in Biotechnology,* 27**,** 199-209.

BOLIVAR, J. M., TRIBULATO, M. A., PETRASEK, Z. & NIDETZKY, B. 2016. Let the substrate flow, not the enzyme: Practical immobilization of D-amino acid oxidase in a glass microreactor for effective biocatalytic conversions. *Biotechnology and Bioengineering,* 113**,** 2342-2349.

BOSKOU, D., TSIMIDOU, M. & BLEKAS, G. 2006. 5 - Polar Phenolic Compounds. *In:* BOSKOU, D. (ed.) *Olive Oil (Second Edition).* AOCS Press, pp. 73-92.

BRADFORD, M. M. 1976. A rapid and sensitive method for the quantitation of microgram quantities of protein utilizing the principle of protein-dye binding. *Analytical Biochemistry,* 72**,** 248-254.

BROEKAERT, W. F., COURTIN, C. M., VERBEKE, K., VAN DE WIELE, T., VERSTRAETE, W. & DELCOUR, J. A. 2011. Prebiotic and other health-related effects of cereal-derived arabinoxylans, arabinoxylan-oligosaccharides, and xylooligosaccharides. *Critical Reviews in Food Science and Nutrition,* 51**,** 178-194.

BURUIANA, C. T., GÓMEZ, B., VIZIREANU, C. & GARROTE, G. 2017. Manufacture and evaluation of xylooligosaccharides from corn stover as emerging prebiotic candidates for human health. *LWT - Food Science and Technology,* 77**,** 449-459.

C

CAMPBELL, J. M., BAUER, L. L., FAHEY, G. C., HOGARTH, A. J. C. L., WOLF, B. W. & HUNTER, D. E. 1997. Selected Fructooligosaccharide (1-Kestose, Nystose, and 1F-ß-Fructofuranosylnystose) Composition of Foods and Feeds. *Journal of Agricultural and Food Chemistry,* 45**,** 3076-3082.

CAO, L., WU, J., LI, X., ZHENG, L., WU, M., LIU, P. & HUANG, Q. 2016. Validated HPAEC-PAD Method for the Determination of Fully Deacetylated Chitooligosaccharides. *International Journal of Molecular Sciences,* 17, 1699.

CAO, Y., LIU, F., CHEN, Y., YU, T., LOU, D., GUO, Y., LI, P., WANG, Z. & RAN, H. 2017. Drug release from core-shell PVA/silk fibroin nanoparticles fabricated by one-step electrospraying. *Scientific Reports,* 7**,** 11913-11913.

CARVALHO, A. F. A., NETO, P. D. O., DA SILVA, D. F. & PASTORE, G. M. 2013. Xylo-oligosaccharides from lignocellulosic materials: Chemical structure, health benefits and production by chemical and enzymatic hydrolysis. *Food Research International,* 51**,** 75-85.

COURTIN, C. M., SWENNEN, K., VERJANS, P. & DELCOUR, J. A. 2009. Heat and pH stability of prebiotic arabinoxylooligosaccharides, xylooligosaccharides and fructooligosaccharides. *Food Chemistry,* 112**,** 831-837.

CRITTENDEN, R. G. & PLAYNE, M. J. 1996. Production, properties and applications of food-grade oligosaccharides. *Trends in Food Science & Technology,* 7**,** 353-361.

CHEN, J., CHEN, X., XU, X., NING, Y., JIN, Z. & TIAN, Y. 2011. Biochemical characterization of an intracellular ^{6}G-fructofuranosidase from *Xanthophyllomyces dendrorhous* and its use in production of neo-fructooligosaccharides (neo-FOSs). *Bioresource Technology,* 102**,** 1715-1721.

CHEN, J., HU, Y., ZHANG, L., WANG, Y., WANG, S., ZHANG, Y., GUO, H., JI, D. & WANG, Y. 2017. Alginate Oligosaccharide DP5 Exhibits Antitumor Effects in Osteosarcoma Patients following Surgery. *Frontiers in Pharmacology,* 8**,** 623-623.

CHRISTAKOPOULOS, P., KATAPODIS, P., KALOGERIS, E., KEKOS, D., MACRIS, B. J., STAMATIS, H. & SKALTSA, H. 2003. Antimicrobial activity of acidic xylo-oligosaccharides produced by family 10 and 11 endoxylanases. *International Journal of Biological Macromolecules,* 31**,** 171-175.

CHUL PARK, M., SOO LIM, J., CHUL KIM, J., WON PARK, S. & WOOK KIM, S. 2005. Continuous production of neo-fructooligosaccharides by immobilization of whole cells of *Penicillium citrinum*. *Biotechnology Letters*, 27, 127-130.

CHUNG, Y. C., HSU, C. K., KO, C. Y. & CHAN, Y. C. 2007. Dietary intake of xylooligosaccharides improves the intestinal microbiota, fecal moisture, and pH value in the elderly. *Nutrition Research,* 27**,** 756-761.

D

DAVIES, G. & HENRISSAT, B. 1995. Structures and mechanisms of glycosyl hydrolases. *Structure,* 3**,** 853-859.

DE LA TORRE, R. 2008. Bioavailability of olive oil phenolic compounds in humans. *Inflammopharmacology,* 16**,** 245-247.

DE ROODE, B. M., FRANSSEN, M. C. R., PADT, A. V. D. & BOOM, R. M. 2003. Perspectives for the Industrial Enzymatic Production of Glycosides. *Biotechnology Progress,* 19**,** 1391-1402.

DE WINTER, K., DEWITTE, G., DIRKS-HOFMEISTER, M. E., DE LAET, S., PELANTOVÁ, H., KŘEN, V. & DESMET, T. 2015. Enzymatic Glycosylation of Phenolic Antioxidants: Phosphorylase-Mediated Synthesis and Characterization. *Journal of Agricultural and Food Chemistry,* 63**,** 10131-10139.

DESMET, T., SOETAERT, W., BOJAROVÁ, P., KŘEN, V., DIJKHUIZEN, L., EASTWICK-FIELD, V. & SCHILLER, A. 2012. Enzymatic Glycosylation of Small Molecules: Challenging Substrates Require Tailored Catalysts. *Chemistry – A European Journal,* 18**,** 10786-10801.

DEUTSCHMANN, R. & DEKKER, R. F. H. 2012. From plant biomass to bio-based chemicals: Latest developments in xylan research. *Biotechnology Advances,* 30**,** 1627-1640.

DRULA, E., GOLACONDA RAMULU, H., COUTINHO, P. M., LOMBARD, V. & HENRISSAT, B. 2013. The carbohydrate-active enzymes database (CAZy) in 2013. *Nucleic Acids Research,* 42**,** D490-D495.

DURIEUX, A., NICOLAY, X. & SIMON, J. P. 2000. Continuous malolactic fermentation by *Oenococcus Oeni* entrapped in LentiKats. *Biotechnology Letters,* 22**,** 1679-1684.

E

EBRINGEROVÁ, A. & HEINZE, T. 2000. Xylan and xylan derivatives – biopolymers with valuable properties, 1. Naturally occurring xylans structures, isolation procedures and properties. *Macromolecular Rapid Communications,* 21**,** 542-556.

EBRINGEROVÁ, A., HROMÁDKOVÁ, Z. & HEINZE, T. 2005. Hemicellulose. *In:* HEINZE, T. (ed.) *Polysaccharides I: Structure, Characterization and Use.* Berlin, Heidelberg: Springer Berlin Heidelberg, pp. 1-67.

EECKHAUT, V., VAN IMMERSEEL, F., DEWULF, J., PASMANS, F., HAESEBROUCK, F., DUCATELLE, R., COURTIN, C. M., DELCOUR, J. A. & BROEKAERT, W. F. 2008. Arabinoxylooligosaccharides from wheat bran inhibit *Salmonella* colonization in broiler chickens. *Poultry Science,* 87**,** 2329-2334.

EFSA PANEL ON DIETETIC PRODUCTS, N. & ALLERGIES 2011. Scientific Opinion on the substantiation of health claims related to polyphenols in olive and protection of LDL particles from oxidative damage (ID 1333, 1638, 1639, 1696, 2865), maintenance of normal blood HDL cholesterol concentrations (ID 1639), maintenance of normal blood pressure (ID 3781), "anti-inflammatory properties" (ID 1882), "contributes to the upper respiratory tract health" (ID 3468), "can help to maintain a normal function of gastrointestinal tract" (3779), and "contributes to body

defences against external agents" (ID 3467) pursuant to Article 13(1) of Regulation (EC) No 1924/2006. *EFSA Journal,* 9**,** 2033.

ESPINOSA-MARTOS, I. & RUPEREZ, P. 2006. Soybean oligosaccharides. Potential as new ingredients in functional food. *Nutrición Hospitalaria,* 21**,** 92-6.

F

FALKEBORG, M., CHEONG, L. Z., GIANFICO, C., SZTUKIEL, K. M., KRISTENSEN, K., GLASIUS, M., XU, X. & GUO, Z. 2014. Alginate oligosaccharides: Enzymatic preparation and antioxidant property evaluation. *Food Chemistry,* 164**,** 185-194.

FERNANDEZ-ARROJO, L., RODRIGUEZ-COLINAS, B., GUTIERREZ-ALONSO, P., FERNANDEZ-LOBATO, M., ALCALDE, M., BALLESTEROS, A. O. & PLOU, F. J. 2013. Dried alginate-entrapped enzymes (DALGEEs) and their application to the production of fructooligosaccharides. *Process Biochemistry,* 48**,** 677-682.

FERNANDEZ-ARROJO, L., SANTOS-MORIANO, P., RODRIGUEZ-COLINAS, B., BALLESTEROS, A. O. & PLOU, F. J. 2015. Micro-scale procedure for enzyme immobilization screening and operational stability assays. *Biotechnology Letters,* 37**,** 1593-1600.

FERNANDEZ, J. G. & INGBER, D. E. 2014. Manufacturing of Large-Scale Functional Objects Using Biodegradable Chitosan Bioplastic. *Macromolecular Materials and Engineering,* 299**,** 932-938.

FLORES-MALTOS, D. A., MUSSATTO, S. I., CONTRERAS-ESQUIVEL, J. C., RODRIGUEZ-HERRERA, R., TEIXEIRA, J. A. & AGUILAR, C. N. 2016. Biotechnological production and application of fructooligosaccharides. *Critical Reviews in Biotechnology,* 36**,** 259-267.

FRANCK, A. 2007. Technological functionality of inulin and oligofructose. *British Journal of Nutrition,* 87**,** S287-S291.

FUNAYAMA, M., ARAKAWA, H., YAMAMOTO, R., NISHINO, T., SHIN, T. & MURAO, S. 1995. Effects of α- and ß-Arbutin on Activity of Tyrosinases from Mushroom and Mouse Melanoma. *Bioscience, Biotechnology, and Biochemistry,* 59**,** 143-144.

G

GHAZI, I., DE SEGURA, A. G., FERNÁNDEZ-ARROJO, L., ALCALDE, M., YATES, M., ROJAS-CERVANTES, M. L., PLOU, F. J. & BALLESTEROS, A. 2005. Immobilisation of fructosyltransferase from *Aspergillus aculeatus* on epoxy-activated Sepabeads EC for the synthesis of fructo-oligosaccharides. *Journal of Molecular Catalysis B: Enzymatic,* 35**,** 19-27.

GIBSON, G. R., PROBERT, H. M., LOO, J. V., RASTALL, R. A. & ROBERFROID, M. B. 2007. Dietary modulation of the human colonic microbiota: updating the concept of prebiotics. *Nutrition Research Reviews,* 17**,** 259-275.

GIBSON, G. R. & ROBERFROID, M. B. 1995. Dietary Modulation of the Human Colonic Microbiota: Introducing the Concept of Prebiotics. *The Journal of Nutrition,* 125**,** 1401-1412.

GIMENO-PÉREZ, M. 2019. Estudio estructural de la *β*-fructofuranosidasa de *Xanthophyllomyces dendrorhous* y su empleo para la producción de oligosacáridos prebióticos y otros derivados fructosilados. Tesis Doctoral. Universidad Autónoma de Madrid.

GIMENO-PÉREZ, M., LINDE, D., FERNÁNDEZ-ARROJO, L., PLOU, F. J. & FERNÁNDEZ-LOBATO, M. 2015. Heterologous overproduction of ß-fructofuranosidase from yeast *Xanthophyllomyces dendrorhous*, an enzyme producing prebiotic sugars. *Applied Microbiology and Biotechnology,* 99**,** 3459-3467.

GIMENO-PEREZ, M., SANTOS-MORIANO, P., FERNANDEZ-ARROJO, L., POVEDA, A., JIMENEZ-BARBERO, J., BALLESTEROS, A. O., FERNANDEZ-LOBATO, M. & PLOU, F. J. 2014. Regioselective synthesis of neo-erlose by the ß-fructofuranosidase from *Xanthophyllomyces dendrorhous*. *Process Biochemistry,* 49**,** 423-429.

GIORDANO, E., DANGLES, O., RAKOTOMANOMANA, N., BARACCHINI, S. & VISIOLI, F. 2015. 3-O-Hydroxytyrosol glucuronide and 4-O-hydroxytyrosol glucuronide reduce endoplasmic reticulum stress in vitro. *Food & Function,* 6**,** 3275-3281.

GÓMEZ, B., GULLÓN, B., REMOROZA, C., SCHOLS, H. A., PARAJÓ, J. C. & ALONSO, J. L. 2014. Purification, Characterization, and Prebiotic Properties of Pectic Oligosaccharides from Orange Peel Wastes. *Journal of Agricultural and Food Chemistry,* 62**,** 9769-9782.

GOMEZ DE SEGURA, A., ALCALDE, M., PLOU, F. J., REMAUD-SIMEON, M., MONSAN, P. & BALLESTEROS, A. 2003. Encapsulation in LentiKats of dextransucrase from *Leuconostoc mesenteroides* NRRL B1299, and its effect on product selectivity. *Biocatalysis and Biotransformation,* 21**,** 325-331.

GONZÁLEZ-ALFONSO, J. L., RODRIGO-FRUTOS, D., BELMONTE-RECHE, E., PEÑALVER, P., POVEDA, A., JIMÉNEZ-BARBERO, J., BALLESTEROS, A. O., HIROSE, Y., POLAINA, J., MORALES, J. C., FERNÁNDEZ-LOBATO, M. & PLOU, F. J. 2018. Enzymatic Synthesis of a Novel Pterostilbene α-Glucoside by the Combination of Cyclodextrin Glucanotransferase and Amyloglucosidase. *Molecules (Basel, Switzerland),* 23**,** 1271.

GULLÓN, P., GONZÁLEZ-MUÑOZ, M. J., GOOL, M. P. V., SCHOLS, H. A., HIRSCH, J., EBRINGEROVÁ, A. & PARAJÓ, J. C. 2011. Structural features and properties of soluble products derived from *Eucalyptus globulus* hemicelluloses. *Food Chemistry,* 127**,** 1798-1807.

GUTIÉRREZ-ALONSO, P., FERNÁNDEZ-ARROJO, L., PLOU, F. J. & FERNÁNDEZ-LOBATO, M. 2009. Biochemical characterization of a *β*-fructofuranosidase from *Rhodotorula dairenensis* with transfructosylating activity. *FEMS Yeast Research,* 9**,** 768-773.

H

HAMED, I., OZOGUL, F. & REGENSTEIN, J. M. 2016. Industrial applications of crustacean by-products (chitin, chitosan, and chitooligosaccharides): A review. *Trends in Food Science & Technology,* 48**,** 40-50.

HAMER, S. N., CORD-LANDWEHR, S., BIARNÉS, X., PLANAS, A., WAEGEMAN, H., MOERSCHBACHER, B. M. & KOLKENBROCK, S. 2015. Enzymatic production of defined chitosan oligomers with a specific pattern of acetylation using a combination of chitin oligosaccharide deacetylases. *Scientific Reports,* 5**,** 8716.

HAMID, R., KHAN, M. A., AHMAD, M., AHMAD, M. M., ABDIN, M. Z., MUSARRAT, J. & JAVED, S. 2013. Chitinases: An update. *Journal of Pharmacy & bioallied sciences,* 5**,** 21-29.

HART, G. W. 2003. Structural and Functional Diversity of Glycoconjugates. *In:* THIBAULT, P. & HONDA, S. (eds.) *Capillary Electrophoresis of Carbohydrates.* Totowa, NJ: Humana Press, pp. 3-24.

HAYES, M. & TIWARI, B. K. 2015. Bioactive Carbohydrates and Peptides in Foods: An Overview of Sources, Downstream Processing Steps and Associated Bioactivities. *International Journal of Molecular Sciences,* 16**,** 22485-22508.

HEGGSET, E. B., DYBVIK, A. I., HOELL, I. A., NORBERG, A. L., SØRLIE, M., EIJSINK, V. G. H. & VÅRUM, K. M. 2010. Degradation of Chitosans with a Family 46 Chitosanase from *Streptomyces coelicolor* A3(2). *Biomacromolecules,* 11**,** 2487-2497.

HERRERA-GONZÁLEZ, A., NÚÑEZ-LÓPEZ, G., MOREL, S., AMAYA-DELGADO, L., SANDOVAL, G., GSCHAEDLER, A., REMAUD-SIMEON, M. & ARRIZON, J. 2017. Functionalization of natural compounds by enzymatic fructosylation. *Applied Microbiology and Biotechnology,* 101**,** 5223-5234.

HG CROUT, D. & VIC, G. 1998. Glycosidases and Glycosyl Transferases in Glycoside and Oligosaccharide Synthesis. *Current Opinion in Chemical Biology*, 2, 98-111.

HIDAKA, H., EIDA, T., TAKIZAWA, T., TOKUNAGA, T. & TASHIRO, Y. 1986. Effects of Fructooligosaccharides on Intestinal Flora and Human Health. *Bifidobacteria and Microflora*, 5, 37-50.

HIGASHIMURA, Y., NAITO, Y., TAKAGI, T., UCHIYAMA, K., MIZUSHIMA, K., USHIRODA, C., OHNOGI, H., KUDO, Y., YASUI, M., INUI, S., HISADA, T.,

HONDA, A., MATSUZAKI, Y. & YOSHIKAWA, T. 2016. Protective effect of agaro-oligosaccharides on gut dysbiosis and colon tumorigenesis in high-fat diet-fed mice. *American Journal of Physiology-Gastrointestinal and Liver Physiology,* 310**,** G367-G375.

HILL, A., KARBOUNE, S. & MATEO, C. 2016. Immobilization and stabilization of levansucrase biocatalyst of high interest for the production of fructooligosaccharides and levan. *Journal of Chemical Technology and Biotechnology,* 91**,** 2440-2448.

HOELL, I. A., VAAJE-KOLSTAD, G. & EIJSINK, V. G. H. 2010. Structure and function of enzymes acting on chitin and chitosan. *Biotechnology and Genetic Engineering Reviews,* 27**,** 331-366.

HOVING, L. R., KATIRAEI, S., HEIJINK, M., PRONK, A., VAN DER WEE-PALS, L., STREEFLAND, T., GIERA, M., WILLEMS VAN DIJK, K. & VAN HARMELEN, V. 2018. Dietary Mannan Oligosaccharides Modulate Gut Microbiota, Increase Fecal Bile Acid Excretion, and Decrease Plasma Cholesterol and Atherosclerosis Development. *Molecular Nutrition & Food Research,* 62**,** e1700942-e1700942.

HUANG, H.-C., HONG, L., CHANG, P., ZHANG, J., LU, S.-Y., ZHENG, B.-W. & JIANG, Z.-F. 2015. Chitooligosaccharides attenuate Cu^{2+}-induced cellular oxidative damage and cell apoptosis involving Nrf2 activation. *Neurotoxicity Research,* 27**,** 411-420.

HUANG, R., MENDIS, E., RAJAPAKSE, N. & KIM, S.-K. 2006. Strong electronic charge as an important factor for anticancer activity of chitooligosaccharides (COS). *Life Sciences,* 78**,** 2399-2408.

I

IMAI, K., SHIOMI, T., UCHIDA, K. & MIYA, M. 1986. Immobilization of Enzyme into Poly(vinyl alcohol) Membrane. *Biotechnology and Bioengineering,* 28**,** 1721-1726.

IMAIZUMI, K., NAKATSU, Y., SATO, M., SEDARNAWATI, Y. & SUGANO, M. 1991. Effects of xylooligosaccharides on blood glucose, serum and liver lipids and-cecum short-chain fatty acids in diabetic rats. *Agricultural and Biological Chemistry,* 55**,** 199-205.

ISHIHARA, M., NOJIRI, M., HAYASHI, N., NISHIMURA, T. & SHIMIZU, K. 1997. Screening of fungal ß-xylanases for production of acidic xylooligosaccharides using in situ reduced 4-O-methylglucuronoxylan as substrate. *Enzyme and Microbial Technology,* 21**,** 170-175.

IUPAC-IUB 1982. IUPAC-IUB Joint Commission on Biochemical Nomenclature (JCBN). Abbreviated terminology of oligosaccharide chains. Recommendations 1980. *European Journal of Biochemistry,* 126**,** 433-437.

J

JANG, K. H., JANG, E. K., KIM, S. H., KIM, I. H., KANG, S. A., KOH, I., PARK, Y. I., KIM, Y. J., HA, S. D. & KIM, C. H. 2006. High-level production of low-branched levan from *Pseudomonas aurantiaca* S-4380 for the production of di-*β*-D-fructofuranose dianhydride IV. *Journal of Microbiology and Biotechnology,* 16**,** 102-108.

K

KANEKO, T., KOHMOTO, T., KIKUCHI, H., SHIOTA, M., IINO, H. & MITSUOKA, T. 1994. Effects of isomaltooligosaccharides with different degrees of polymerization on human fecal bifidobacteria. *Bioscience, Biotechnology and Biochemistry,* 58**,** 2288-2290.

KANG, J., KIM, Y.-M., KIM, N., KIM, D.-W., NAM, S.-H. & KIM, D. 2009. Synthesis and characterization of hydroquinone fructoside *using Leuconostoc mesenteroides* levansucrase. *Applied Microbiology and Biotechnology*, 83, 1009-1016.

POTOCKÁ, E., MASTIHUBOVÁ, M. & MASTIHUBA, V. 2019. Enzymatic synthesis of tyrosol and hydroxytyrosol *β*-D-fructofuranosides. *Biocatalysis and Biotransformation,* 37**,** 18-24.

KASAI, A., ARAFUKA, S., KOSHIBA, N., TAKAHASHI, D. & TOSHIMA, K. 2015. Systematic synthesis of low-molecular weight fucoidan derivatives and their effect on cancer cells. *Organic and Biomolecular Chemistry*, 13, 10556.

KATCHALSKI-KATZIR, E. & KRAEMER, D. M. 2000. Eupergit C, a carrier for immobilization of enzymes of industrial potential. *Journal of Molecular Catalysis B: Enzymatic,* 10**,** 157-176.

KIDIBULE, P. E., SANTOS-MORIANO, P., JIMÉNEZ-ORTEGA, E., RAMÍREZ-ESCUDERO, M., LIMÓN, M. C., REMACHA, M., PLOU, F. J., SANZ-APARICIO, J. & FERNÁNDEZ-LOBATO, M. 2018. Use of chitin and chitosan to produce new chitooligosaccharides by chitinase Chit42: enzymatic activity and structural basis of protein specificity. *Microbial Cell Factories,* 17**,** 47-47.

KILIAN, S., KRITZINGER, S., RYCROFT, C., GIBSON, G. & DU PREEZ, J. 2002. The effects of the novel bifidogenic trisaccharide, neokestose, on the human colonic microbiota. *World Journal of Microbiology and Biotechnology,* 18**,** 637-644.

KIM, K. H., KIM, Y. W., KIM, H. B., LEE, B. J. & LEE, D. S. 2006. Anti-apoptotic activity of laminarin polysaccharides and their enzymatically hydrolyzed oligosaccharides from *Laminaria japonica*. *Biotechnology Letters,* 28**,** 439-446.

KIM, S. J. & RAJAPAKSE, N. 2005. Enzymatic production and biological activities of chitosan oligosaccharides (COS): A review. *Carbohydrate Polymers*, 62, 357-368.

KIM, W. J., KOO, Y.-K., JUNG, M.-K., MOON, H. R., KIM, S. M., SYNYTSYA, A., YUN-CHOI, H. S., KIM, Y. S., PARK, J. K. & PARK, Y. I. 2010. Anticoagulating activities of low-molecular weight fuco-oligosaccharides prepared by enzymatic digestion of fucoidan from the sporophyll of Korean *Undaria pinnatifida*. *Archives of Pharmacal Research,* 33**,** 125-131.

KITTUR, F. S., KUMAR, A. B. V., GOWDA, L. R. & THARANATHAN, R. N. 2003. Chitosanolysis by a pectinase isozyme of *Aspergillus niger*—A non-specific activity. *Carbohydrate Polymers,* 53**,** 191-196.

KOLENOVÁ, K., VRŠANSKÁ, M. & BIELY, P. 2006. Mode of action of endo-ß-1,4-xylanases of families 10 and 11 on acidic xylooligosaccharides. *Journal of Biotechnology,* 121**,** 338-345.

KUROSU, J., SATO, T., YOSHIDA, K., TSUGANE, T., SHIMURA, S., KIRIMURA, K., KINO, K. & USAMI, S. 2002. Enzymatic synthesis of α-arbutin by α-anomer-selective glucosylation of hydroquinone using lyophilized cells of *Xanthomonas campestris* WU-9701. *Journal of Bioscience and Bioengineering,* 93**,** 328-330.

L

LAIRSON, L. L., HENRISSAT, B., DAVIES, G. J. & WITHERS, S. G. 2008. Glycosyltransferases: Structures, Functions, and Mechanisms. *Annual Review of Biochemistry,* 77**,** 521-555.

LE DÉVÉDEC, F., BAZINET, L., FURTOS, A., VENNE, K., BRUNET, S. & MATEESCU, M. A. 2008. Separation of chitosan oligomers by immobilized metal affinity chromatography. *Journal of Chromatography A,* 1194**,** 165-171.

LI, K., XING, R., LIU, S., LI, R., QIN, Y., MENG, X. & LI, P. 2012. Separation of chito-oligomers with several degrees of polymerization and study of their antioxidant activity. *Carbohydrate Polymers,* 88**,** 896-903.

LI, M., LI, G., ZHU, L., YIN, Y., ZHAO, X., XIANG, C., YU, G. & WANG, X. 2014. Isolation and Characterization of an Agaro-Oligosaccharide (AO)-Hydrolyzing Bacterium from the Gut Microflora of Chinese Individuals. *PLOS ONE,* 9**,** e91106.

LI, K., XING, R., LIU, S. & LI, P. 2016. Advances in preparation, analysis and biological activities of single chitooligosaccharides. *Carbohydrate Polymers,* 139**,** 178-190.

LI, M., SHANG, Q., LI, G., WANG, X. & YU, G. 2017. Degradation of Marine Algae-Derived Carbohydrates by Bacteroidetes Isolated from Human Gut Microbiota. *Marine Drugs,* 15**,** 92.

LIAQAT, F. & ELTEM, R. 2018. Chitooligosaccharides and their biological activities: A comprehensive review. *Carbohydrate Polymers,* 184**,** 243-259.

LIM, J. S., LEE, J. H., KANG, S. W., PARK, S. W. & KIM, S. W. 2007. Studies on production and physical properties of neo-FOS produced by co-immobilized *Penicillium citrinum* and neo-fructosyltransferase. *European Food Research and Technology,* 225**,** 457-462.

LINARES-PASTÉN, J. A., ARONSSON, A. & NORDBERG KARLSSON, E. 2018. Structural considerations on the use of endo-xylanases for the production of prebiotic xylooligosaccharides from biomass. *Current Protein and Peptide Science,* 19**,** 48-67.

LINDE, D., MACIAS, I., FERNÁNDEZ-ARROJO, L., PLOU, F. J., JIMÉNEZ, A. & FERNÁNDEZ-LOBATO, M. 2009. Molecular and biochemical characterization of a beta-fructofuranosidase from *Xanthophyllomyces dendrorhous*. *Applied and Environmental Microbiology,* 75**,** 1065-1073.

LINDE, D., RODRIGUEZ-COLINAS, B., ESTEVEZ, M., POVEDA, A., PLOU, F. J. & FERNANDEZ LOBATO, M. 2012. Analysis of neofructooligosaccharides production mediated by the extracellular beta-fructofuranosidase from *Xanthophyllomyces dendrorhous*. *Bioresource Technology,* 109**,** 123-130.

LODHI, G., KIM, Y.-S., HWANG, J.-W., KIM, S.-K., JEON, Y.-J., JE, J.-Y., AHN, C.-B., MOON, S.-H., JEON, B.-T. & PARK, P.-J. 2014. Chitooligosaccharide and its derivatives: preparation and biological applications. *BioMed Research International,* 2014**,** 654913.

LORENZONI, A. S. G., AYDOS, L. F., KLEIN, M. P., AYUB, M. A. Z., RODRIGUES, R. C. & HERTZ, P. F. 2015. Continuous production of fructooligosaccharides and invert sugar by chitosan immobilized enzymes: Comparison between in fluidized and packed bed reactors. *Journal of Molecular Catalysis B: Enzymatic,* 111**,** 51-55.

LOZINSKY, V. I. & PLIEVA, F. M. 1998. Poly(vinyl alcohol) cryogels employed as matrices for cell immobilization. 3. Overview of recent research and developments. *Enzyme and Microbial Technology,* 23**,** 227-242.

LU, L., GUO, Y., XU, L., QI, T., JIN, L., XU, L. & XIAO, M. 2015. Galactosylation of caffeic acid by an engineered ß-galactosidase. *Drug Discoveries & Therapeutics,* 9**,** 123-128.

M

MAHATA, M., SHINYA, S., MASAKI, E., YAMAMOTO, T., OHNUMA, T., BRZEZINSKI, R., MAZUMDER, T. K., YAMASHITA, K., NARIHIRO, K. & FUKAMIZO, T. 2014. Production of chitooligosaccharides from *Rhizopus oligosporus* NRRL2710 cells by chitosanase digestion. *Carbohydrate Research,* 383**,** 27-33.

MATEOS-APARICIO, I., MENGIBAR, M. & HERAS, A. 2016. Effect of chito-oligosaccharides over human faecal microbiota during fermentation in batch cultures. *Carbohydrate Polymers,* 137**,** 617-624.

MAYER, J., KRANZ, B. & FISCHER, L. 2010. Continuous production of lactulose by immobilized thermostable ß-glycosidase from *Pyrococcus furiosus*. *Journal of Biotechnology,* 145**,** 387-393.

MENA-ARIZMENDI, A., ALDERETE, J., AGUILA, S., MARTY, A., MIRANDA-MOLINA, A., LOPEZ MUNGUIA, A. & CASTILLO, E. 2011. Enzymatic fructosylation of aromatic and aliphatic alcohols by Bacillus subtilis levansucrase: Reactivity of acceptors. *Journal of Molecular Catalysis B: Enzymatic*, 70, 41-48.

MÍGUEZ, N., RAMÍREZ-ESCUDERO, M., GIMENO-PÉREZ, M., POVEDA, A., JIMÉNEZ-BARBERO, J., BALLESTEROS, A. O., FERNÁNDEZ-LOBATO, M., SANZ-APARICIO, J. & PLOU, F. J. 2018. Fructosylation of Hydroxytyrosol by the *β*-Fructofuranosidase from *Xanthophyllomyces dendrorhous*: Insights into the Molecular Basis of the Enzyme Specificity. *ChemCatChem,* 10**,** 4878-4887.

MIRO-CASAS, E., COVAS, M.-I., FARRE, M., FITO, M., ORTUÑO, J., WEINBRENNER, T., ROSET, P. & DE LA TORRE, R. 2003. Hydroxytyrosol Disposition in Humans. *Clinical Chemistry,* 49**,** 945.

MOUELHI, R., ABIDI, F. & MARZOUKI, M. N. 2016. An improved method for the production of fructooligosaccharides by immobilized *β*-fructofuranosidase from *Sclerotinia sclerotiorum*. *Biotechnology and Applied Biochemistry,* 63**,** 281-291.

MUANPRASAT, C. & CHATSUDTHIPONG, V. 2017. Chitosan oligosaccharide: Biological activities and potential therapeutic applications. *Pharmacology & Therapeutics,* 170**,** 80-97.

MUROTA, K., MATSUDA, N., KASHINO, Y., FUJIKURA, Y., NAKAMURA, T., KATO, Y., SHIMIZU, R., OKUYAMA, S., TANAKA, H., KODA, T., SEKIDO, K. & TERAO, J. 2010. α-Oligoglucosylation of a sugar moiety enhances the bioavailability of quercetin glucosides in humans. *Archives of Biochemistry and Biophysics,* 501**,** 91-97.

MUSSATTO, S. I. & MANCILHA, I. M. 2007. Non-digestible oligosaccharides: A review. *Carbohydrate Polymers,* 68**,** 587-597.

N

NADIM, M., AURIOL, D., LAMERANT-FAYEL, N., LEFÈVRE, F., DUBANET, L., REDZINIAK, G., KIEDA, C. & GRILLON, C. 2014. Improvement of polyphenol properties upon glucosylation in a UV-induced skin cell ageing model. *International Journal of Cosmetic Science,* 36**,** 579-587.

NIETO-DOMÍNGUEZ, M., DE EUGENIO, L. I., PEÑALVER, P., BELMONTE-RECHE, E., MORALES, J. C., POVEDA, A., JIMÉNEZ-BARBERO, J., PRIETO, A., PLOU, F. J. & MARTÍNEZ, M. J. 2017a. Enzymatic Synthesis of a Novel Neuroprotective Hydroxytyrosyl Glycoside. *Journal of Agricultural and Food Chemistry,* 65**,** 10526-10533.

NIETO-DOMÍNGUEZ, M., DE EUGENIO, L. I., YORK-DURÁN, M. J., RODRÍGUEZ-COLINAS, B., PLOU, F. J., CHENOLL, E., PARDO, E., CODOÑER, F. & JESÚS MARTÍNEZ, M. 2017b. Prebiotic effect of xylooligosaccharides produced from birchwood xylan by a novel fungal GH11 xylanase. *Food Chemistry,* 232**,** 105-113.

NING, Y., WANG, J., CHEN, J., NA, Y., JIN, Z. & XU, X. 2010. Production of neo-fructooligosaccharides using free-whole-cell biotransformation by *Xanthophyllomyces dendrorhous*. *Bioresource Technology*, 101, 7472-7478.

NOBRE, C., TEIXEIRA, J. A. & RODRIGUES, L. R. 2015. New Trends and Technological Challenges in the Industrial Production and Purification of Fructo-oligosaccharides. *Critical Reviews in Food Science and Nutrition,* 55**,** 1444-1455.

NORDLUND, J. J., GRIMES, P. E. & ORTONNE, J. P. 2006. The safety of hydroquinone. *Journal of the European Academy of Dermatology and Venereology,* 20**,** 781-787.

NUNES, M. A. P., FERNANDES, P. C. B. & RIBEIRO, M. H. L. 2013. Microtiter plates versus stirred mini-bioreactors in biocatalysis: A scalable approach. *Bioresource Technology,* 136**,** 30-40.

NUNES, M. A. P., GOIS, P. M. P., ROSA, M. E., MARTINS, S., FERNANDES, P. C. B. & RIBEIRO, M. H. L. 2016. Boronic acids as efficient cross linkers for PVA: synthesis and application of tunable hollow microspheres in biocatalysis. *Tetrahedron,* 72**,** 7293-7305.

NUNES, M. A. P., ROSA, M. E., FERNANDES, P. C. B. & RIBEIRO, M. H. L. 2014. Operational stability of naringinase PVA lens-shaped microparticles in batch stirred reactors and mini packed bed reactors-one step closer to industry. *Bioresource Technology,* 164**,** 362-370.

NÚÑEZ-LÓPEZ, G., HERRERA-GONZÁLEZ, A., HERNÁNDEZ, L., AMAYA-DELGADO, L., SANDOVAL, G., GSCHAEDLER, A., ARRIZON, J., REMAUD-SIMEON, M. & MOREL, S. 2019. Fructosylation of phenolic compounds by levansucrase from *Gluconacetobacter diazotrophicus*. *Enzyme and Microbial Technology,* 122**,** 19-25.

O

OHBUCHI, T., SAKAINO, M., TAKAHASHI, T., AZUMI, N., ISHIKAWA, K., KAWAZOE, S., KOBAYASHI, Y. & KIDO, Y. 2010. Oral administration of acidic xylooligosaccharides prevents the development of atopic dermatitis-like skin lesions in NC/Nga mice. *Journal of Nutritional Science and Vitaminology,* 56**,** 54-59.

OHBUCHI, T., TAKAHASHI, T., AZUMI, N. & SAKAINO, M. 2009. Structural analysis of neutral and acidic xylooligosaccharides from hardwood kraft pulp, and their utilization by intestinal bacteria in vitro. *Bioscience, Biotechnology and Biochemistry,* 73**,** 2070-2076.

ONO, Y., TOMIMORI, N., TATEISHI, N., MORIWAKI, M., EMURA, K., & OKUYAMA, S. 2006. Quercetin Glycoside Composition and Method of Preparing the Same. US patent US20090143317A1.

P

PANTALEONE, D., YALPANI, M. & SCOLLAR, M. 1992. Unusual susceptibility of chitosan to enzymatic hydrolysis. *Carbohydrate Research,* 237**,** 325-332.

PARK, P.-J., JE, J.-Y. & KIM, S.-K. 2003. Angiotensin I Converting Enzyme (ACE) Inhibitory Activity of Hetero-Chitooligosaccharides Prepared from Partially Different Deacetylated Chitosans. *Journal of Agricultural and Food Chemistry,* 51**,** 4930-4934.

PARK, J. S., PARK, H. Y., RHO, H. S., KIM, D. H., & CHANG, I. S. 2008. Method for preparing kaempferol-3-0-rutinoside and composition of skin external application comprising thereof. International patent WO2008044818A1

PIEDRABUENA, D., MÍGUEZ, N., POVEDA, A., PLOU, F. J. & FERNÁNDEZ-LOBATO, M. 2016. Exploring the transferase activity of Ffase from *Schwanniomyces occidentalis*, a ß-fructofuranosidase showing high fructosyl-acceptor promiscuity. *Applied Microbiology and Biotechnology,* 100**,** 8769-8778.

PLOU, F. J., FERNANDEZ-ARROJO, L., SANTOS-MORIANO, P. & BALLESTEROS, A. O. 2014. Application of Immobilized Enzymes for the Synthesis of Bioactive Fructooligosaccharides. *In: MORENO F.J. (ed.) Food Oligosaccharides: Production, Analysis and Bioactivity*, Wiley Blackwell, 200-216.

POLIZELI, M. L. T. M., RIZZATTI, A. C. S., MONTI, R., TERENZI, H. F., JORGE, J. A. & AMORIM, D. S. 2005. Xylanases from fungi: properties and industrial applications. *Applied Microbiology and Biotechnology,* 67**,** 577-591.

POTOCKÁ, E., MASTIHUBOVÁ, M. & MASTIHUBA, V. 2015. Enzymatic synthesis of tyrosol glycosides. *Journal of Molecular Catalysis B: Enzymatic,* 113**,** 23-28.

R

RAKMAI, J. & CHEIRSILP, B. 2016. Continuous production of ß-cyclodextrin by cyclodextrin glycosyltransferase immobilized in mixed gel beads: Comparative study in continuous stirred tank reactor and packed bed reactor. *Biochemical Engineering Journal,* 105, Part A**,** 107-113.

RAMÍREZ-ESCUDERO, M., GIMENO-PÉREZ, M., GONZÁLEZ, B., LINDE, D., MERDZO, Z., FERNÁNDEZ-LOBATO, M. & SANZ-APARICIO, J. 2016. Structural Analysis of ß-Fructofuranosidase from *Xanthophyllomyces dendrorhous* Reveals Unique Features and the Crucial Role of N-Glycosylation in Oligomerization and Activity. *The Journal of Biological Chemistry,* 291**,** 6843-6857.

RE, R., PELLEGRINI, N., PROTEGGENTE, A., PANNALA, A., YANG, M. & RICE-EVANS, C. 1999. Antioxidant activity applying an improved ABTS radical cation decolorization assay. *Free Radical Biology and Medicine,* 26**,** 1231-1237.

RESCIGNANO, N., FORTUNATI, E., MONTESANO, S., EMILIANI, C., KENNY, J. M., MARTINO, S. & ARMENTANO, I. 2014. PVA bio-nanocomposites: A new take-off using cellulose nanocrystals and PLGA nanoparticles. *Carbohydrate Polymers,* 99**,** 47-58.

ROBERFROID, M. 1993. Dietary fiber, inulin, and oligofructose: A review comparing their physiological effects. *Critical Reviews in Food Science and Nutrition,* 33**,** 103-148.

ROBLES-ALMAZAN, M., PULIDO-MORAN, M., MORENO-FERNANDEZ, J., RAMIREZ-TORTOSA, C., RODRIGUEZ-GARCIA, C., QUILES, J. L. & RAMIREZ-TORTOSA, M. 2018. Hydroxytyrosol: Bioavailability, toxicity, and clinical applications. *Food Research International,* 105**,** 654-667.

RODRIGUES, R. C., ORTIZ, C., BERENGUER-MURCIA, A., TORRES, R. & FERNANDEZ-LAFUENTE, R. 2013. Modifying enzyme activity and selectivity by immobilization. *Chemical Society Reviews,* 42**,** 6290-6307.

RODRIGUES, R. C., VIRGEN-ORTÍZ, J. J., DOS SANTOS, J. C. S., BERENGUER-MURCIA, Á., ALCANTARA, A. R., BARBOSA, O., ORTIZ, C. & FERNANDEZ-LAFUENTE, R. 2019. Immobilization of lipases on hydrophobic supports: immobilization mechanism, advantages, problems, and solutions. *Biotechnology Advances.*

RODRIGUEZ-COLINAS, B., KOLIDA, S., BARAN, M., BALLESTEROS, A. O., RASTALL, R. A. & PLOU, F. J. 2013. Analysis of fermentation selectivity of purified galacto-oligosaccharides by in vitro human faecal fermentation. *Applied Microbiology and Biotechnology,* 97**,** 5743-5752.

RODRIGUEZ-GOMEZ, R., JIMENEZ-DIAZ, I., ZAFRA-GOMEZ, A. & MORALES, J. C. 2015. Improved sample treatment for the determination of fructooligosaccharides in milk related products by liquid chromatography with electrochemical and refractive index detection. *Talanta,* 144**,** 883-889.

RYE, C. S. & WITHERS, S. G. 2000. Glycosidase mechanisms. *Current Opinion in Chemical Biology,* 4**,** 573-580.

S

SABATER-MOLINA, M., LARQUE, E., TORRELLA, F. & ZAMORA, S. 2009. Dietary fructooligosaccharides and potential benefits on health. *Journal of Physiology and Biochemistry,* 65**,** 315-328.

SAMANTA, A. K., JAYAPAL, N., JAYARAM, C., ROY, S., KOLTE, A. P., SENANI, S. & SRIDHAR, M. 2015. Xylooligosaccharides as prebiotics from agricultural by-products: Production and applications. *Bioactive Carbohydrates and Dietary Fibre,* 5**,** 62-71.

SANTOS-MORIANO, P., FERNANDEZ-ARROJO, L., POVEDA, A., JIMENEZ-BARBERO, J., BALLESTEROS, A. O. & PLOU, F. J. 2015. Levan versus fructooligosaccharide synthesis using the levansucrase from *Zymomonas mobilis*: Effect of reaction conditions. *Journal of Molecular Catalysis B: Enzymatic,* 119**,** 18-25.

SANTOS-MORIANO, P., WOODLEY, J. M. & PLOU, F. J. 2016. Continuous production of chitooligosaccharides by an immobilized enzyme in a dual-reactor system. *Journal of Molecular Catalysis B: Enzymatic,* 133**,** 211-217.

SANTOS-MORIANO, P., FERNANDEZ-ARROJO, L., MENGIBAR, M., BELMONTE-RECHE, E., PEÑALVER, P., ACOSTA, F. N., BALLESTEROS, A. O., MORALES, J. C., KIDIBULE, P., FERNANDEZ-LOBATO, M. & PLOU, F. J. 2018a. Enzymatic production of fully deacetylated chitooligosaccharides and their neuroprotective and anti-inflammatory properties. *Biocatalysis and Biotransformation,* 36**,** 57-67.

SANTOS-MORIANO, P., KIDIBULE, P. E., ALLEYNE, E., BALLESTEROS, A. O., HERAS, A., FERNANDEZ-LOBATO, M. & PLOU, F. J. 2018b. Efficient conversion of chitosan into chitooligosaccharides by a chitosanolytic activity from *Bacillus thuringiensis*. *Process Biochemistry,* 73**,** 102-108.

SCOTT, K. P., MARTIN, J. C., DUNCAN, S. H. & FLINT, H. J. 2014. Prebiotic stimulation of human colonic butyrate-producing bacteria and bifidobacteria, in vitro. *FEMS Microbiology Ecology,* 87**,** 30-40.

SCHLIEKER, M. & VORLOP, K.-D. 2006. A Novel Immobilization Method for Entrapment: LentiKats®. *In:* GUISAN, J. M. (ed.) *Immobilization of Enzymes and Cells*. Totowa, NJ: Humana Press, pp. 333-343.

SCHMALTZ, R. M., HANSON, S. R. & WONG, C.-H. 2011. Enzymes in the Synthesis of Glycoconjugates. *Chemical Reviews,* 111**,** 4259-4307.

SEMEŇUK, T., KRIST, P., PAVLÍČEK, J., BEZOUŠKA, K., KUZMA, M., NOVÁK, P. & KŘEN, V. 2001. Synthesis of chitooligomer-based glycoconjugates and their binding to the rat natural killer cell activation receptor NKR-P1. *Glycoconjugate Journal,* 18**,** 817-826.

SHARON, N. 1986. Nomenclature of glycoproteins, glycopeptides and peptidoglycans. *European Journal of Biochemistry,* 159**,** 1-6.

SHELDON, R. A. 2007. Enzyme immobilization: The quest for optimum performance. *Advanced Synthesis & Catalysis,* 349**,** 1289-1307.

SHELDON, R. A., SCHOEVAART, R. & VAN LANGEN, L. M. 2005. Cross-linked enzyme aggregates (CLEAs): A novel and versatile method for enzyme immobilization (a review). *Biocatalysis and Biotransformation,* 23**,** 141-147.

SHELDON, R. A. & VAN PELT, S. 2013. Enzyme immobilisation in biocatalysis: Why, what and how. *Chemical Society Reviews,* 42**,** 6223-6235.

SHEU, D.-C., CHANG, J.-Y., CHEN, Y.-J. & LEE, C.-W. 2013. Production of high-purity neofructooligosaccharides by culture of *Xanthophyllomyces dendrorhous*. *Bioresource Technology*, 132, 432-435.

SHI, Y., LIU, J., YAN, Q., YOU, X., YANG, S. & JIANG, Z. 2018. In vitro digestibility and prebiotic potential of curdlan $(1 \rightarrow 3)$-β-D-glucan oligosaccharides in Lactobacillus species. *Carbohydrate Polymers,* 188**,** 17-26.

SINGH, M., ARSENEAULT, M., SANDERSON, T., MURTHY, V. & RAMASSAMY, C. 2008. Challenges for Research on Polyphenols from Foods in Alzheimer's Disease: Bioavailability, Metabolism, and Cellular and Molecular Mechanisms. *Journal of Agricultural and Food Chemistry,* 56**,** 4855-4873.

SINGH, R. K., CHANG, H.-W., YAN, D., LEE, K. M., UCMAK, D., WONG, K., ABROUK, M., FARAHNIK, B., NAKAMURA, M., ZHU, T. H., BHUTANI, T. & LIAO, W. 2017. Influence of diet on the gut microbiome and implications for human health. *Journal of Translational Medicine,* 15**,** 73.

SONG, J. Y., ALNAEELI, M. & PARK, J. K. 2014. Efficient digestion of chitosan using chitosanase immobilized on silica-gel for the production of multisize chitooligosaccharides. *Process Biochemistry,* 49**,** 2107-2113.

SUN, Y., YANG, B., WU, Y., LIU, Y., GU, X., ZHANG, H., WANG, C., CAO, H., HUANG, L. & WANG, Z. 2015. Structural characterization and antioxidant activities of κ-carrageenan oligosaccharides degraded by different methods. *Food Chemistry,* 178**,** 311-318.

T

TANG, J., ZHEN, H., WANG, N., YAN, Q., JING, H. & JIANG, Z. 2019. Curdlan oligosaccharides having higher immunostimulatory activity than curdlan in mice treated with cyclophosphamide. *Carbohydrate Polymers,* 207**,** 131-142.

TELEMAN, A., TENKANEN, M., JACOBS, A. & DAHLMAN, O. 2002. Characterization of O-acetyl-(4-O-methylglucurono)xylan isolated from birch and beech. *Carbohydrate Research,* 337**,** 373-377.

THUAN, N. H. & SOHNG, J. K. 2013. Recent biotechnological progress in enzymatic synthesis of glycosides. *Journal of Industrial Microbiology & Biotechnology,* 40**,** 1329-1356.

TORRES-SALAS, P., DEL MONTE-MARTINEZ, A., CUTIÑO-AVILA, B., RODRIGUEZ-COLINAS, B., ALCALDE, M., BALLESTEROS, A. O. & PLOU, F. J.

2011. Immobilized Biocatalysts: Novel Approaches and Tools for Binding Enzymes to Supports. *Advanced Materials,* 23**,** 5275-5282.

TORRES, P., POVEDA, A., JIMENEZ-BARBERO, J., PARRA, J. L., COMELLES, F., BALLESTEROS, A. O. & PLOU, F. J. 2011. Enzymatic Synthesis of α-Glucosides of Resveratrol with Surfactant Activity. *Advanced Synthesis & Catalysis,* 353**,** 1077-1086.

TRINCONE, A. 2010. Five Years Patenting Time Frame Concerning Enzymatic Preparation of Glycosides. *Recent Patents on Biotechnology,* 4**,** 30-47.

TRINCONE, A., PAGNOTTA, E. & TRAMICE, A. 2012. Enzymatic routes for the production of mono- and di-glucosylated derivatives of hydroxytyrosol. *Bioresource Technology,* 115**,** 79-83.

TSAO, R. 2010. Chemistry and biochemistry of dietary polyphenols. *Nutrients,* 2**,** 1231-1246.

TUSI, S. K., KHALAJ, L., ASHABI, G., KIAEI, M. & KHODAGHOLI, F. 2011. Alginate oligosaccharide protects against endoplasmic reticulum- and mitochondrial-mediated apoptotic cell death and oxidative stress. *Biomaterials,* 32**,** 5438-5458.

V

VALLS, C., PASTOR, F. I. J., VIDAL, T., RONCERO, M. B., DÍAZ, P., MARTÍNEZ, J. & VALENZUELA, S. V. 2018. Antioxidant activity of xylooligosaccharides produced from glucuronoxylan by Xyn10A and Xyn30D xylanases and eucalyptus autohydrolysates. *Carbohydrate Polymers,* 194**,** 43-50.

VARKI, A. 1993. Biological roles of oligosaccharides: all of the theories are correct. *Glycobiology,* 3**,** 97-130.

VARKI, A. 2017. Biological roles of glycans. *Glycobiology,* 27**,** 3-49.

VAZQUEZ, M. J., ALONSO, J. L., DOMÍNGUEZ, H. & PARAJO, J. C. 2001. Xylooligosaccharides: Manufacture and applications. *Trends in Food Science and Technology,* 11**,** 387-393.

VISIOLI, F., BELLOMO, G. & GALLI, C. 1998. Free Radical-Scavenging Properties of Olive Oil Polyphenols. *Biochemical and Biophysical Research Communications,* 247**,** 60-64.

W

WANG, X., WANG, L., CHE, J., LI, X., LI, J., WANG, J. & XU, Y. 2014. In vitro non-specific immunostimulatory effect of alginate oligosaccharides with different molecular weights and compositions on sea cucumber (*Apostichopus japonicus*) coelomocytes. *Aquaculture,* 434**,** 434-441.

WANG, Y., HAN, F., HU, B., LI, J. & YU, W. 2006. In vivo prebiotic properties of alginate oligosaccharides prepared through enzymatic hydrolysis of alginate. *Nutrition Research,* 26**,** 597-603.

WEN, L., EDMUNDS, G., GIBBONS, C., ZHANG, J., GADI, M. R., ZHU, H., FANG, J., LIU, X., KONG, Y. & WANG, P. G. 2018. Toward Automated Enzymatic Synthesis of Oligosaccharides. *Chemical Reviews,* 118**,** 8151-8187.

WU, S.-J., PAN, S.-K., WANG, H.-B. & WU, J.-H. 2013a. Preparation of chitooligosaccharides from cicada slough and their antibacterial activity. *International Journal of Biological Macromolecules,* 62**,** 348-351.

WU, X., CHU, J., LIANG, J. & HE, B. 2013b. Efficient enzymatic synthesis of mangiferin glycosides in hydrophilic organic solvents. *RSC Advances,* 3**,** 19027-19032.

WU, X., CHU, J., WU, B., ZHANG, S. & HE, B. 2013c. An efficient novel glycosylation of flavonoid by ß-fructosidase resistant to hydrophilic organic solvents. *Bioresource Technology,* 129**,** 659-662.

X

XIA, W., LIU, P. & LIU, J. 2008. Advance in chitosan hydrolysis by non-specific cellulases. *Bioresource Technology,* 99**,** 6751-6762.

XU, L., QI, T., XU, L., LU, L. & XIAO, M. 2016. Recent progress in the enzymatic glycosylation of phenolic compounds. *Journal of Carbohydrate Chemistry,* 35**,** 1-23.

XU, Q., ZHENG, X., HUANG, M., WU, M., YAN, Y., PAN, J., YANG, Q., DUAN, C.-J., LIU, J.-L. & FENG, J.-X. 2015. Purification and biochemical characterization of a novel ß-fructofuranosidase from *Penicillium oxalicum* with transfructosylating activity producing neokestose. *Process Biochemistry,* 50**,** 1237-1246.

XU, S.-Y., KAN, J., HU, Z., LIU, Y., DU, H., PANG, G.-C. & CHEONG, K.-L. 2018. Quantification of Neoagaro-Oligosaccharide Production through Enzymatic Hydrolysis and its Anti-Oxidant Activities. *Molecules (Basel, Switzerland),* 23**,** 1354.

Y

YAMAMOTO, I., MUTO, N., NAGATA, E., NAKAMURA, T. & SUZUKI, Y. 1990. Formation of a stable L-ascorbic acid α-glucoside by mammalian α-glucosidase-catalyzed transglucosylation. *Biochimica et Biophysica Acta (BBA) - General Subjects,* 1035**,** 44-50.

YAMASAKI, T., ENOMOTO, A., KATO, A., ISHII, T., KAMEYAMA, M., ANZAI, H. & SHIMIZU, K. 2012. Enzymatically derived aldouronic acids from *Cryptomeria japonica* arabinoglucuronoxylan. *Carbohydrate Polymers,* 87**,** 1425-1432.

YAO, Z.-A., XU, L. & WU, H.-G. 2014. Immunomodulatory Function of κ-Carrageenan Oligosaccharides Acting on LPS-Activated Microglial Cells. *Neurochemical Research,* 39**,** 333-343.

YOSHINO, K., HIGASHI, N. & KOGA, K. 2006a. Inhibitory Effects of Acidic Xylooligosaccharide on Stress-induced Gastric Inflammation in Mice. *Food Hygiene and Safety Science (Shokuhin Eiseigaku Zasshi),* 47**,** 284-287.

YOSHINO, K., HIGASHI, N. & KOGA, K. 2006b. Preventive Effects of Acidic Xylooligosaccharide on Contact Hypersensitivity in Mice. *Journal of Health Science,* 52**,** 628-632.

YOUNES, I. & RINAUDO, M. 2015. Chitin and chitosan preparation from marine sources. Structure, properties and applications. *Marine Drugs,* 13**,** 1133-1174.

YUN, J. W. 1996. Fructooligosaccharides— Occurrence, preparation, and application. *Enzyme and Microbial Technology,* 19**,** 107-117.

YUN, J. W., KANG, S. C. & SONG, S. K. 1995. Continuous production of fructooligosaccharides from sucrose by immobilized fructosyltransferase. *Biotechnology Techniques,* 9**,** 805-808.

Z

ZAMBELLI, P., FERNANDEZ-ARROJO, L., ROMANO, D., SANTOS-MORIANO, P., GIMENO-PEREZ, M., POVEDA, A., GANDOLFI, R., FERNÁNDEZ-LOBATO, M., MOLINARI, F. & PLOU, F. J. 2014. Production of fructooligosaccharides by mycelium-bound transfructosylation activity present in *Cladosporium cladosporioides* and *Penicilium sizovae*. *Process Biochemistry,* 49**,** 2174-2180.

ZOU, P., YANG, X., WANG, J., LI, Y., YU, H., ZHANG, Y. & LIU, G. 2016. Advances in characterisation and biological activities of chitosan and chitosan oligosaccharides. *Food Chemistry,* 190**,** 1174-1181.

ZOU, Y., FU, X., LIU, N., DUAN, D., WANG, X., XU, J. & GAO, X. 2019. The synergistic anti-inflammatory activities of agaro-oligosaccharides with different degrees of polymerization. *Journal of Applied Phycology*.

APPENDIX I

SUPPLEMENTARY MATERIAL

Mass spectrometry and NMR

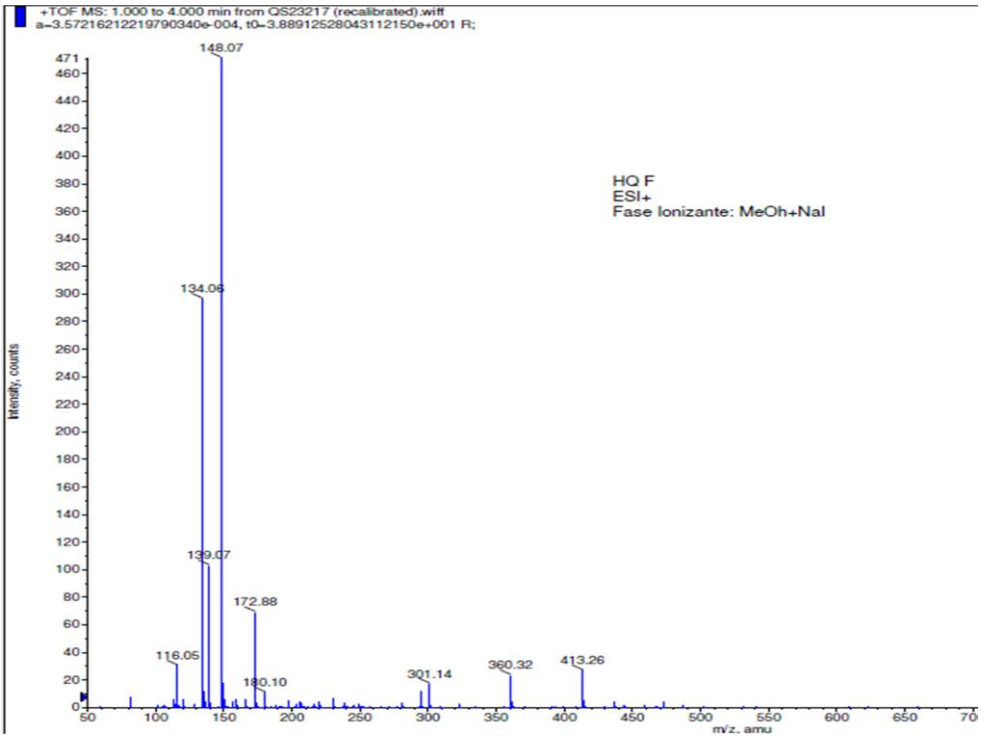

Figure S1 Mass spectrometry (ESI-TOF) of the HQ fructosides.

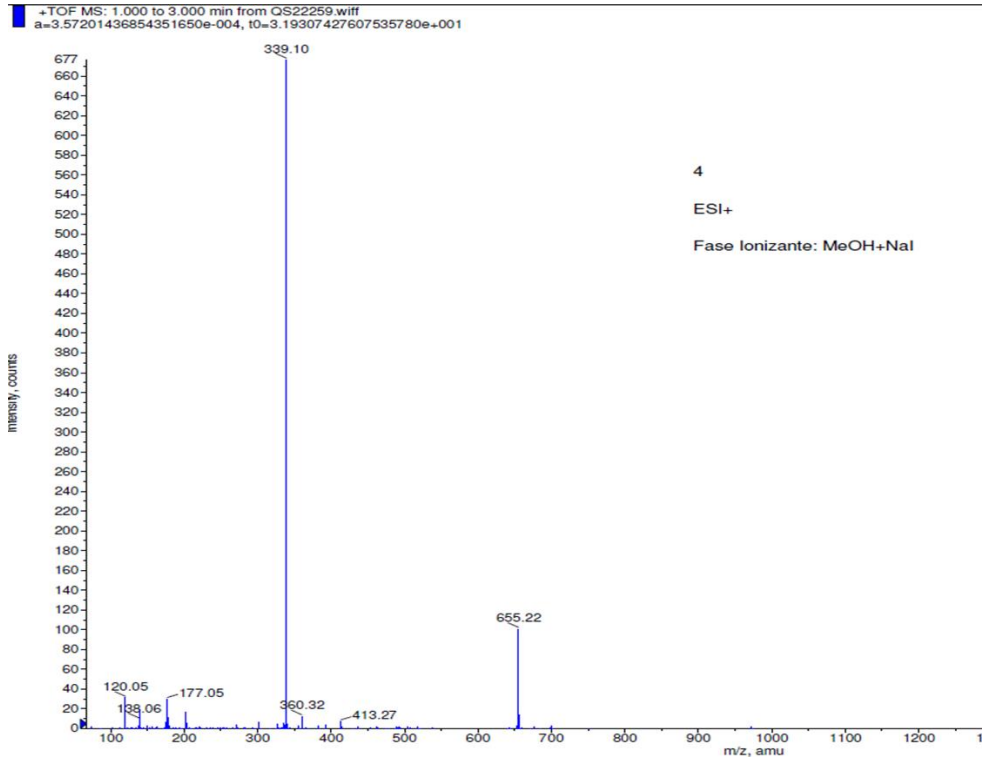

Figure S2 Mass spectrometry (ESI-TOF) of the HT fructosides.

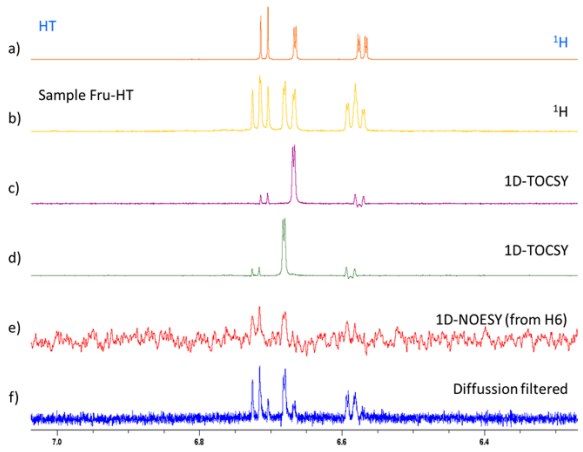

Position	δ_C (ppm), type	δ_H (ppm)
1	135.3, C	-
2	120.1, CH	6.68
3	146.5, C	-
4	145.0, C	-
5	118.9, CH	6.72
6	124.3, CH	6.59
A	64.9, CH2	3.55 / 3.60
B	37.4, CH2	2.58
1'	62.3, CH2	3.45 / 3.56
2'	106.1, C	-
3'	78.9, CH	3.94
4'	77.8, CH	3.62
5'	83.8, CH	3.56
6'	65.6, CH2	2.51 / 3.21

Figure S3 NMR Spectroscopic Data (800 MHz, D2O, 298K) for compound Fru-HT1.

Table S1 NMR Spectroscopic Data (800 MHz, D2O, 298K) for compound X2_MeGlcA.

Unit	H1/C1	H2/C2	H3/C3	H4/C4	H5/C5	OMe [4]	CO2H [6]
X1 α	5.1 ($^2J_{H1H2}$= 3.6 Hz)[a] /94.6	3.46/73.9	3.78/73.55	3.71/**78.72**	3.78,3.72/61.25	-	-
X1 β	4.5 ($^2J_{H1H2}$= 7.9 Hz)[b] /99.1	3.16/76.56	3.49/76.56	3.68/**74.87**	4.0, 3.37/65.45	-	-
X2	4.52 ($^2J_{H1H2}$= 7.6 Hz)[c] /104.3	3.33/**79.0**	3.4/76.95	3.57/72.0	3.9, 3.23/67.5	-	-
GA3	5.23,5.25 ($^2J_{H1H2}$= 3.9 Hz)[d] /100.1	3.5/73.8	3.7/78.7	3.14/**85.14**	4.23 ($^2J_{H1H2}$= 10.1 Hz)[e] /74.79	3.4/62.45	-/179.3[f]

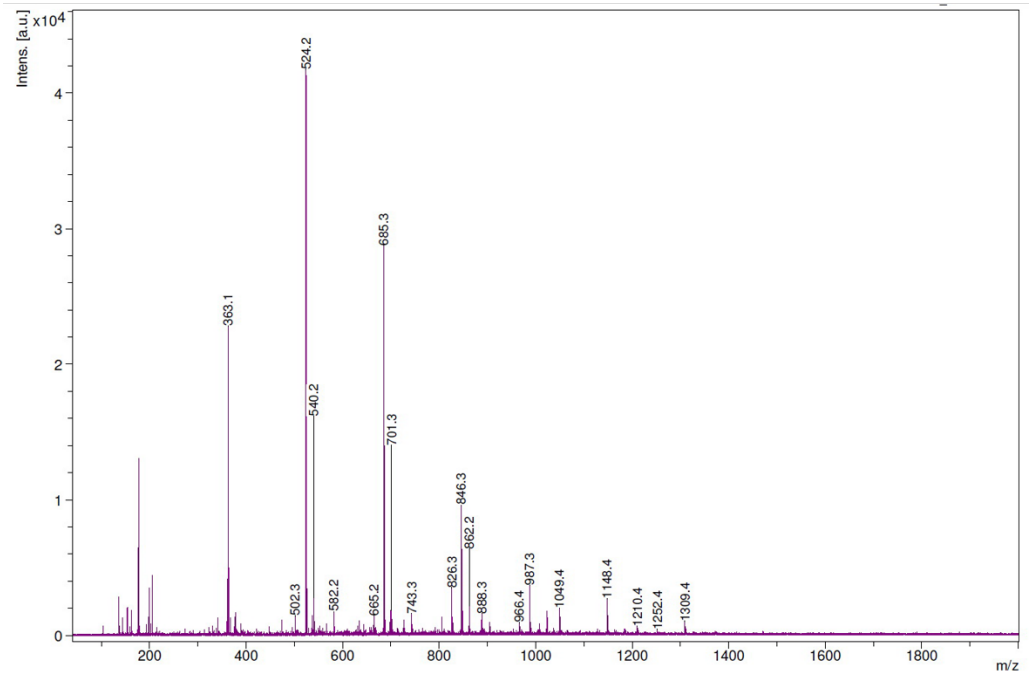

Figure S4 Mass spectrometry (MALDI-TOF) of the fdCOS mixture (obtained with chitosan CHIT600 + Neutrase 0.8L).

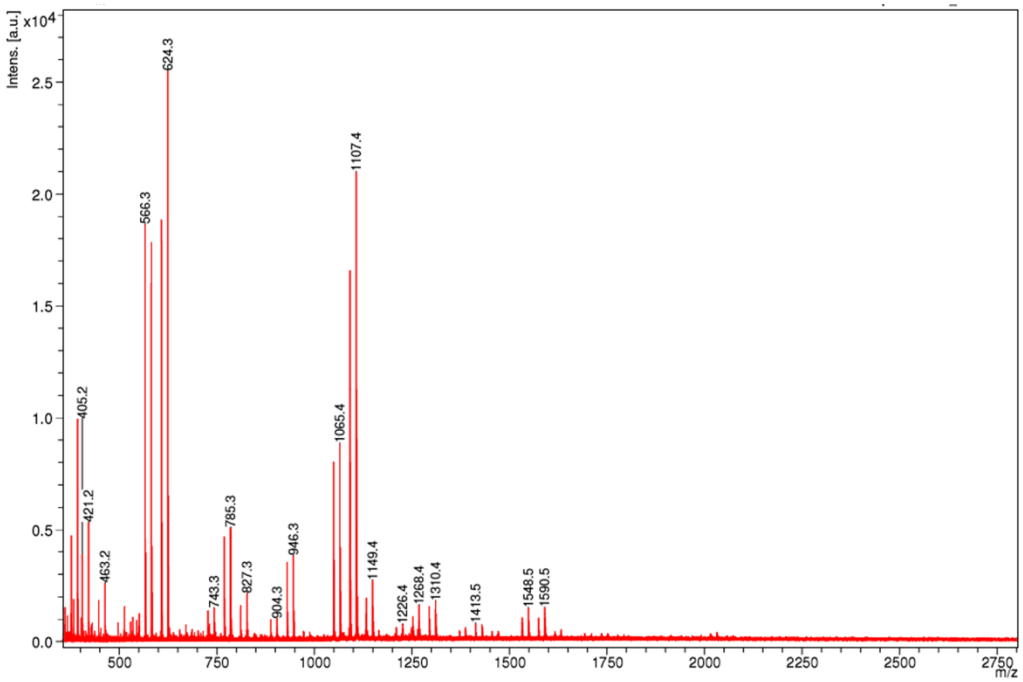

Figure S5 Mass spectrometry (MALDI-TOF) of the paCOS mixture (obtained with chitosan QS1 + CHIT42).

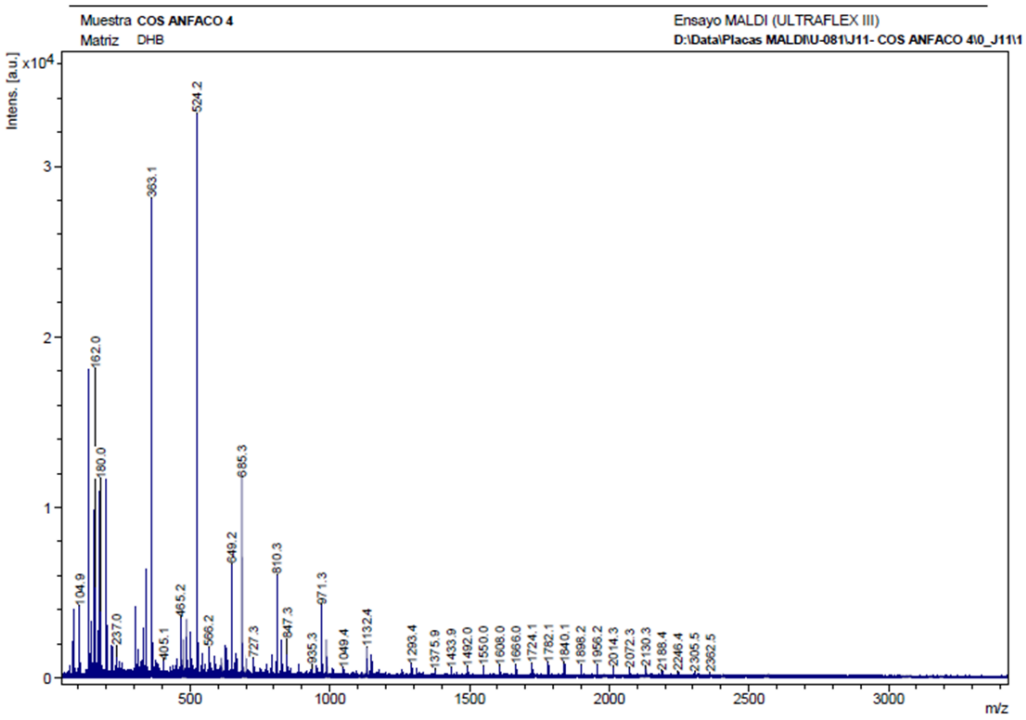

Figure S6 Mass spectrometry (MALDI-TOF) of the fdCOS and paCOS mixture (obtained with chitosan CHIT1 + Neutrase 0.8L).

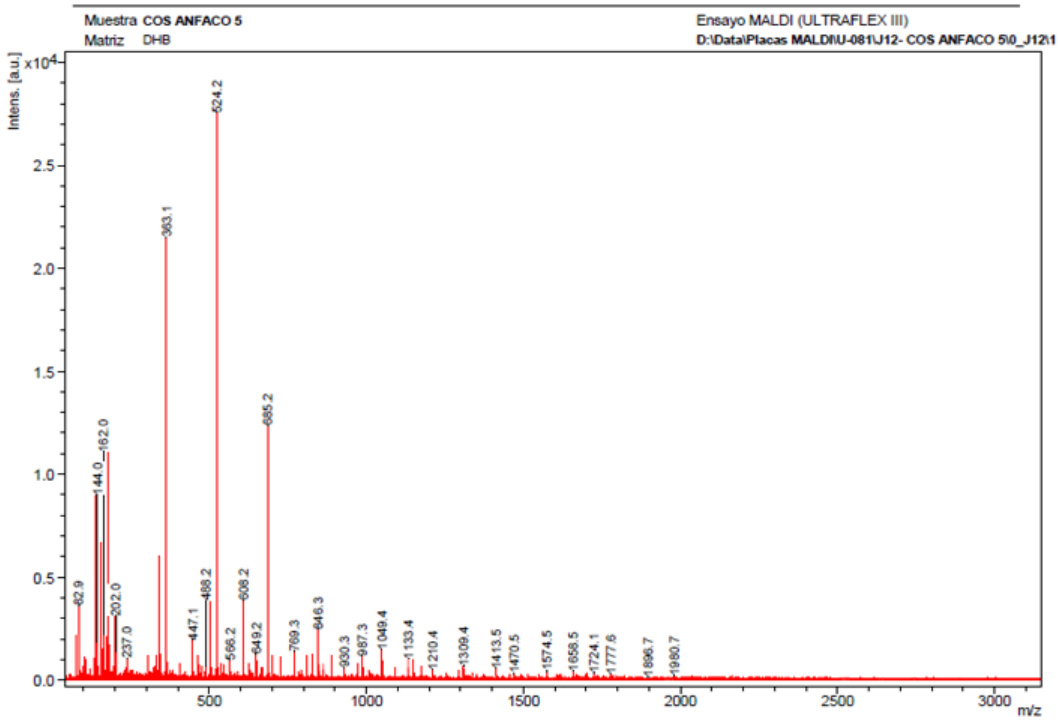

Figure S7 Mass spectrometry (MALDI-TOF) of the fdCOS and paCOS mixture (obtained with CHIT2 + Neutrase 0.8L).

APPENDIX II

PUBLICATIONS

Publications related with the Thesis

"Fructosylation of hydroxytyrosol by the *β*-fructofuranosidase from *Xanthophyllomyces dendrorhous*: Insights into the molecular basis of the enzyme specificity". N. Míguez, M. Ramírez-Escudero, M. Gimeno-Pérez, A. Poveda, J. Jiménez-Barbero, A. O. Ballesteros, M. Fernández-Lobato, J. Sanz-Aparicio* and F. J. Plou* *ChemCatChem* **(2018)**, 10.1002/cctc.201801171.

"Immobilization of the β-fructofuranosidase from *Xanthophyllomyces dendrorhous* by entrapment in polyvinyl alcohol and its application to neo-fructooligosaccharides production". N. Miguez, M. Gimeno-Perez, D. Fernandez-Polo, F.V. Cervantes, A.O. Ballesteros, M. Fernandez-Lobato, M.H. Ribeiro, F.J Plou*. *Catalysts* 8(5), 201 **(2018)**, 10.3390/catal8050201.

"Tailored enzymatic synthesis of chitooligosaccharides with different deacetylation degree and their anti-inflammatory activity". P. Santos-Moriano, P. Kidibule, N. Míguez, L. Fernández-Arrojo, A.O. Ballesteros, M. Fernández-Lobato and F.J. Plou*. *Catalysts* **(2019)**, 10.3390/catal9050405.

Other publications

"Optimization of regioselective α-glucosylation of hesperetin catalyzed by cyclodextrin glucanotransferase". J.L. González-Alfonso, N. Míguez, J.D. Padilla, L. Leemans, A. Poveda, J. Jimenez-Barbero, A.O. Ballesteros, G. Sandoval and F.J. Plou*. *Molecules* 23 (11) **(2018)**, 10.3390/molecules23112885.

"Exploring the transferase activity of Ffase from *Schwanniomyces occidentalis*, a β-fructofuranosidase showing high fructosyl-acceptor promiscuity". D. Piedrabuena, N. Miguez, A. Poveda, F.J. Plou, M. Fernández-Lobato*. *Applied Microbiology and Biotechnology* 100, 8769–8778 **(2016)**, 10.1007/s00253-016-7628-z.